Synthesis and Characterization

of Terpyridine-based

Fluorescent Coordination Polymers

vorgelegt von
Rainer Anton Dobrawa
aus Kaufbeuren

Würzburg 2004

Eingereicht am: _____
bei der Fakultät für Chemie und Pharmazie

1. Gutachter: _____

2. Gutachter: _____
der Dissertation

1. Prüfer: _____

2. Prüfer: _____

3. Prüfer: _____
des öffentlichen Promotionscolloquiums

Tag des öffentlichen Promotionscolloquiums: _____

Doktorurkunde ausgehändigt am: _____

für meine Eltern

Acknowledgement / Danksagung

List of Abbreviations

ACN	Acetonitrile
AFM	Atomic Force Microscopy
bpy	2,2'-Bipyridine
DOSY	Diffusion Ordered Spectroscopy
HOPG	Highly Ordered Pyrolytic Graphite
ITC	Isothermal Titration Calorimetry
MALDI-TOF	Matrix-Assisted Laser Desorption Injection Time-of-Flight
MeOH	Methanol
OPV	Oligo-*p*-phenylene-vinylene
phen	Phenanthroline
ptpy	4'-*p*-Phenyl-2,2':6',2"-terpyridine
STM	Scanning Tunneling Microscopy
TMS	Tetramethylsilane
tpy	2,2':6',2"-Terpyridine

Note:

- For the sake of clarity, always the 2,2':6',2"-terpyridine isomer is referred to whenever the terms "tpy" or "terpyridine" are used within this thesis.
- Although the conformation of the pyridine units in the uncomplexed terpyridine ligand is *trans*/*trans* with respect to the nitrogen atoms, the ligand units are in most cases depicted in the *cis*/*cis* conformation to emphasize the ability to act as a chelating ligand.

Table of Contents

Introduction and Aim
of this Thesis

The organization of functional molecular building blocks by noncovalent interactions is a central topic in modern supramolecular chemistry[1] and numerous applications of functional self-assembled systems including sensors[2], electronic[3] and photonic[4] materials or ion transport channels[5] have been reported. New supramolecular materials or devices are based on two requirements: first, the individual units must provide some sort of functionality like ion recognition or redoxactivity and have to be suited for the transformation into supramolecular building blocks containing appropriate receptor groups. The second requirement is the recognition-directed formation of a multichromophoric architecture which promotes or produces the desired functionality like ion transport, charge transport or light harvesting. A large variety of self-assembled structures has been published in the last decades[6] including layers,[7] membranes,[8] micelles,[9] vesicles,[10] gels[11] or liquid crystals.[12] Functional systems, however, are just now beginning to emerge for these "bulk" assemblies.

The application of the principles of supramolecular chemistry and self-assembly to direct chain growth added a new and highly diverse class of materials to modern polymer chemistry. Supramolecular polymers[13] offer the opportunity to be sensitive to external influences (like temperature, mechanic energy, solvent effects etc.) due to their construction from reversible bonds. Therefore, many supramolecular polymers can be switched between the polymeric and the monomeric state, thus offering new prospects for the design of sensor materials. On the other hand, photoactive polymers[14] play an important role for the manufacturing of organic electronic devices like transistors, light-emitting diodes or solar cells. Also these applications

could benefit from the advantage of supramolecular polymer chemistry which allows casting of well-ordered films from solution.

The aim of this thesis is the formation of photoluminescent supramolecular polymers, which are soluble and sufficiently stable to be processed and characterized in solution. For these requirements, metal-ligand coordination bonds seem to be best suited to realize polymeric chain dimensions. By proper choice of one of the large number of accessible ligand types and a suitable metal ion, diverse binding strength as well as various functional properties are accessible. The 2,2':6',2''-terpyridine ligand seems to be especially suited for this purpose due to its easy synthetic accessibility and the defined complexation behavior with various transition metal ions. The present work reports on the construction and characterization of two types of terpyridine-based dyes, which exhibit red and blue fluorescence, and the subsequent supramolecular polymer formation (figure 1).
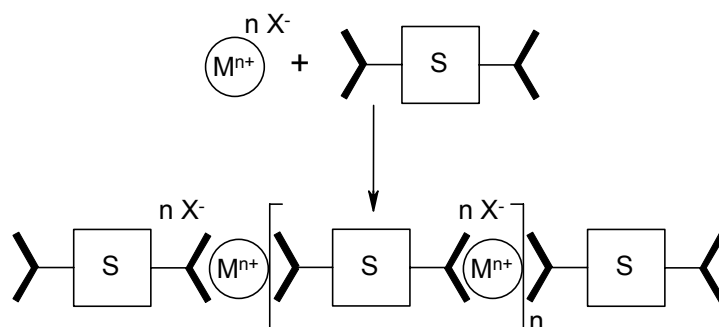
Figure 1. Schematic representation of a supramolecular polymerization process based on metal-ligand coordination chemistry, M: metal ion, X: counter ion, S: organic spacer equipped with the two terpyridine receptor units (bold).

Chapter 1 gives an overview of known supramolecular metal-ligand coordination polymers and discusses the basic relationship between binding strength and degree of polymerization.

In *chapter 2* the complex formation for the parent terpyridine unit with a series of transition metal ions is investigated by titration experiments applying UV-vis and NMR spectroscopy and isothermal titration calorimetry (ITC).

In *chapter 3* the construction of perylene bisimide containing terpyridine-based coordination polymers is established by NMR titrations upon comparison with a model dimer complex. The titrations reveal the reversibility of the complexation. The optical properties of the resulting complex units are investigated by UV-vis and fluorescence spectroscopy.

Chapter 4 provides a deeper insight into the properties of the perylene bisimide containing coordination polymers by DOSY (diffusion ordered spectroscopy) NMR and by fluorescence

anisotropy investigations. AFM micrographs provide proof for the presence of polymeric structures. Evaluation of the micrographs allows the determination of the polymer length.

In *chapter 5* a second class of fluorescent terpyridine-based coordination polymers is introduced, taking advantage of the blue fluorescence of 4'-phenyl-substituted terpyridine derivatives. However, due to the incorporation of a flexible tetraethylene glycol linker group, complexation of the ditopic ligand with Zn^{2+} yields a mixture of macrocyclic compounds and linear coordination polymers, as could be shown by DOSY NMR.

Chapter 6 reports on further structural hierarchy by applying the principle of electrostatic self-assembly to the polycationic coordination polymers, that have been reported in the previous chapters. Blue and red fluorescent layers could be constructed from both types of polymers.

The thesis concludes with summaries in English (*chapter 7*) and German (*chapter 8*).

References

(1)   (a) Lehn, J.-M. *Supramolecular Chemistry: Concepts and Perspectives* VCH, Weinheim: **1995**; (b) Schneider, H.-J.; Yatsimirski, A. *Principles and Methods of Supramolecular Chemistry* John Wiley & Sons, Ltd., Chichester: **2000**; (c) Steed, J. W.; Atwood, J. L. *Supramolecular Chemistry* John Wiley & Sons, Ltd., Chichester: **2000**.

(2)   (a) Prodi, L.; Bolletta, F.; Montalti, M.; Zaccheroni, N. *Coord. Chem. Rev.* **2000**, *205*, 59-83 (b) McQuade, D. T.; Pullen, A. E.; Swager, T. M. Chem. Rev. **2000**, *100*, 2537-2574.

(3)   (a) Tour, J. M. *Acc. Chem. Res.* **2000**, *33*, 791-804; (b) Würthner, F. *Angew. Chem. Int. Ed.* **2001**, *40*, 1037-1039; (c) Chabinyc, M.; Chen, X.; Holmlin, R. E.; Jacobs, H.; Skulason, H.; Frisbie, C. D.; Mujica, V.; Ratner, M. A.; Rampi, M. A.; Whitesides, G. M. *J. Am. Chem. Soc.* **2002**, *124*, 11730-11736.

(4)   (a) Würthner, F. *Chem. Commun.* 2004, *14*, 1564-1579; (b) Würthner, F.; Chen, Z.; Hoeben, F. J. M.; Osswald, P.; You, C.-C.; Jonkheijm, P.; von Herrikhuyzen, J.; Schenning, A. P. H. J.; van der Schoot, P. P. A. M.; Meijer, E. W.; Beckers, E. H. A.; Meskers, S. C. J.; Janssen, R. A. J. *J. Am. Chem. Soc.* **2004**, *126*, 10611-10618 (c) Friend, R. H. *Pure Appl. Chem.* **2001**, *73*, 425-430 and references cited therein; (d) Brabec, C. J.; Saricifci, N. S.; Hummelen, J. C. *Adv. Funct. Mater.* **2001**, *11*, 15-26.

(5)   (a) Sakai, N.; Matile, S. *Chem. Commun.* **2003**, 2514-2523; (b) Bong, D. T.; Clark, T. D.; Granja, J. R.; Ghadiri, M. R. *Angew. Chem. Int. Ed.* **2001**, *40*, 988-1011; (c) Beginn, U. *Adv. Mater.* **1998**, *10*, 1391-1393.

(6)   Lehn, J,-M. *Science* **2002**, *295*, 2400-2403

(7)   (a) Arys, X.; Jonas, A. M., Laschewsky, A.; Legras, R. *Supramolecular Polyelectrolyte Assemblies* in: A. Ciferri (Ed.) *Supramolecular Polymers*, 505-564, Marcel Dekker, New York, Basel: **2000**; (b) Decher, G.; Schlenloff, J. B. *Multilayer Thin Films. Sequential Assembly of Nanocomposite Materials*, 177-205, Wiley-VCH, Weinheim: **2003**.

(8)   Kimizuka, N. *Curr. Opin. Chem. Biol.* **2003**, *7*, 702-709.

(9)   Furhop, J.-H.; Wang, T. *Chem. Rev.* **2004**, *104*, 2901-2937.

(10)   Antonietti, M.; Förster, S. *Adv. Mater.* **2003**, *15*, 1323-1333.

(11)   (a) Terech, P.; Weiss, R. G. *Chem. Rev.* **1997**, *97*, 3133-3159; (b) van Esch, J. H.; Feringa, B. L. *Angew. Chem. Int. Ed.* **2000**, *39*, 2263-2266.

(12)   Percec, V. *Macromol. Symp.* **1997**, *117*, 267-273.

(13)   (a) Schmuck, C.; Wienand, W. *Angew. Chem. Int. Ed.* **2001**, *40*, 4363-4369; (b) Brunsveld, L.; Folmer, B. J. B.; Meijer, E. W.; Sijbesma, R. P. *Chem. Rev.* **2001**, *101*, 4071-4097.

(14)   Köhler, A.; Wilson, J. S.; Friend, R. H. *Adv. Mater.* **2002**, *14*, 701-707.

1

Supramolecular Coordination Polymers:
From Structure to Function

Abstract: The first introductory chapter gives a definition of supramolecular coordination polymers and presents the relation between polymer length, binding constant and concentration. The possibility for influencing the binding constant by chelating ligands is discussed by an example of different Zn^{2+} complexes and their respective binding constants. In the main part, supramolecular coordination polymers constructed from different metal-ligand systems are reviewed and some applications as functional materials for artificial membrane and enzyme models, light harvesting systems as well as materials for organic light emitting diodes are discussed by individual examples.

Introduction

The development of supramolecular chemistry in the last two decades of the past century added a whole new perspective to modern chemistry by going one step further from the molecular level to the "chemistry beyond the molecule"[1], by controlling the organization of molecular building blocks in space by rational design. The use of noncovalent interactions offers the possibility for the synthesis of large, complex aggregates enabling applications as receptors or devices as well as their use in catalysis.[2] The concepts of supramolecular chemistry have also been applied to other established fields like polymer science,[3] solid state chemistry,[4] and liquid crystal research.[5] Further steps are taken towards applying the principle of self-assembly to derive systems on the mesosocopic and macroscopic scale.[6] The construction of highly complex systems is virtually impossible by application of only one noncovalent interaction. In contrast, a series of interactions with different strength and reversibility have to be tuned and balanced to achieve the structure formation over multiple levels with the assembly process gradually increasing in strength – a concept, which is known as "hierarchical self-assembly".[7]

An area of special interest is supramolecular polymer chemistry.[8] Polymers which are synthesized not by classical covalent polymerization reactions but by noncovalent interactions offer new possibilities, since these interactions can be influenced by external parameters like temperature or mechanic stimuli causing drastic changes in the polymer properties, especially elasticity and solution viscosity. A large number of supramolecular polymers could be built by hydrogen bonding,[9] in some cases in combination with further interactions like π-π-aggregation, which significantly determines the structure of the polymers. Also more 'exotic' interactions like dipolar aggregation have been applied successfully for the formation of highly complex polymeric dye aggregates.[10]

Metal-ligand coordination provides an excellent means for the synthesis of supramolecular systems since the coordination bond is highly directional, the ligand structures can be varied in almost any way by classical organic chemistry, and the strength and reversibility can be varied in a high degree due to the large number of available ligand types and metal ions. Supramolecular systems constructed from metal-ligand bonds include lattice, cyclic and filamentous motives as well as interlaced systems.[11]

This introductory chapter collects examples of metallosupramolecular coordination polymers and illustrate their evolution from pure structure towards functional systems which possess additional properties like redox- or photoactivity or which have already been applied in devices.

Coordination Polymer: Definition, Formation and Interactions

Definition: The keyword "coordination polymer" is abundantly found in modern chemistry literature. However, care must be taken since the term "coordination polymer" is defined quite differently in the inorganic and in the supramolecular chemistry communities. Inorganic chemists define infinite 1D, 2D and 3D coordination compounds as coordination polymers. These systems are in the great majority characterized in the solid state and it is also the solid state properties, which are of interest. Alternative names for this type of compounds are "metal-organic coordination networks" or "metal-organic frameworks".[12] One highlight of recent research in this field is the construction of functional porous coordination polymers.[13]

In the field of supramolecular chemistry, the definition is more restricted and related to macromolecular chemistry. A coordination polymer in this sense is a compound consisting of a backbone, which is held together by metal-ligand interactions. These interactions have to be strong enough to retain the polymer chain also in solution. The coordination polymers should exhibit properties which are characteristic for polymers like enhanced viscosity in comparison with their monomeric building blocks. In his review on organic/inorganic hybrid polymers, Rehahn[14] gives a classification on the different structures of coordination polymers.

Within this chapter, only those coordination polymers will be discussed which are constructed from an alternating incorporation of metal ions and organic ligand molecules (figure 1). The systems have to be soluble and stable in solution and should be synthesized by a supramolecular approach, i.e. formation of the polymer chain by metal ion complexation. The latter should be accomplished under the condition of reversibility in contrast to traditional polymerization by formation of covalent bonds.[15]
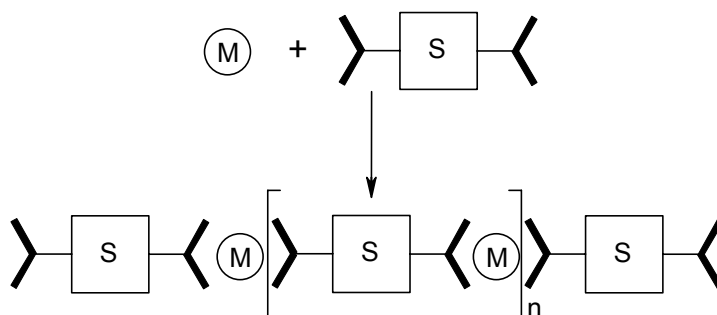
Figure 1. Schematic representation of the supramolecular definition for a coordination polymer with "M" depicting the metal ion and "S" the organic spacer equipped with two receptor units (bold).

Coordination Polymer Formation: The main difference between classical covalent polymers and supramolecular polymers is the dependence of the chain length on the solvent

and temperature dependent binding constant and, connected therewith, the concentration. The degree of polymerization DP and the binding constant K are connected by the following relation:[16]

$$DP \sim (K\,[\text{M}])^{1/2}$$

According to this relation, high degrees of polymerization DP can only be achieved at high monomer concentration [M] and by using a system with a large binding constant. This relationship pf course holds only true if complexation is a fully reversible process. Many advantageous properties of supramolecular structures like self-healing or formation of the thermodynamically favored structure are only possible if the binding site can be opened and subsequently closed again in another orientation. As already mentioned above, external stimuli can be applied for reversible polymers to enable switching from the monomeric to the polymeric state. In contrast to classical covalent polymers, which can only be polymerized once, some of these systems can be repeatedly switched. The synthesis of copolymer systems is also easy since the simple addition of a second compound, equipped with the same ligand unit, is easily built in into the existing reversible polymers.

For intermolecular interactions, realization of high binding constants and reversibility is challenging. In general, these properties are strongly anticorrelated meaning that high binding constants often lead to low reversibility has to be accepted and vice versa. Only a small number of examples exist which offer high binding constants combined with reversibility.[17]

Metallosupramolecular Interactions: As discussed above, the nature of the metal-ligand interaction has a significant influence on the properties of the resulting coordination polymer and the binding constant is the first parameter that has to be considered. Since for most applications high degrees of polymerization are preferred and an increase of concentration is not possible in many cases due to practical limitations or insufficient solubility, control of the binding strength is of paramount importance. An increased K can be achieved by combining multiple interacting binding sites, the most simplest one being the use of chelate ligands and multivalent metal ions. The analogous strategy was applied for hydrogen bonded polymers when quadruple hydrogen bonds[3] had been used instead of triple hydrogen bond, which resulted in a drastic increase in binding constant and subsequently in the formation of systems with typical polymer properties.[9] The increase in binding constant by application of chelating ligands is illustrated by the comparison of the Zn^{2+} complexation with pyridine donor ligands.
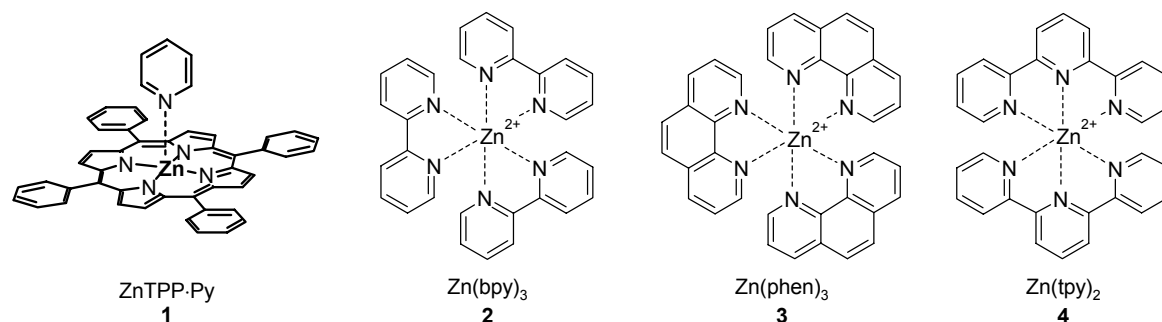
Chart 1. Examples for compounds with a single, a bidentate and a tridentate pyridine/Zn^{2+} interaction.

Table 1. Literature values for binding constants of Zn^{2+} with aromatic N-donor ligands of increasing chelation giving the binding constant for the first binding event K_1 and the overall binding constant β.[18]

Ligand Type	K_1 [M^{-1}]	β_n [M^{-n}]		Solvent / Counterion	Ref.
Pyridine / ZnTPP **1**	4.1×10^3	4.1×10^3	(n = 1)	CHCl$_3$ / - - -	19
	3.3×10^3	3.3×10^3	(n = 1)	CHCl$_3$ / - - -	20
	3.8×10^3	3.8×10^3	(n = 1)	benzene / - - -	19
	2.0×10^4	2.0×10^4	(n = 1)	CCl$_4$ / - - -	19
bpy / Zn^{2+} **2**	2.5×10^5	2×10^{13}	(n = 3)	aq. KNO$_3$	21
	2.0×10^5	4.2×10^{13}	(n = 3)	0.1 M aq. NaNO$_3$	22
phen / Zn^{2+} **3**	2.7×10^6	1×10^{17}	(n = 3)	aq. KNO$_3$	21
	3.5×10^6	2.5×10^{17}	(n = 3)	0.1 M aq. NaNO$_3$	22
tpy / Zn^{2+} **4**	$> 10^8$	$> 10^8$	(n = 2)	CH$_3$CN / ClO$_4^-$	23
	1×10^5	8×10^9	(n = 2)	CH$_3$CN / ClO$_4^-$	24[†]
	2.5×10^8	2×10^{14}	(n = 2)	CH$_3$CN / ClO$_4^-$ / TBAPF	25[‡]

[†] determined for a 4'-substituted terpyridine unit;

[‡] determined for a 4'-substituted unit, TBAPF = 0.01 M tetrabutylammonium hexafluorophosphate

Although the data given in table 1 refers to experiments in different solvents and with different counterions, the significant increase in binding constant ranging from K = 10^3 M^{-1} for the single Zn^{2+}/pyridine interaction to K > 10^8 M^{-1} for the threefold chelating terpyridine unit is not questioned. Comparison of the binding constants for the bpy and phen complexes **2** and **3** shows that the value for phen is higher by approx. a factor of 10. The reason for this effect is the fixed *cis*-conformation of the nitrogen atoms in the pheanthronline ligand, whereas the bpy ligand is flexible around the py-py bond. This flexibility has to be frozen upon complexation, thereby decreasing the binding constant for entropical reason. With this

information, the length of a coordination polymer for a stoichiometric 1 mM solution of metal ion and ligand can be estimated for hypothetic polymers constructed of each of the interactions given above. In the case of a binding constant of $K = 10^3$ M^{-1} no significant polymer formation will be observed. An increase of the binding constant by the factor of 100 to $K = 10^5$ M^{-1} results in a polymer length of approx. 10 units, whereas a binding constant of $K = 10^7$ would give a chain length of approx. 100 repeat units. The same estimation can be used to determine the effect of dilution, which gradually decreases the chain length. However, it is not yet established how molecular weight correlates with polymer-like properties for such supramolecular polymers. The dynamic nature of these noncovalent bonds will clearly influence the properties, especially under the influence of shearing forces or other kinds of stress. Indeed, quite often the traditional polymer characterization techniques like GPC, viscosimetry etc. fail for supramolecular polymers and other techniques like AFM or ultracentrifugation or NMR are applied. Recently, DOSY (diffusion ordered spectroscopy) NMR was shown to be particularly suited, since the compounds remain in equilibrium with the surrounding solution during the whole measurement.

Overview of Supramolecular Coordination Polymers

Content and Organization. The literature overview is organized by the nature of the metal-ligand interaction. After a short description of some individual examples with O, S and P ligands the class of imine ligands will be discussed, followed by the large field of aromatic nitrogen ligands, which will be subdivided into classes with increasing chelating effect.

First Soluble and Reversible Coordination Polymer. The first soluble coordination polymer, the beryllium phosphinate system **5**, was published by Ripamonti and coworkers in 1968.[26] They observed reversible degradation of the polymer depending on the solvent nature, temperature and concentration, which are exactly the conditions defined for a supramolecular polymer. The polymer **5** is soluble in hydrocarbon and halogenated solvents and was characterized by viscosimetry and X-ray powder diffraction. The nature of the polymer backbone was proposed to be a linear chain as depicted in chart 2.
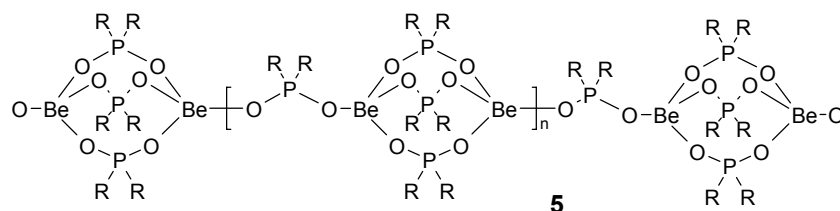
Chart 2. First soluble, reversible coordination polymer published by the group of Ripamonti.26

Various Metal-Ligand Systems. A relatively new concept for the synthesis is the application of ionophore ligands, which are known to bind with high affinity to alkali ions. Paquette and coworkers[27] synthesized tris(spirotetrahydrofuranyl) ionophores which were found to bind selectively to Li^+ in a 2:1 complex. Ditopic receptors **6** with rigid spacers constructed of 1,3-butadiyne units were applied as the monomers and coordination with Li^+ yielded the respective rigid rod-like coordination polymers **7** (scheme 1), which is, however, of limited solubility.
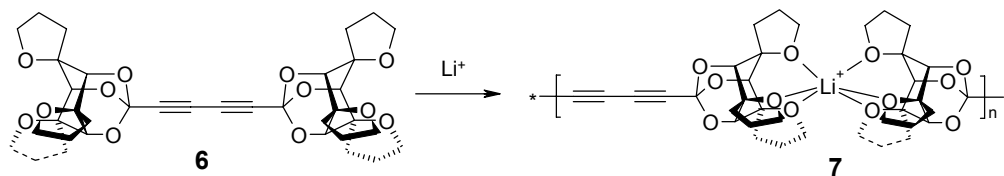
Scheme 1. Synthesis of a coordination polymer based on a tris(spirotetrahydrofuranyl) ionophore and Li^+.[27]

Bis-dithiolene Coordination Polymers. Also in the field of conducting polymers, early examples for coordination polymers are found, e.g. metal-sulfur complexes.[28] (Chart 3). As can be expected for the structure **8,** which lacks any solubilizing groups, these systems were

completely insoluble in all solvents. Conductivity and magnetic susceptibility measurements revealed that the material is paramagnetic and exhibits conductivities of 10^{-4} – 0.2 S cm^{-1}. In contrast to these insoluble compounds, Wang and Reynolds[29] reported soluble and electroactive nickel bis(dithiolene) polymers **9** and **10**, which had been obtained by metal complexation polymerization (scheme 2). The length and chemical nature of the flexible spacer groups were varied from short spacers like R = O, S and CH$_2$ to long spacer units such as R = (CH$_2$)$_{10}$, (CH$_2$)$_{22}$ and (OCH$_2$CH$_2$)$_3$O. The polymers with short spacers are reported to be highly soluble in both aqueous and organic solvents in the dianionic form **9** and slightly soluble in the oxidized, neutral form **10**, whereas the compounds equipped with long spacers exhibit good solubility in both forms in organic solvents. Electrochemical studies revealed that two reversible oxidations can be observed from the dianionic to the monoanionic and subsequently to the neutral form.
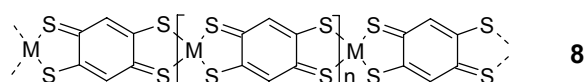
Chart 3. Poly(benzodithiolene) compounds published by Wudl and Heeger et al. as conductive materials (M = Fe, Co).[28]
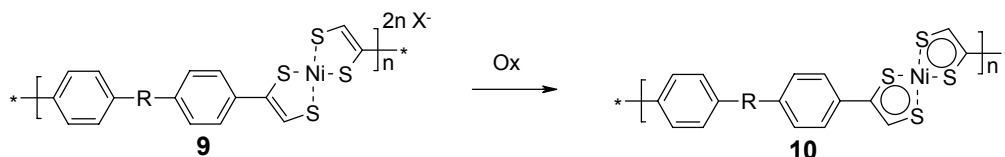
Scheme 2. Soluble and electroactive nickel bis(dithiolene) coordination polymers. The nature of the spacer group R and the oxidation state determine the solubility.[29]

Salicylidene and Hydroxyazobenzene Based Coordination Polymers. An early and extensively studied class of soluble coordination polymers are the Schiff-base systems **11** (chart 4), which have been published in the early 1990ies by Archer and coworkers.[30,31] Tetracationic rare earth ions like Zr^{4+} and Ce^{4+} were used as well as tricationic ions like Y^{3+}, Yb^{3+} and Gd^{3+} together with one additional Na$^+$ counterion. All polymers are highly stable against dissociation and can be characterized by GPC, viscosimetry and NMR spectroscopy. Polymers containing Eu^{3+} or mixtures of metal ions like Y^{3+}/Eu^{3+} exhibit intense luminescence[32] since the ligands acts as an energy donor and transfers its excitation energy to the Eu^{3+} ion. The concept of Schiff-base coordination polymers and the procedure for their synthesis have been applied recently to obtain stepwise growth of such polymers perpendicular to a substrate by alternating deposition of Zn^{4+} and ditopic ligand molecules.[33]
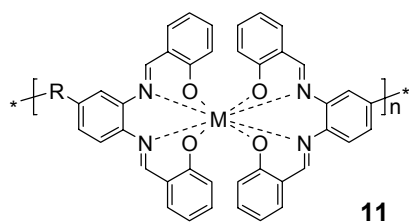
Chart 4. General structure of the Schiff-base coordination polymers published by Archer and coworkers with R representing any spacer unit.[31,32]

The metal coordination property of *o,o'*-dihydroxy-functionalized azobenzene **12** was applied by the group of Suh for the construction of polymeric coordination compounds **13**, which have been named polyazometals (Scheme 3).[34] As metal centers, Fe^{2+}/Fe^{3+}, Co^{2+}, Ni^{2+} and Cu^{2+}/Cu^{3+} have been applied. Identical to the investigations of Heeger et al. on the poly(benzodithiolene) compounds, also the polyazometals were first synthesized as conducting organic compounds and the conductivity of a Fe^{2+}/Fe^{3+} (1:1) polyazometal reached a conductivity of 1.4×10^{-2} Ω^{-1} cm^{-1} when doped with BF_3. Since no solubilizing substituents are present in the ligand, also these compounds are insoluble and structural characterization remained elusive.
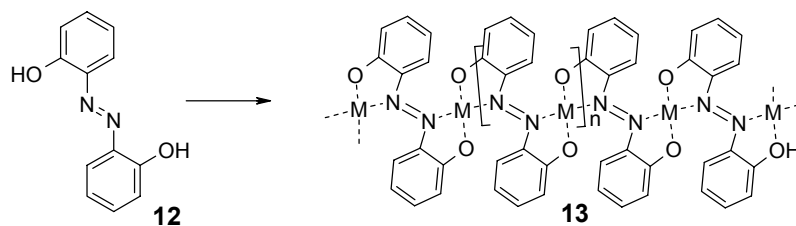
Scheme 3. The basic structure and coordination motif of polyazometals published by Suh et al. (M = Ni^{2+}, Cu^{2+}/Cu^{3+}, Co^{2+}, Fe^{2+}/Fe^{3+}).[34]

Since the polyazometals provide a stable and defined polymeric platform, this motif was incorporated into an amphiphilic structure (**14**). Complexation of the amphiphiles with one equivalent of a metal ion (Fe^{2+}, Fe^{3+}, Co^{2+}, Co^{3+}, Cu^{2+}) provided highly stabilized bilayer membranes **15**, as could be shown by UV-vis and IR spectroscopy and surface-pressure measurements at the air-water interface (scheme 4).[35] Similar polyazometal structures, which had been conjugated with poly(allylamin), were found to catalyze the hydrolytic cleavage of bovine serum albumine and therefore constitute an artificial metalloproteinase.[36] The concept for coordinative stabilization of membranes was also applied to other structures based on Schiff-base ligands like compound **16**, which additionally shows blue fluorescence (chart 5).[37]
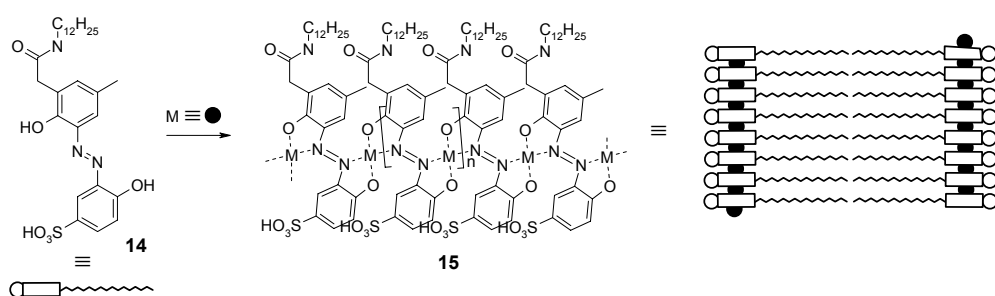
Scheme 4. Formation and stabilization of bilayer membranes by complexation of *o,o'*-dihydroxyazobenzene amphiphiles.[35]
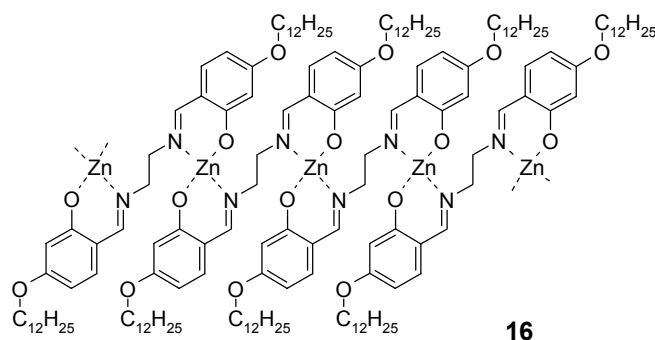
Chart 5. Blue-fluorescent stable monolayersby coordination polymerization of long-chained Schiff-base units.[37]

Coordination Polymers by Pyridine-Metal Coordination. Craig and coworkers[38] recently published a basic structural study on a pyridine-palladium coordination polymer system **19**, where the dissociation dynamics can be tuned independent of the systems binding constant. The effect is produced by variation of the substituents at the amino-functions (R) of the palladium-pincer **17** (scheme 5). Whereas the binding constant in dimethylsulfoxide is almost identical for the methyl- and ethyl-substituted compounds, the dissociation rates differ almost by a factor of 100, an effect, which is attributed to the different steric situation at the metal center. Interestingly, the binding constant seems not to be significantly influenced by the nature of the solvent ($K(CDCl_3) = 2 \times 10^3$ M^{-1}, $K(MeOD) = 1 \times 10^3$ M^{-1}, $K(D_2O/DMSO,$ 1:1) = 1 \times 10^3$ M^{-1}).
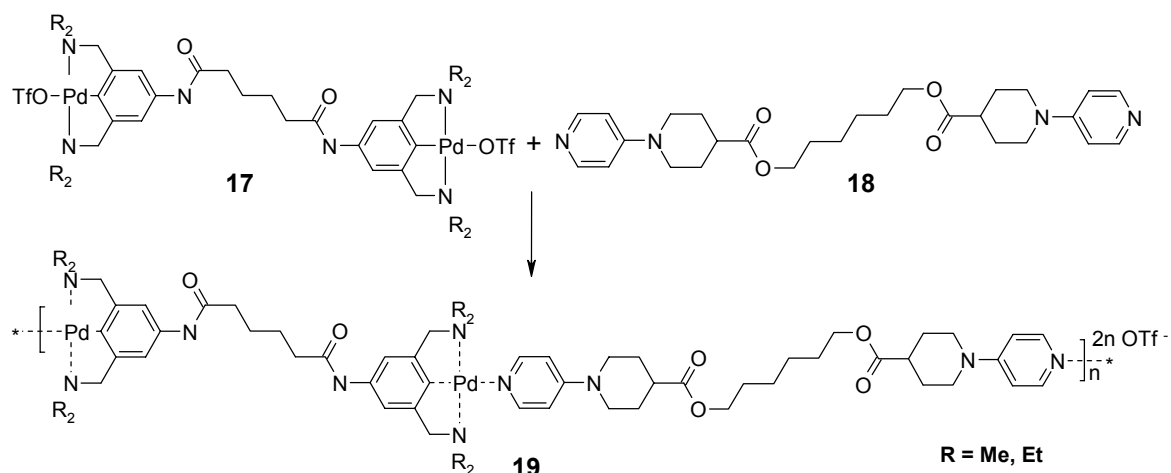
Scheme 5. palladium-pyridine coordination polymers.[38]

The coordination of pyridine ligands to silver(I) ions offers the possibility for the connection of two ligands in a linear fashion. Since the Ag^+-pyridine complex does not exhibit a high binding constant, but nevertheless represents an interesting topology, it is abundantly used for 1D inorganic solid state coordination polymers.[39] A highly soluble dye capable of forming a coordination polymer with Ag^+ was introduced by Würthner and Sautter.[40] The tetraphenoxy-diazadibenzoperylene ligand forms a complex with Ag^+ (**20**) and NMR studies revealed significant line broadening and an increased viscosity of the system suggesting the presence of a polymeric species at a 1:1 ratio of ligand and Ag^+.
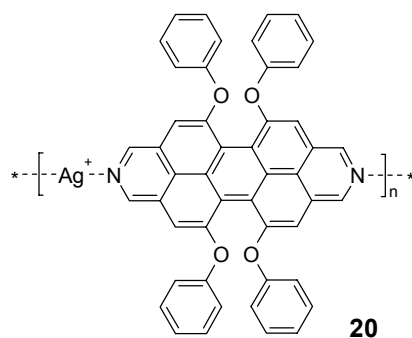
Chart 6. Ag^+-diazadibenzoperylene polymer.[40]

The concept of formation and/or stabilization of membranes or monolayers by metal ion coordination, which has already been shown for the polyazometals, has also been applied to aromatic nitrogen ligands. Monolayer formation at the water/air interface is reported for benzimidazole[41] or naphthimidazole[42] systems like **21** (chart 7). Remarkably, the latter form a helical assembly from the achiral building blocks, as supported by CD spectroscopy.
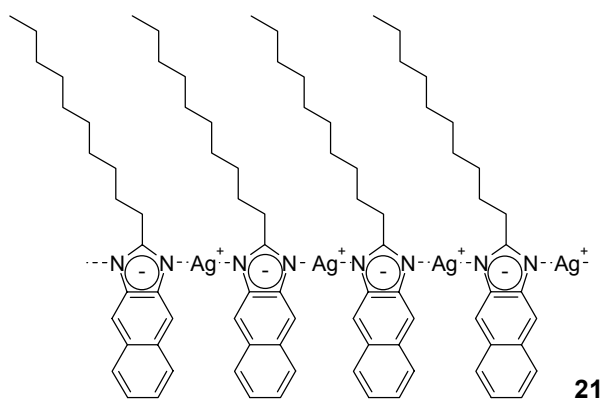
Chart 7. Self-assembled monolayer stabilized by silver(I)/naphthimidazol coordination at the water/air interface.[42]

Vermonden and coworkers[43] utilized oligoethylene glycol spacered pyridine-2,6-dicarboxylic acid receptors **22** (chart 8) for the construction of water soluble coordination macromolecules which were extensive studied utilizing viscosity measurements, DOSY (diffusion ordered spectroscopy) NMR and ITC (isothermal titration calorimetry), to determine the influence of concentration, temperature and stoichiometry on the formation of linear chains and cyclic species.
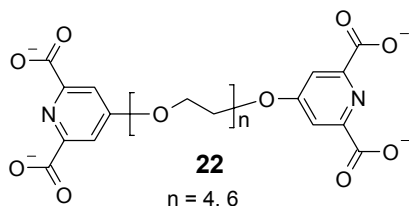
Chart 8. Ditopic ligand bearing pyridine-2,6-dicarboxylic acid receptor groups utilized for the synthesis of water soluble coordination polymers with Zn^{2+} ions.[43]

Polymeric Porphyrin-Systems Connected by Pyridine-Metal Interaction. The construction of self-assembled porphyrin systems gained significant attention in the last decade, especially as models for natural light harvesting systems.[44] The structure of porphyrin metal complexes makes them ideally suited for coordination compounds with pyridine. The four porphyrin nitrogens embed the metal ion a square planar fashion whilst one or two coordination sites remain accessible. The first example of a porphyrin-pyridine coordination polymer was reported by Fleischer and Shachter,[45] who synthesized a self-complementary zinc-4-pyridyl-triphenyl-porphyrin, which forms a staircase-like coordination polymer that was characterized by X-ray single crystal analysis, but also in the dissolved state by concentration dependent UV-vis and NMR spectroscopy.

As already mentioned, the binding constant of pyridine unit to zincporphyrin is in the order of 10^3 M^{-1} in chloroform, which is not enough for the self-assembly of high molecular weight

polymers in dilute solution. Since the application of chelating ligands is not applicable for zinc-porphyrin systems, higher binding constants can therefore be achieved by utilizing not only one, but more interactions of the same type. Michelsen and Hunter[46] realized this concept by equipping the porphyin with a cobalt(II) center, which in contrast to zinc(II) exhibits octahedral coordination allowing the coordination of one pyridine ligand **23** above and below the porphyrin plane respectively (scheme 6). The symmetric structure of the pyridine ligand arms allowed the formation of a soluble extended polymeric structure, which was characterized by PGSE (pulsed-gradient spin-echo) NMR diffusion experiments and by GPC.
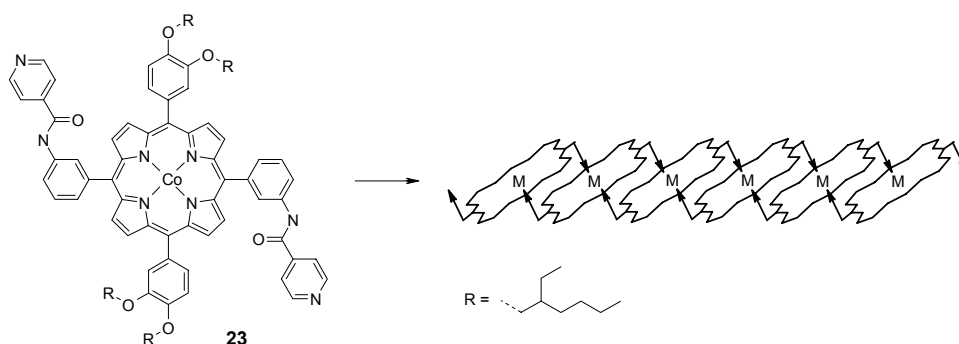
Scheme 6. Linear coordination polymer from self-complementary cobalt-porphyrin published by Michelsen and Hunter.[46]

Breaking the symmetry of this self-complementary Co-porphyrin ligand resulted in an curved coordination motif **24**.[47] If the system is equilibrated to allow for the formation of the thermodynamically favored structure, a macrocyclic compound is obtained instead of a coordination polymer (scheme 7). Hunter and coworkers characterized the resulting macrocycles by GPC.
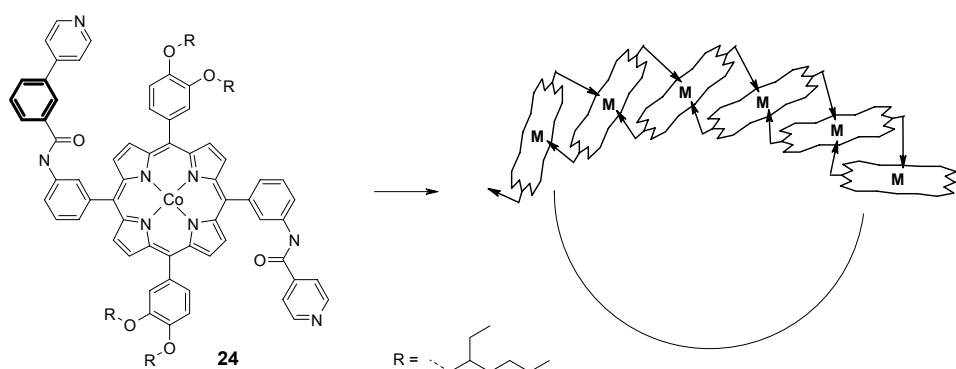
Scheme 7. Self-assembled formation of a macrocyclic cobalt-porphyrin coordination compound by variation of the length of one ligand 'arm' (bold), thereby creating curvature.[47]

A related approach was followed by the group of Kobuke,[48] who applied the pentacoordinating zinc-porphyrin scaffold due to its favorable fluorescence properties. Since only one ligand can bind to the zinc-porphyrin, covalent linking of two units equipped with one imidazol-ligand each yields the necessary ditopic self-complementary building block **25**

for coordination polymer formation (figure 2). The polymers were found to be stable in chloroform in the absence of protic solvents and GPC analysis revealed a remarkable length of 150 units. The addition of monotopic, chain-terminating compounds did not decrease the chain length which raises some questions if maybe already more extended structures have formed by hierarchical self-assembly. However, addition of methanol decreased the chain length significantly by acting as a competitive ligand.
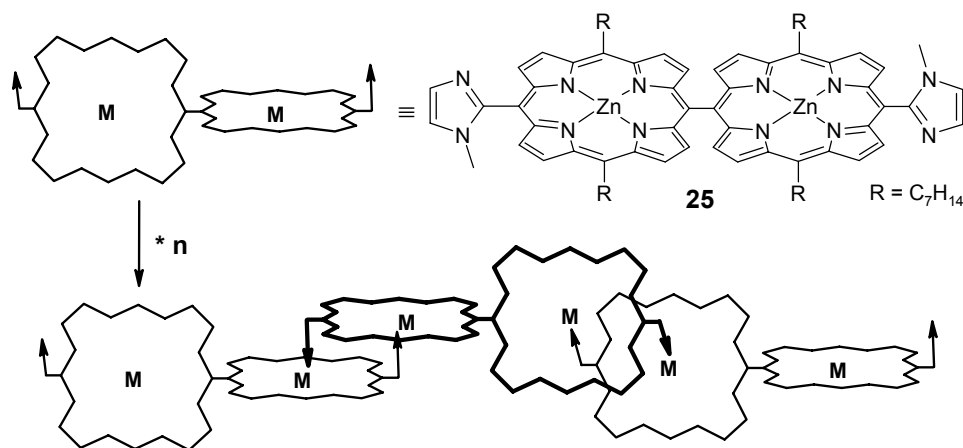
Figure 2. Linear, rigid coordination polymer from bis- zinc-porphyrin imidazole ligands.[48]

Also here, macrocyclic hexamers have been obtained from the same construction principle by connecting the two imidazolyl-zinc-porphyrin subunits through a *meta*-phenylene bridge (**26**) which introduces a 120° angle (figure 3).[49] The selective synthesis of the hexameric macrocycle was achieved by a reorganization process, in which the units were dissolved in the presence of methanol as a competitive ligand under high dilution followed by evaporation of the solvent mixture. Characterization by GPC, AFM and small angle X-ray scattering (SAXS) revealed the exclusive formation of the macrocycle.
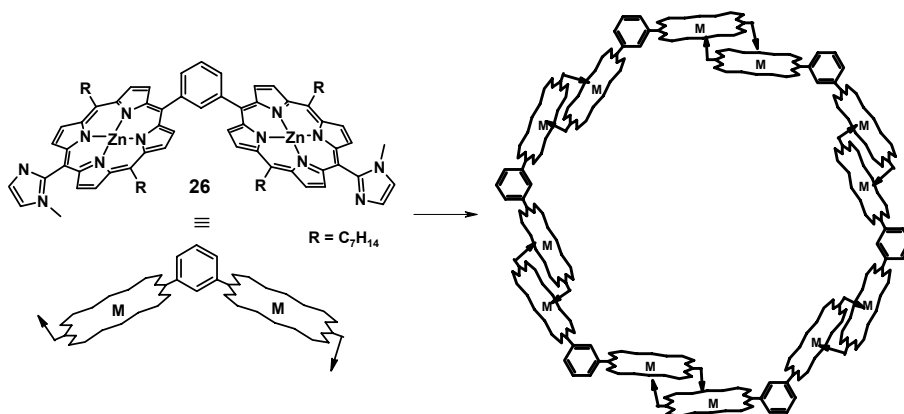
Figure 3. Macrocyclic hexamer from self-complementary bis-porphyrin building blocks.[49]

Another fascinating polymeric porphyrin system was presented by the group of Shinkai.[50] The three-dimensional polymeric hollow-capsules **27a,b** are constructed of a porphyrin unit

bearing eight rigid pyridine ligands, which are coordinated in a 90° angle by a palladium 1,3-bis-(diphenylphospino)propane [Pd(dppp)] complex, thereby bridging two units (chart 9). The UV-vis titration of the metal complex to the porphyrin ligand proved the stoichiometry of the system by revealing a 4:1 ratio as expected for the polymer formation. The coordination polymer was characterized by NMR and dynamic light scattering. Substitution of the dppp-ligand by a chiral binaphtyl-based ligand caused the formation of a chiral polymeric structure **27b**, which was substantiated by CD spectroscopy.
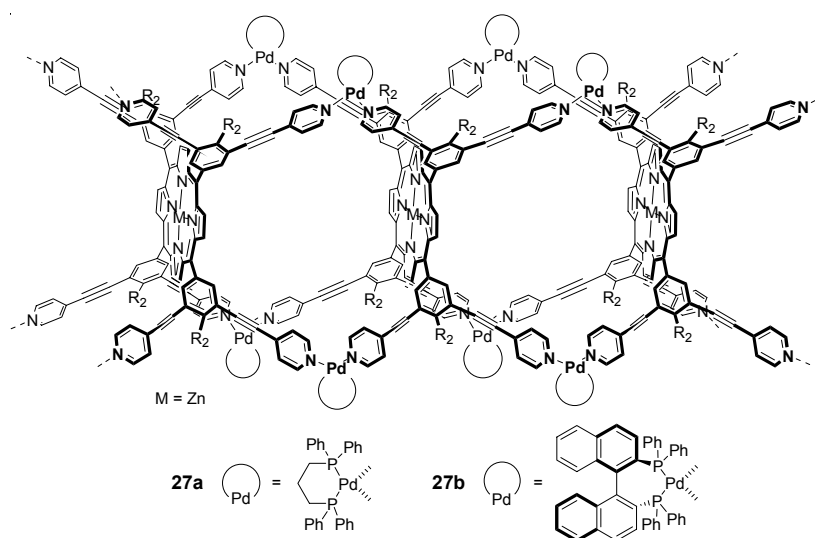
Chart 9. Polymeric hollow capsules formed by four palladium phosphane complexes which act as bridging units.

Coordination Polymers from 2,2'-Bipyridine. As already mentioned, the application of chelating complexes is an effective way to obtain higher binding constants. The first example of a well-defined coordination polymer constructed from kinetically labile metal complexes was published by the group of Rehahn[51] and is based on a ditopic building block **28** bearing two phenanthroline ligand units. The polymer complexes **29** obtained from addition of silver(I) or copper(I) are highly labile and are therefore only stable in noncoordinating solvents. Detailed NMR studies showed that the presence of small amount of a competitive solvent like acetonitrile drastically decreases the coordination polymer length. The solubility of the polymer was high enough for viscosimetric characterization.
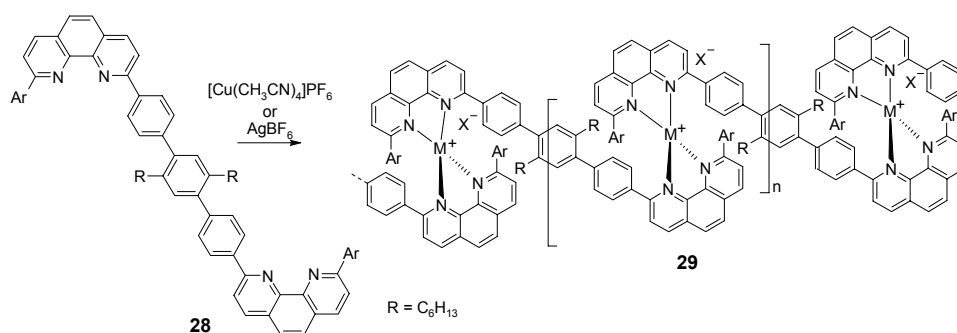
Scheme 8. Synthesis of kinetically labile silver(I) and copper(I) phenanthroline coordination polymers by rigorous exclusion of any competitive ligands or solvent molecules published by Rehahn et al.

The formation of zinc phenanthroline complexes **31**, which are further stabilized by an *o*-carboxylic acid group to provide octahedral coordination, is the basis of the porphyrin coordination polymers introduced by Groves and coworker.[52] The complexation of the units upon addition of zinc acetate was monitored spectrophotometrically revealing that complex formation takes place distinctly faster that the metalation of the porphyrin macrocycle. The average length of the structures was determined by a kinetic study to 12 units.
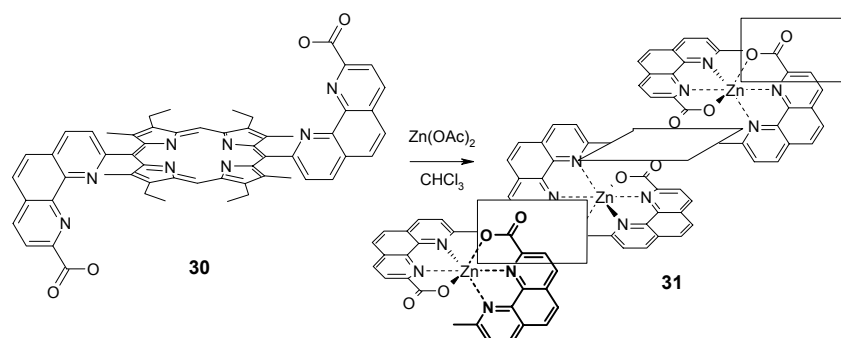
Scheme 9. Porphyrin-containing coordination polymer based on a phenanthroline carboxylic acid.

In contrast to the kinetic instability of phenanthroline complexes with silver(I) and copper(I), the respective ruthenium(II) complexes are highly stable. Accordingly metalation is a virtually irreversible process.. The group of Rehahn[53] published the synthesis of polymers **34** from the tetrapyridophenazine bridging unit **33** and the 2,2'-bipyridine fragment Ru(bpy)Cl₃ **32** (chart 10a). Variation of the steric stress by the substituents R at the bipyridine unit was found to have significant influence on the chain conformation. Since the polymer **34** is built by complex formation there is no control of the chirality of the complexes. MacDonnell and coworker[54] prepared the same type of coordination polymer by formation of the bridging ligand in the polymerization step (chart 10b). The use of enantiomerically pure complexes **35** and **36** as starting materials allowed the preparation of a coordination polymer with defined chirality as proved by CD spectroscopy.
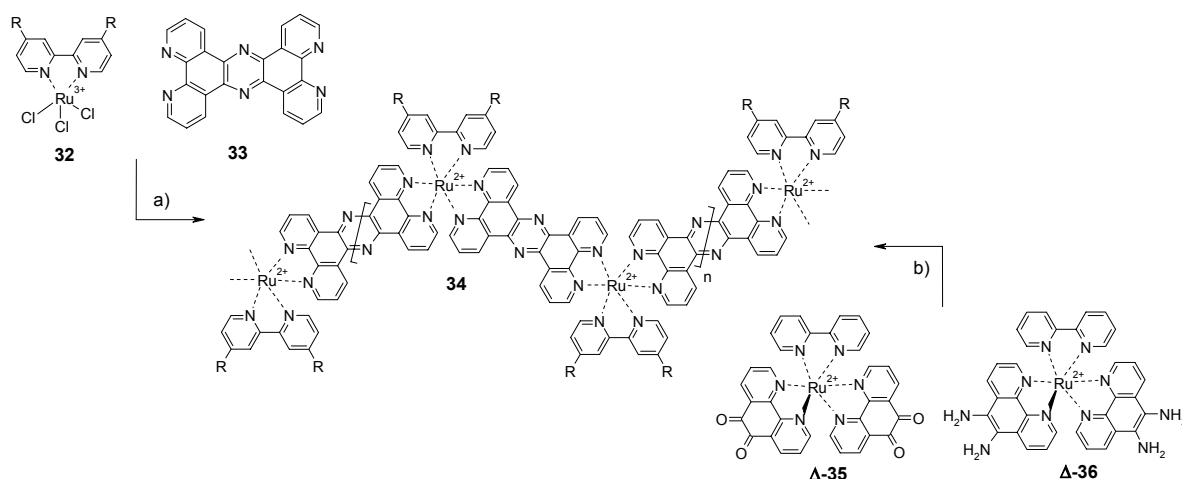
Chart 10. Synthesis of ruthenium(II)-tetrapyridophenazine coordination polymer, (a) by complex formation leading to a racemic mixture of complexes[53] or (b) by synthesis of the tetrapyridophenazine ligand from enantiomerically pure starting materials.[54]

Mallouk, Fendler and coworkers[55] applied ruthenium tris(bipyridine) coordination polymers **37** for the preparation of a self-assembled diode junction on TiO$_2$. The polymer was prepared by complexation of a ditopic alkyl-spacered bipyridine ligand with ruthenium(II) and subsequent addition of the third bipyridine unit. Titanium dioxide electrodes were covered with the resulting polyelectrolyte by using the electrostatic self-assembly method and the resulting devices were characterized for their current/voltage properties showing diode behavior.
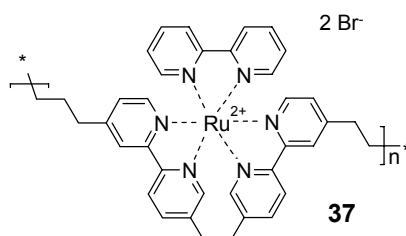
Chart 11. Ruthenium tris(bipyridine) coordination polymer used for the preparation of self-assembled diode junctions.[55]

Terpyridine Coordination Polymers. The 2,2':6',2"-terpyridine (tpy) ligand is ideally suited as a ligand for coordination polymers .[56] The three chelating pyridine units offer high binding constants and the formation of octahedral 2:1 ligand-metal complexes does not give rise to enantiomers like is the case for octahedral coordination by three phenanthroline or 2,2'-bipyridine ligands. Additionally, the easy synthetic access of 4'-substituted terpyridine derivatives offers the possibility for the construction of a perfectly linear coordination motif like discussed for the pyridine/Ag$^+$ system, but with a strongly increased binding constant. The general concept for coordination polymer formation on the basis of terpyridine[57] and the

synthesis of basic building blocks **38**, **39** and **40** (chart 12)[58] were introduced by Constable and coworkers.
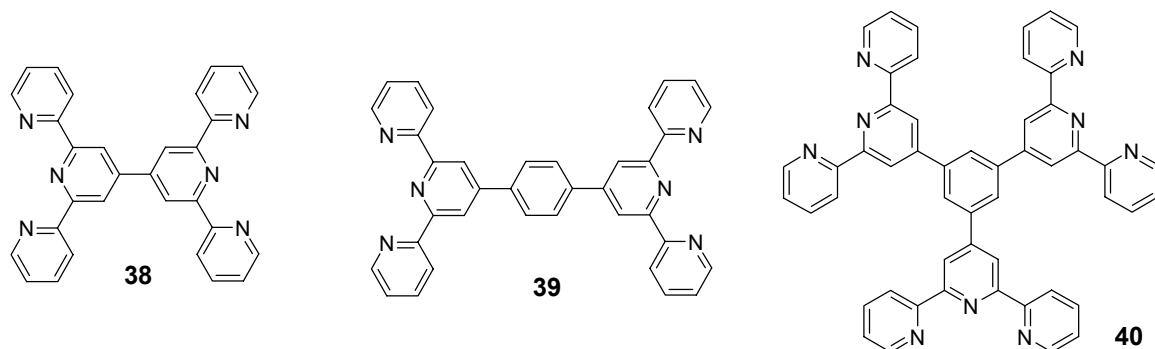
Chart 12. Basic ditopic and tritopic ligands for the construction of tpy-based coordination compounds reported by Constable et al.[57,58]

Two series of ditopic terpyridine ligands based on amide and imide linked 4'-*p*-aminophenyl-terpyridines were synthesized by the groups of Colbran[59] (chart 12) and Chan[60] (chart 14). Colbran et al. synthesized the respective iron(II) coordination polymers from ligand **41a-c** and characterized them by NMR end-group analysis to find an average polymer length of 17 units. Mass spectrometry and GPC were not applicable to these systems, which is the case also for the large majority of other tpy-based coordination polymers synthesized by other groups. The ruthenium coordination polymers **42a-f** published by Chan have not been prepared by metal complexation polymerization but by a polyimidization reaction of the preformed kinetically stable ruthenium complexes. The compounds have been fabricated into light-emitting diodes and also showed electron and hole carrier mobilities in the order of 10^{-4} cm^2 V^{-1} s^{-1}.
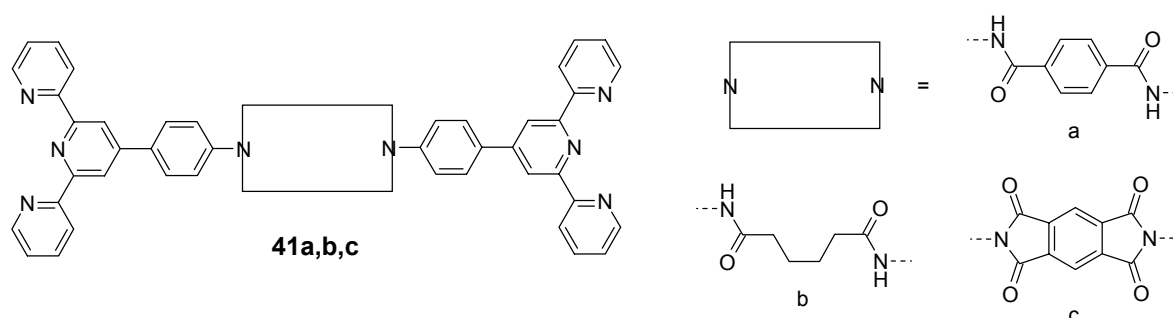
Chart 13. Series of ditopic tpy-ligands published by Colbran et al.[59]
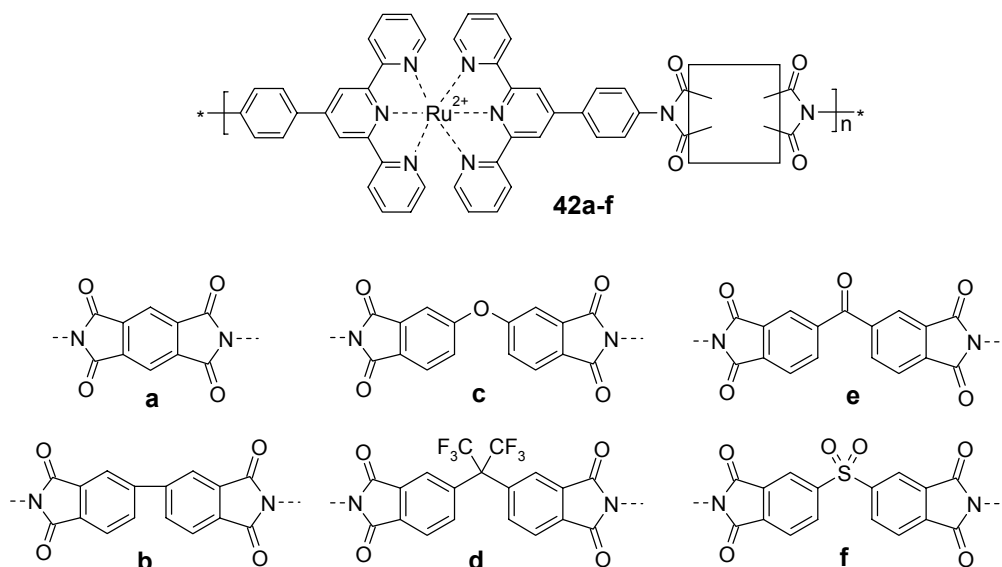
Chart 14. Ruthenium-terpyridine containing polyimides applied as electroluminescent materials by Chan et al.[60]

Rehahn and coworkers[61] synthesized a soluble ruthenium-terpyridine polymer **43** (chart 15) applying two orthogonal methods, which are the metal complexation polymerization of an activated ruthenium(II) species with the ditopic ligand and the polymerization by synthesis of the ditopic ligand by metal-catalyzed aryl-aryl coupling of the previously formed Ru(tpy)$_2$ units. Whereas the latter strategy only produced oligomeric compounds, the complexation polymerization yielded coordination polymers which were thoroughly characterized by viscosity in salt-free and salt-containing solvents revealing a pronounced polyelectrolyte effect. The polymer length was estimated by NMR end group analysis to >30 repeat units.
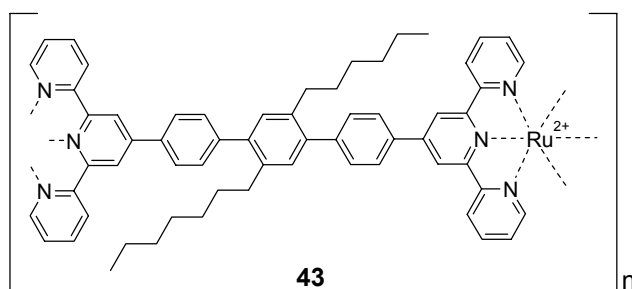
Chart 15. Ruthenium-terpyridine based coordination polymer with a length of >30 units presented by Rehahn.

Application of simple tpy-based coordination polymers **44** as building blocks for further hierarchical self-assembly of complex layer architectures have been reported by Kurth and coworkers (figure 4). Due to their polyelectrolyte nature, these coordination polymers can be applied in the 'layer-by-layer' method to form alternating layer assemblies with polyanions.[62] The same method can also be applied with polystyrene latex particles as a template for the formation of core-shell particles.[63] If the central template is a weakly linked melamine-formaldehyde particle, which can be decomposed and removed, also the construction of

hollow shell particles is possible. Exchange of the original counter ions by amphiphilic anions can be applied for the fabrication of polyelectrolyte-amphiphile complexes.[64]
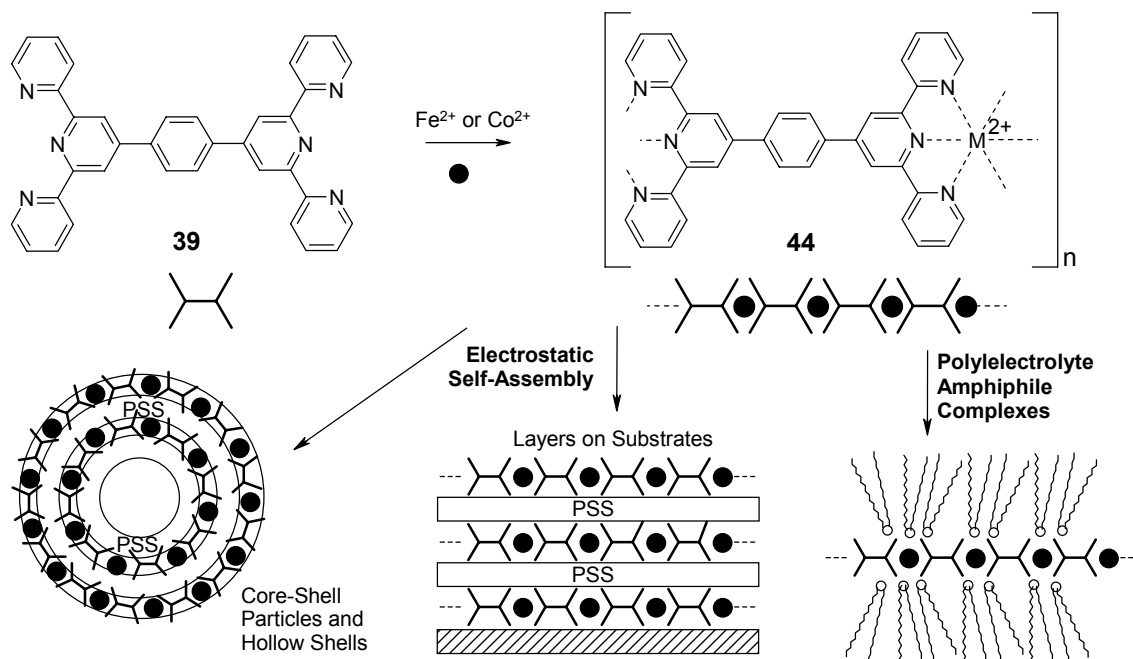
Figure 4. Examples for hierarchical self-assembly of tpy-based coordination polymers by electrostatic self-assembly by Kurth et al.

Terpyridine ligands **45** and **46** bearing flexible oligomeric and polymeric spacers have been reported by the group of Schubert.[65] Depending on the metal ion used for complexation[66] and the nature of the spacer unit more or less polymer-type properties have been observed..
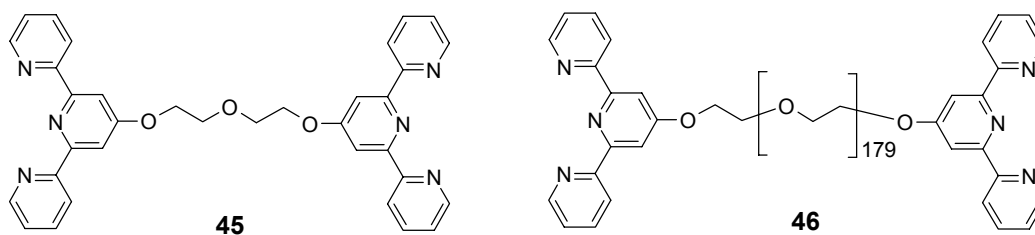
Chart 16. Building blocks applied by Schubert for the construction of supramolecular polymers from oligomeric and polymeric spacers.

A helical tpy-based coordination polymer originating from a chiral binaphthyl-spacered ligand **47** was synthesized by Kimura and coworkers by complexation with Fe^{2+} (chart 17).[67] Depending on the chirality of the applied ligand the polymer exhibits different helicity as proven by CD spectroscopy. Another ditopic and chiral tpy building block was published by Abruña and coworkers[68], who investigated the coordination of the enantiomerically pure ligands **48** with Fe^{2+} by UV-vis and CD spectroscopy, the latter allowing an absolute assignment of the configuration of the helical polymers. Highly ordered domains of the polymer were found by scanning tunneling microscopy (STM) and the electrochemical

properties were investigated using cyclic voltammetry revealing the independence of each Fe(tpy)$_2$ unit.
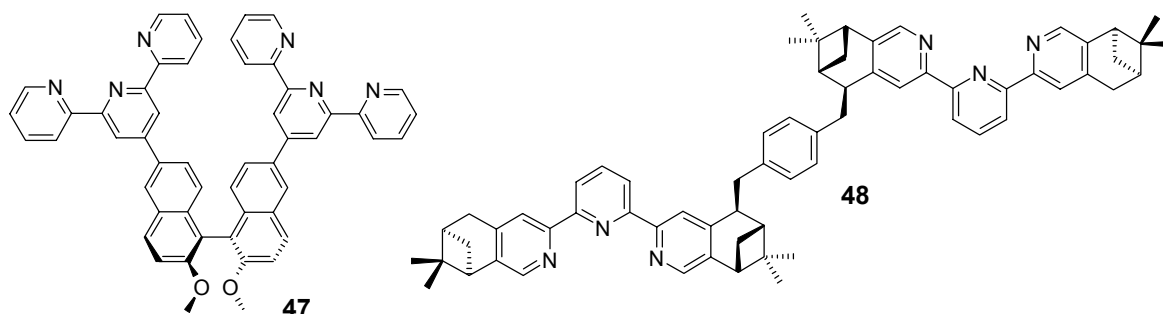
Chart 17. Chiral building blocks for the synthesis of helical Fe^{2+} coordination polymers presented by the groups of Kimura[67] (left) and Abruña[68] (right).

The introduction of electroactive oligo-*p*-phenylenevinylene (OPV) functional units was achieved by the group of Meijer,[69] who showed the formation of a coordination polymer **49** (chart 18) upon addition of Fe^{2+} by UV-vis spectroscopy. A whole set of ditopic electro- and photoactive terpyridine ligands **50a-i** (chart 19) and their coordination polymers were published only recently by Che et al.[70], who studied the polymers by NMR and viscosimetry. The fluorescence properties of the ligand were retained upon complexation of Zn^{2+} (compare also Chapter 3 and 4 of this work). The successful fabrication of organic light emitting diodes from such materials was exemplified for two Zn^{2+}-polymers based on ligands **50a** and **50i**.
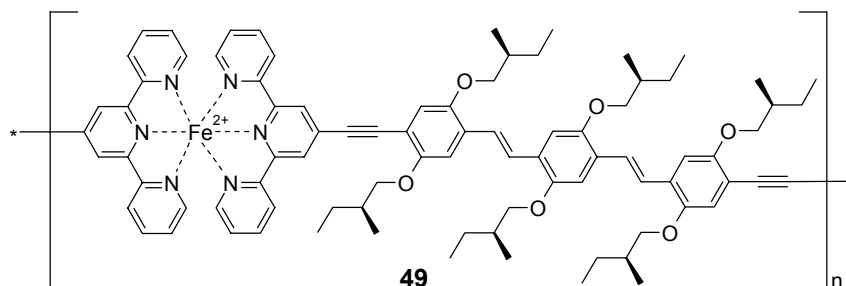
Chart 18. A coordination polymer bearing an OPV spacer published by Meijer et al.[69]
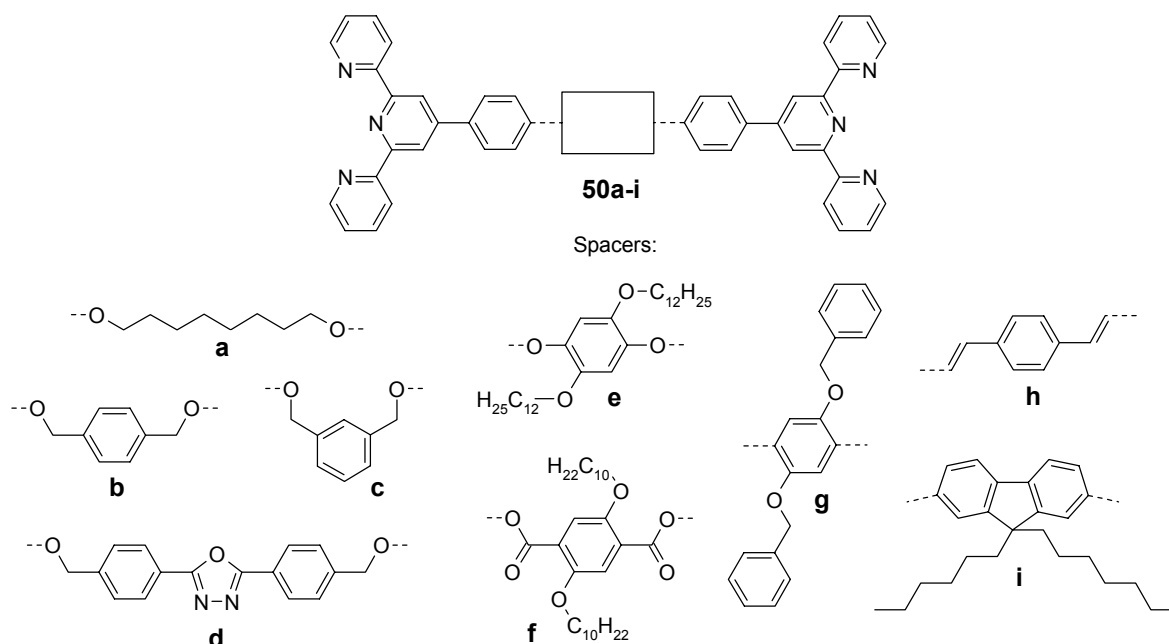
Chart 19. Ditopic terpyridine ligands which were used for the synthesis of Zn^{2+} coordination polymers.

A very innovative approach using the tpy-related ligand 1,6-bis(*1'*-methylbenzimidazolyl)-4-hydroxypyridine was presented by Beck and Rowan[71] for the synthesis of photoactive mechanoresponsive gels. The ditopic unit **51** can form 2:1 metal complexes with transition metal ions, but also forms 3:1 complexes with lanthanide ions (figure 5). The later complexes act as branching points and are responsible for gelation, when applied in a small percentage in a coordination polymer. Since the lanthanide complexes are less stable, the branching points open when the gel is heated or if mechanic stress is exerted by shaking, both causing the gel to liquefy. After cooling or leaving the sample motionless the gel is reformed. The Eu^{3+}-based gels show the characteristic red luminescence of the complexed Eu^{3+} ion, which is sensitized by energy transfer from the ligand to the ion. If the Eu^{3+} complex is opened by heat or mechanical stress, the luminescence color changes to blue which is related to the ligand centered emission.
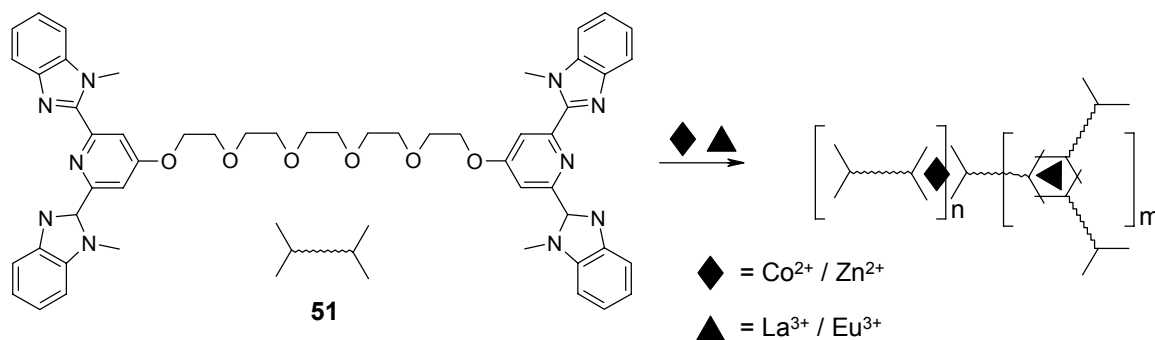
Figure 5. Formation of a supramolecular thermo- and mechanoresponsive gel from a ditopic 1,6-bis(*1'*-methylbenzimidazolyl)-4-hydroxypyridine ligand presented by Beck and Rowan.[71]

Macrocyclic Terpyridine Coordination Compounds. In analogy to the examples of porphyrin macrocycles, which have been obtained by self-assembly by means of sterical constraints, also tpy-based macrocycles could be prepared. A fascinating examples is published by Newkome and coworkers, who prepared hexameric macrocycles **52** of approx. 30 Å in diameter (chart 20, left) using a ditopic terpyridine unit with a *m*-phenylene spacer. The cycles have been synthesized either by stepwise construction of oligomeric building blocks or by classic self-assembly of a 1:1 mixture of metal and ligand.[72]

The isolation and characterization of a [3+3] (**53**) and related [4+4] cycles (chart 20, right) from a highly flexible oligoethylene glycol spacered ligand has been reported by Constable and coworkers. The cycle formation was observed after rearrangement of initially polymeric material upon extended reaction time of four days and could be chromatographically separated from the residual polymeric fraction.[73]
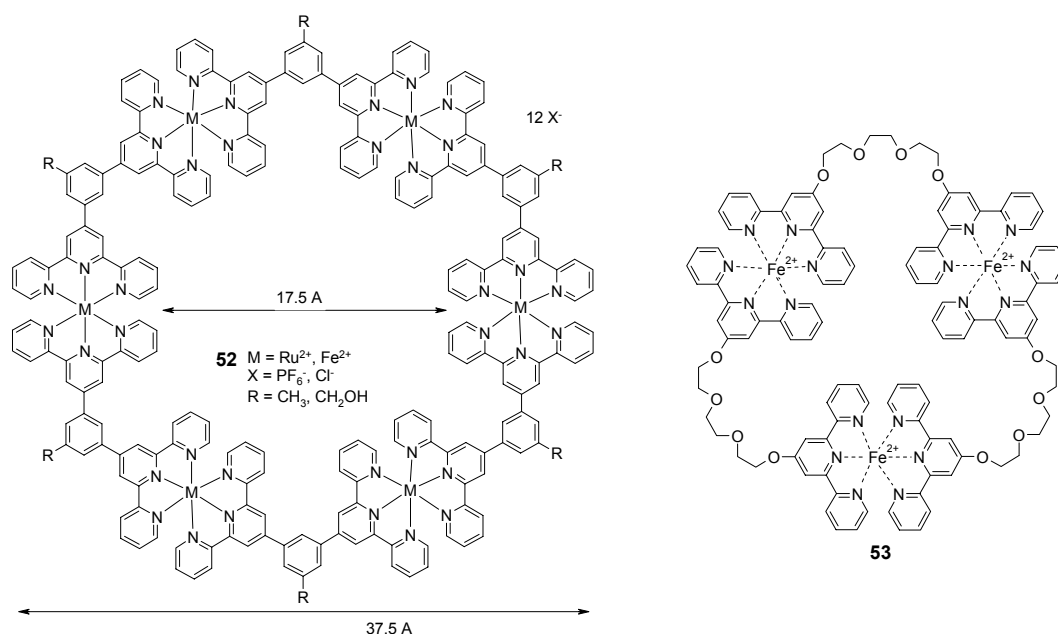
Chart 20. A hexameric macrocycle presented by Newkome et al. (left) and a discrete trimeric iron complex (right) published by Constable et al., both formed in self-assembly processes.

This last example points at two important facettes of metallosupramolecular chemistry which require further exploration in the future. One is the competition between polymer formation and macrocyclization (compare chart 16 and 20), the other the question unter which conditions thermodynamic products are formed and where kinetic products are trapped.

Conclusion

The present introductory chapter gives an overview of the large variety of coordination polymers and their applications in materials science. The relation between binding constant, concentration and degree of polymerization can be used to assess the polymer properties of the system. As shown in this overview, the wide range of metal ions and ligand units presents a means for the construction of polymeric systems with highly varying length, stability and reversibility. The application of some of these structures as functional materials, especially for charge transport, light emitting diodes and mechanoresponsive sensors has been described.

Introduction of luminescent units like perylene bisimide fluorophores into supramolecular polymers therefore seems a promising way to yield luminescent materials that can be organized on a supramolecular level in one, two and three dimensions. The application of this concept is presented in the following chapters of this thesis.

References

(1)   (a) Lehn, J.-M. *Angew. Chem. Int. Ed.* **1988**, *27*, 89; (b) Lehn, J,-M. *Science* **2002**, *295*, 2400-2403.

(2)   The application of supramolecular systems for synthesis, catalysis, and devices is discussed in: Reinhoudt, D. N; Crego-Calama, M. *Science* **2002**, *295*, 2403-2407.

(3)   Ikkala, O.; ten Brinke, G. *Science* **2002**, *295*, 2407-2409.

(4)   Hollingsworth, M. D. *Science* **2002**, *205*, 2410-2413.

(5)   Kato, T. *Science* **2002**, *295*, 2414-2418.

(6)   Whitesides, G. M.; Grzybowski, B. *Science* **2002**, *295*, 2418-2421.

(7)   Elemans, J. A. A. W.; Rowan, A. E.; Nolte, R. J. M. *J. Mater. Chem.* **2003**, *13*, 2661-2670.

(8)   A general review on supramolecular polymers is presented in: Brunsveld, L.; Folmer, B. J. B.; Meijer, E. W.; Sijbesma, R. P. *Chem. Rev.* **2001**, *101*, 4071-4197.

(9)   ten Cate; A. T.; Sijbesma, R. P. *Macromol. Rapid Commun.* **2002**, *23*, 1094-1112.

(10) Yao, S.; Beginn, U.; Gress, T.; Lysetska, M.; Würthner, F. *J. Am. Chem. Soc.* **2004**, *126*, 8336-8348.

(11)   An extensive review on supramolecular metal-ligand systems is presented in: Swiegers, G. F.; Malefetse, T. J. *Chem. Rev.* **2000**, *100*, 3463-3537.

(12)   Janiak, C. *J. Chem. Soc., Dalton Trans.* **2003**, 2781-2804.

(13)   Kitagawa, S.; Kitaura, R.; Noro, S. *Angew. Chem. Int. Ed.* **2004**, *43*, 2334-2375.

(14)   Rehahn, M. *Acta Polymer.* **1998**, *49*, 201-224.

(15)   Also organometallic polymers will not be discussed here. For reviews refer to: (a) Nguyen, P.; Gomez-Elipe, P.; Manners, I. *Chem. Rev.* **1999**, *99*, 1515-1548; and (b) the review of Rehahn.[14]

(16)   Ciferri, A. *Macromol. Rapid. Commun.* **2002**, *23*, 511-529.

(17)   Yount, W. C.; Juwarker, H.; Craig, S. L. *J. Am. Chem. Soc.* **2003**, *125*, 15302-15303.

(18)   The overall binding constant is defined as the product of the individual binding constants K: $\beta_n = K_1 \cdot K_2 \cdot ... \cdot K_n$

(19)   Zielenkiewicz, W.; Lebedeva, N. S.; Antina, E. V.; Vyugin, A. I.; Kaminski, M. *J. Solution Chem.* **1998**, *27*, 879-886.

(20)   Würthner, F. personal communication, determined by ITC.

(21)   Yamasaki, K.; Yasuda, M. *J. Am. Chem. Soc.* **1956**, *78*, 1324.

(22)   Anderegg, G. *Helv. Chim. Acta* **1963**, *315*, 2813-2822.

(23)   Chapter 2 of this thesis.

(24)   Benniston, A. C.; Harriman, A.; Lawrie, D. J.; Mayeux, A.; Rafferty, K.; Russell, O. D. *J. Chem. Soc., Dalton Trans.* **2003**, 4762-4769.

(25)   Goze, C.; Ulrich, G.; Charbonnière, L.; Cesario, M.; Prangé, T.; Ziessel, R. *Chem. Eur. J.* **2003**, *9*, 3748-3755.

(26)   Gemiti, F.; Giancotti, V.; Ripamonti, A. *J. Chem. Soc.* **1968**, 763-768.

(27)   Paquette, L. A.; Tae, J. *J. Am. Chem. Soc.* **2001**, *123*, 4974-4984.

(28)   Dirk, C. W.; Bousseau, M.; Barrett, P. H.; Moraes, F.; Wudl, F.; Heeger, A. J. *Macromolecules* **1986**, *19*, 266-269.

(29)   Wang, F.; Reynolds, J. R. *Macromolecules* **1990**, *23*, 3219-3225.

(30)   Chen, H.; Cronin, J. A.; Archer, R. D. *Macromolecules* **1994**, *27*, 2174-2180; Chen, H.; Archer, R. D. *Macromolecules* **1995**, *28*, 1609-1617; Chen, H.; Cronin, J. A.; Archer, R. D. *Inorg. Chem.* **1995**, *34*, 2306-2315.

(31)   For a review on Schiff-base coordination polymers refer to: Archer, R. D. *Coord. Chem. Rev.* **1993**, *128*, 49-68.

(32) Chen, H.; Archer, R. D. *Macromolecules* **1996**, *29*, 1957-1964.

(33) Byrd, H.; Holloway, C. E.; Pogue, J.; Kircus, S.; Advincula, R. C.; Knoll, W. *Langmuir* **2000**, *16*, 10322-10328.

(34) (a) Suh, J.; Oh, E. *Synthetic Metals* **1990**, *39*, 177-181. (b) Suh, J.; Oh, E.; Kim, H. C. *Synthetic Metals* **1992**, *48*, 325-329.

(35) Suh, J.; Shim, H.; Shin, S. *Langmuir* **1996**, *12*, 2323-2324.

(36) Suh, J.; Moon, S. J. *Bioorg. Med. Chem. Lett.* **1998**, *8*, 2751-2756.

(37) Luo, X.; Wang, X.; Wu, S.; Liang, Y. *J. Colloid Interface Sci.* **2003**, *258*, 432-434.

(38) Yount, W. C.; Juwarker, H,; Craig, S. L. *J. Am. Chem. Soc.* **2003**, *125*, 15302-15303.

(39) Khlobystov, A. N.; Blake, A. J.; Champness, N. R.; Lemenkovskii, D. A.; Majouga, A. G.; Zyk, N. V.; Schröder, M. *Coord. Chem. Rev.* **2001**, *222*, 155-192.

(40) Würthner, F.; Sautter, A.; Thalacker, C. *Angew. Chem. Int. Ed.* **2000**, *39*, 1243-1245.

(41) Liu, M.; Kira. A.; Nakahara, H. *Langmuir* **1997**, *13*, 4807-4809.

(42) Luo, X.; Wang, X.; Wu, S.; Liang, Y. *J. Colloid. Interface. Sci.* **2003**, *258*, 432-434.

(43) Vermonden, T.; van der Gucht, J.; de Waard, P.; Marcelis, A. T. M.; Besseling, N. A. M.; Sudhölter, E. J. R.; Fleer, G. J.; Cohen Stuart, M. A. *Macromolecules* **2003**, *36*, 7035-7044.

(44) For a recent review on porphyrin supramolecules for artificial photosynthesis and molecular photonic/electronic materials refer to: Kobuke, Y.; Ogawa, K. *Bull. Chem. Soc. Jpn.* **2003**, *76*, 689-707.

(45) Fleischer, E. B.; Shachter, A. M. *Inorg. Chem.* **1991**, *30*, 3763-3769.

(46) Michelsen, U.; Hunter, C. A. *Angew. Chem. Int. Ed.* **2000**, *39*, 764-767.

(47) Haycock, R. A.; Hunter, C. A.; James, D. A.; Michelsen, U.; Sutton, L. R. *Org. Lett.* **2000**, *2*, 2435-2438.

(48) Ogawa, K.; Kobuke, Y. *Angew. Chem. Int. Ed.* **2000**, *39*, 4070-4073.

(49) Takahashi, R.; Kobuke, Y. *J. Am. Chem. Soc.* **2003**, *125*, 2372-2373.

(50) Ayabe, M.; Yamashita, K.; Sada, K.; Shinkai, S.; Ikeda, A.; Sakamoto, S.; Yamaguchi, K. *J. Org. Chem.* **2003**, *68*, 1059-1066.

(51) Velten, U.; Lahn, B.; Rehahn, M. *Macromol. Chem. Phys.* **1997**, *198*, 2789-2816.

(52) Phillips-McNaughton, K.; Groves, J. T. *Org. Lett.* **2003**, *5*, 1829-1832.

(53)   (a) Knapp, R.; Schott, A.; Rehahn, M. *Macromolecules* **1996**, 29, 478-480. (b) Kelch, S.; Rehahn, M. *Macromolecules* **1997**, 30, 6185-6193. (c) Kelch, S.; Rehahn, M. *Macromolecules* **1998**, *31*, 4102-4106.

(54)   Chen, J.; MacDonnell, F. M. *Chem. Commun.* **1999**, 2529-2530.

(55)   Cassagneau, T.; Fendler, J. H.; Johnson, S. A.; Mallouk, T. E. *Adv. Mater.* **2000**, *12*, 1363-1366.

(56)   For a recent review on 2,2'-bipyridine and 2,2':6',2''-terpyridine containing polymers refer to: Schubert, U. S.; Eschbaumer, C. *Angew. Chem. Int. Ed.* **2002**, *41*, 2892-2926.

(57)   Constable, E. C. *Macromol. Symp.* **1995**, *98*, 503-524.

(58)   (a) Constable, E. C.; Cargill Thompson, A. M. W. *J. Chem. Soc., Dalton Trans.* **1992**, 3467-3475. (b) E. C. Constable, Cargill Thompson, A. M. W.; Tocher, D. A. *Macromol. Symp.* **1994**, *77*, 219-228.

(59)   Storrier, G. D.; Colbran, S. B.; Craig, D. C. *J. Chem. Soc., Dalton Trans.* **1997**, 3011-3028.

(60)   Ng, W. Y.; Gong, X.; Chan, W. K. *Chem. Mater.* **1999**, *11*, 1165-1170.

(61)   Kelch, S.; Rehahn, M. *Macromolecules* **1999**, *32*, 5818-5828.

(62)   Schütte, M.; Kurth, D. G.; Linford, M. R.; Cölfen, H.; Möhwald, H. *Angew. Chem. Int. Ed.* **1998**, *37*, 2891-2893.

(63)   Caruso, F.; Schüler, C.; Kurth, D. G. *Chem. Mater.* **1999**, *11*, 3394-3399.

(64)   Kurth, D. G.; Lehmann, P.; Schütte, M. *PNAS* **2000**, *97*, 5704-5707.

(65)   (a) Schmatloch, S.; González, M.; Schubert, U. S. *Macromol. Rapid Commun.* **2002**, *23*, 957-961. (b) Schmatloch, S.; van den Berg, A.; Alexeev, A. S.; Hofmeier, H.; Schubert, U. S. *Macromolecules* **2003**, *36*, 9943-9949. (c) Hofmeier, H.; Schmatloch, S.; Wouters, D.; Schubert, U. S. *Macromol. Chem. Phys.* **2003**, *204*, 2197-2203.

(66)   Schmatloch, S.; Schubert, U. S. *Macromol. Symp.* **2003**, *199*, 483-497.

(67)   Kimura, M.; Sano, M.; Muto, T.; Hanabusa, K.; Shirai, H. *Macromolecules* **1999**, *32*, 7951-7953.

(68)   Bernhard, S.; Takada, K.; Díaz, D. J.; Abruña, H. D.; Mürner, H. *J. Am. Chem. Soc.* **2001**, *123*, 10265-10271.

(69)   El-Ghayoury, A.; Schenning, A. P. H. J.; Meijer, E. W. *J. Polym. Sci. A: Polym. Chem.* **2002**, *40*, 4020-4023.

(70)   Yu, S.-C.; Kwok, C.-C.; Chan, W.-K.; Che, C.-M. *Adv. Mater.* **2003**, *15*, 1643-1647.

(71)   Beck, J. B.; Rowan, S. J. *J. Am. Chem. Soc.* **2003**, *125*, 13922-13923.

(72)   (a) Newkome, G. R.; Cho, T. J.; Moorefield, C. N.; Baker, G. R.; Cush, R.; Russo, P. S. *Angew. Chem. Int. Ed.* **1999**, *38*, 3717-2721. (b) Newkome, G. R.; Cho, T. J.; Moorefield, C. N.; Cush, R.; Russo, P. S.; Godínez, L. A.; Saunders, M. J.; Mohapatra, P. C*hem. Eur. J.* **2002**, 8, 2946-2954.

(73)   Constable, E. C.; Housecroft, C. E.; Smith, C.B. *Inorg. Chem. Commun.* **2003**, *6*, 1011-1013.

2

Thermodynamics of 2,2':6',2''-Terpyridine - Metal Ion Complexation

Abstract: The complexation of 2,2':6',2''-terpyridine, which is an important building block in metallosupramolecular chemistry, has been studied by titration experiments with the perchlorate hexahydrate salts of Fe^{2+}, Co^{2+}, Ni^{2+}, Cu^{2+} and Zn^{2+} in acetonitrile solution applying UV-vis and NMR spectroscopy and isothermal titration calorimetry (ITC). UV-vis titrations show characteristic spectral changes for the formation of the $M(tpy)_2^{2+}$ complexes at a metal/ligand ratio of 1:2, and only for the Cu^{2+} system a further processes can be observed when the Cu^{2+}/tpy ratio exceeds 1:2, which indicates reversible complexation equilibria. ^{1}H NMR experiments revealed that also the Zn^{2+}-tpy bonding is reversible and $Zn(tpy)^{2+}$ species are formed at Zn^{2+} excess. ITC experiments were performed in both titration directions and gave *ΔH* values between -14.5 and -22.2 kcal/mol for the complexation of the metal ions to tpy together with estimates for the lower limit of the binding constants, which are in the range of 10^8 and higher. Again, the Cu^{2+}/tpy system behaves unusual, supporting the view that one tpy unit only acts as a bidentate ligand in the $Cu(tpy)_2^{2+}$ complex. The results of the complexation experiments present fundamental information for the proper choice of metal ion and solvent in metallosupramolecular polymerization of terpyridine-substituted perylene bisimides, which is presented in the following chapters.

Introduction

Terpyridine complexes in supramolecular chemistry. With the evolution of supramolecular chemistry[1,2] and the use of metal complexes for the construction of noncovalently bound architectures,[3,4] the 2,2':6,'2''-terpyridine (tpy) ligand became an often used receptor unit for metal-ligand mediated self-assembly due to its easy availability and its predictable complexation behavior. Terpyridine derivatives with residues in the 4'-position are of special importance as they allow the arrangement of two units in an exactly collinear fashion.

In the last decade an increasing number of examples for supramolecular structures based on the tpy ligand have been published combined with an increase in complexity and functionality of the systems. An impressing example of the potential lying in metal-terpyridine self-assembly was introduced by Newkome and coworkers,[5] who published the self-assembled construction of cyclic hexamers built from six $M(tpy)_2^{2+}$ units, utilizing Fe^{2+} and Ru^{2+} as central ions. A number of groups are working on the construction of coordination polymers based on the tpy ligand, a field which was pioneered by the work of Constable,[6] and extensively studied by several groups.[7] Further classes of supramolecular systems constructed by tpy-metal complexes are dendrimers,[8] grid-like structures[9] and helicates.[10] Due to their luminescence properties, especially the Ru^{2+} and Os^{2+} complexes of terpyridine have been widely used to construct functional supramolecular systems, for example molecular rods with tpy complexes as energy donor and/or acceptor units. Extensive research has been done in this field by the groups of Sauvage, Balzani, and Ziessel.[11] Various ruthenium-terpyridine compounds have been studied for application as photoactive dyes in dye sensitized solar cells.[12] Furthermore, terpyridine is used as a receptor unit in fluorescence sensors for the recognition of metal ions[13,14] and amino acids.[15,16] Recently even more elaborate supramolecular systems, so-called molecular muscles, based on catenanes and rotaxanes have been introduced.[17] The systems take advantage of the different stability of tpy and phenanthroline complexes with metals in different oxidation states.

Ligand and Complex Structure. Terpyridine is typically depicted in the *cis*/*cis* conformation with regard to the dihedral angle of the N-C-C-N bonds in order to emphasize its ability to act as a chelate ligand (figure 1). However, it has to be kept in mind that the solid state conformation of the uncomplexed and unprotonated form is *trans*/*trans*, which is explained by the steric repulsion of the *ortho*-hydrogen atoms (3/3' and 5'/3'') in combination with an electrostatic repulsion of the three nitrogen lone pairs. The steric effect can be seen in

the space-filling model in figure 1. Theoretical calculations[18] of different conformations also gave support for the *trans*/*trans* conformation as the energetically favored one, and showed that the *cis*/*cis* conformation should be twisted with a dihedral angle of ca. 48°. The conformation of tpy in solution follows the same trend but is dependent on the hydrogen-bonding properties of the solvent. In acidic media, stabilization of the *cis*/*cis* conformation can be achieved by protonation of one pyridine unit, which leads to a favorable hydrogen-bonding between the proton and the lone pairs of the remaining free nitrogen atoms. The lowest energy structure is one with the central nitrogen protonated and the lateral pyridine units forming hydrogen bonds, which leads to the *cis*/*cis* conformation being energetically favored.
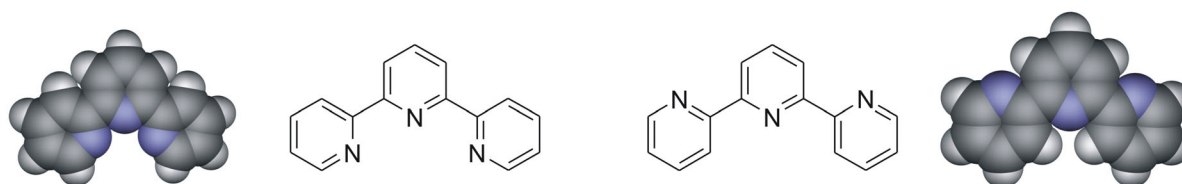
Figure 1. Scheme and molecular model[19] of the tpy ligand in the *cis*/*cis* (left) and the *trans*/*trans* (right) conformation. Note the proximity of the 3/3' and 5/5' hydrogen atoms in the space-filled model of the *cis*/*cis* conformation (left).

In the decades after its discovery, tpy complexes with a large number of metal ions were studied. Crystal structures revealed that there are two predominant complex types to be found, depending on the metal ion and on the stoichiometry applied in the crystallization process: a 2:1 complex showing a slightly distorted octahedral coordination with the two tpy units arranged perpendicular to each other, and a 1:1 complex with the metal ion coordinated in a distorted trigonal pyramidal way, the tpy coordinating the axial sites and one site in the trigonal plane, and the counterions situated in the two residual planar positions. Figure 2 shows both the 1:1 and 2:1 complex. The distortion of the complex from its ideal structure can be seen clearly by the deviation of the axial N-M-N bond from an ideal 180° angle.
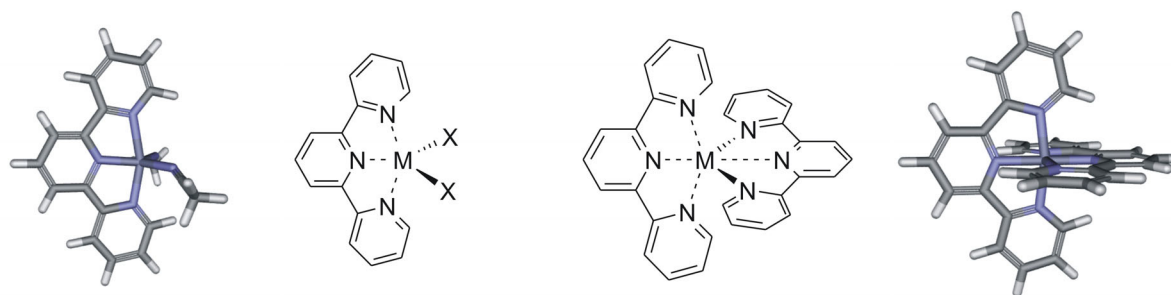
Figure 2. Schemes and molecular models of 1:1 (left) and 2:1 (right) tpy complexes. The 1:1 complex is modeled with two acetonitrile molecules, X represents any counterion or coordinating solvent molecule.

To characterize the coordination of some frequently used first row transition metals to terpyridine in a nonaqeous solvent, especially with regard to its application for the synthesis of supramolecular structures under proper thermodynamic control, a series of titration experiments has been conducted applying UV-vis and NMR spectroscopy and isothermal titration calorimetry (ITC). In the following the results will be reported.

UV-vis Titration Studies

UV-vis titrations have been performed to study the complexation of terpyridine with the metals of the first transition metal row from iron(II) to zinc(II). All metals ions were applied as the metal perchlorate hexahydrate salts, since they offer some advantages: the salts are all commercially available and have already been used in the construction of supramolecular systems. Due to their hydrated form they are not hygroscopic, which facilitates the precise preparation of stock solutions, and all salts are readily soluble in acetonitrile, as is the ligand itself. Acetonitrile was chosen since it acts as a competitive ligand for the complexation which should lead to a decreased binding constant and additionally facilitate ligand exchange. Furthermore, it is not protic, which eliminates any effects due to protonation or hydrogen bonding to the pyridine units.

The UV-vis spectrum of terpyridine in acetonitrile shows a broad, unstructured band at 235 nm and a second, broad band with a maximum at 280 nm and two shoulders at 300 nm and 310 nm (Figure 3, solid line). Both bands are attributed to π-π* transitions and the broadness of the bands and the absence of vibronic finestructure indicates the population of various conformatios.[20] Apart from some special features, which will be discussed for each metal ion in the following paragraph, all metal ions used in this series cause similar changes in the tpy spectrum which are closely related to those caused by protonation of tpy. Figure 3 shows the UV-vis spectrum of tpy in acetonitrile solution before (solid line) and after (dashed line) addition of trifluoroacetic acid. Both absorption bands sharpen considerably pointing at a more coplanaer chromophore. In addition, a new band is coming up between 300-350 nm. The latter process is characteristic for the conformational change in the tpy from the *trans*/*trans* conformation in solution to the perfectly planarized *cis*/*cis* conformation in the complex. In the protonated species, the *cis*/*cis* conformation is stabilized by hydrogen bonds from the lateral pyridine units to the proton.
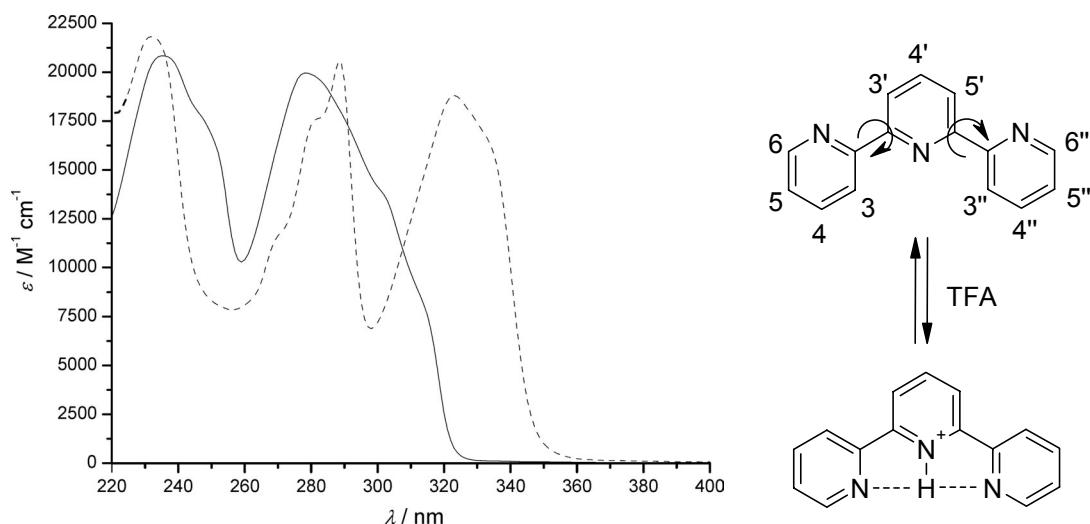
Figure 3. Left: Spectra of tpy in acetonitrile (0.5 mM, solid line) and same solution after addition of one equivalent of trifluoroacetic acid (dashed line) yielding the protonated tpy ligand; Right: Structure and numbering scheme of the 2,2':6',2''-terpyridine ligands and its protonated form.

Figure 4 shows the UV-vis titrations of terpyridine with the perchlorate hexahydrate salts of iron(II), cobalt(II), nickel(II) and zinc(II). The characteristic feature of the $Fe(tpy)_2^{2+}$ complex (figure 4A) is the quite intense ($\varepsilon = 6000$ M^{-1} cm^{-1}) metal-ligand charge transfer (MLCT) band with a maximum at 550 nm, which is responsible for its deep violet, permanganate-like color. The $Co(tpy)_2^{2+}$ complex (figure 4B) also shows absorbance in the visible wavelength region but only with a small extinction coefficient of approx. 700 $M^{-1}cm^{-1}$. A very weak absorption band can also be observed for $Ni(tpy)_2^{2+}$ (figure 4C) at approx. 550 nm and 725 nm ($\varepsilon \approx 200$ $M^{-1}cm^{-1}$). The respective zinc(II) complex with the closed shell (d^{10}, figure 4D) shows no absorption at all at wavelengths > 350 nm, confirms the absence of charge transfer transitions arising from metal-ligand coordination. The titration curves were evaluated for characteristic bands, show that all spectral changes occur at metal/ligand ratios below 0.5 indicating the formation of the $M(tpy)_2^{2+}$ complex. The straight slope and its abrupt saturation at a ratio of 0.5 indicate a high binding constant which can not be determined from this set of data. All titrations show very clear isosbestic points suggesting that only two species, which are the uncomplexed tpy and the metal-complexed tpy are present during the titration process. $M(tpy)^{2+}$ and $M(tpy)_2^{2+}$ cannot be distinguished but based on the saturation at a ratio of 0.5 it can be concluded that all added metal ions are directly converted to $M(tpy)_2^{2+}$ up to a ration of 0.5.

The absence of spectral change at higher metal/ligand ratios does not necessarily mean that there is no further change in the system. As it has been mentioned, the most significant change in the UV-vis absorption spectrum of terpyridine is due to the *cis*/*trans* conformation in the tpy and concomitant formation of a planar chromophore, which is identical in the 1:1

and the 2:1 complex. Therefore, UV-vis spectroscopy is not suited to examine the reversibility of tpy complexes and to reveal the composition of the system at ratios > 0.5.
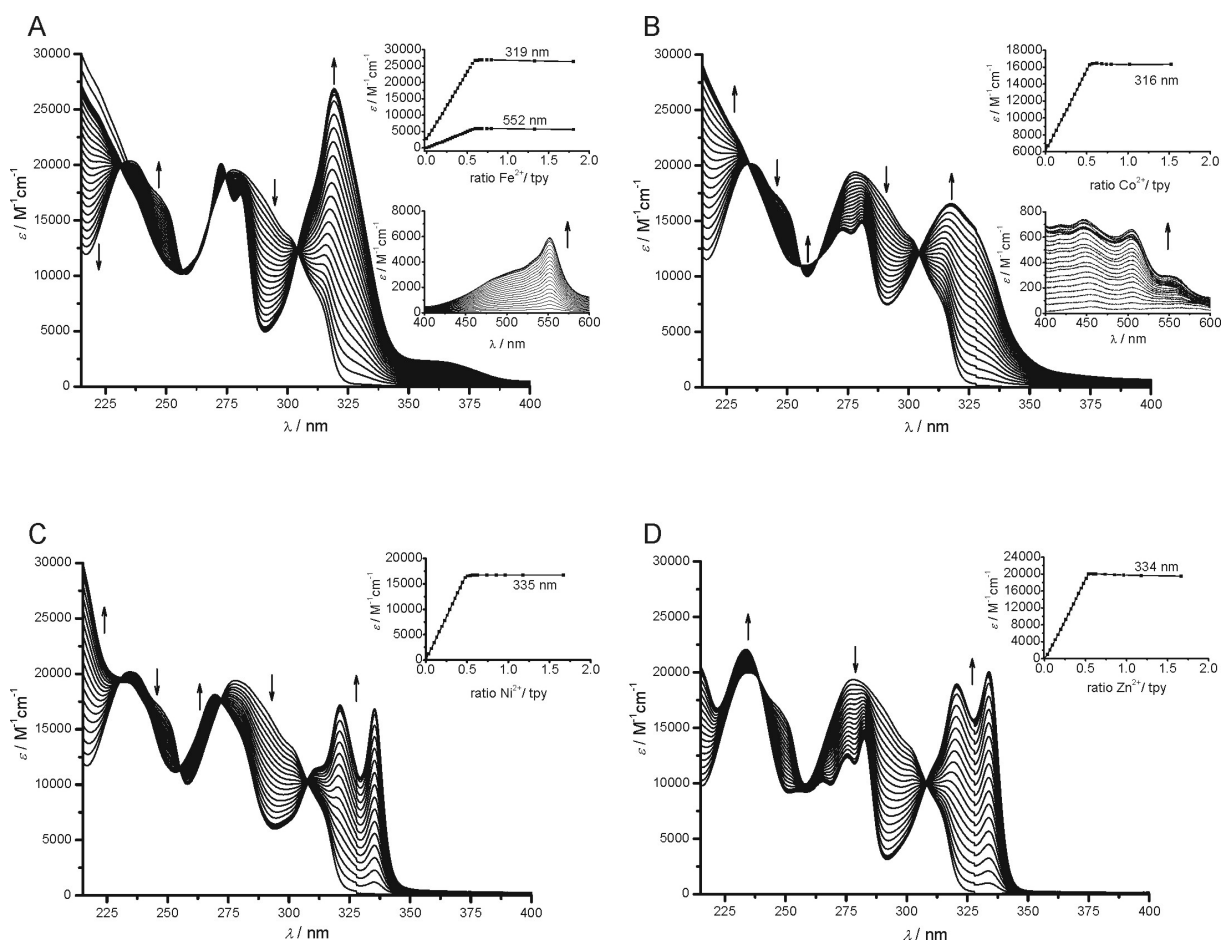
Figure 4. Constant-host titrations of tpy (0.05 mM in acetonitrile) with the metal perchlorate hexahydrate salts (0.5 mM in tpy solution) of iron(II) (A), cobalt(II) (B), nickel(II) (C), and zinc(II) (D). Insets show titration curves at significant wavelengths.

The titration of terpyridine with copper(II) is the only example in this series where a significant spectral change can be observed also in the range of metal/ligand ratio between 0.5 and 1. Figure 5 (left) shows the titration up to a molar ratio of 0.5 with the same features as mentioned previously for Fe^{2+}, Co^{2+}, Ni^{2+} and Zn^{2+}. In contrast, a sharp change is observed when the ratio of 0.5 is exceeded, characterized by the increasing intensity of three sharp bands between 260 nm and 280 nm and the shift of the long-wavelength band by ca. 10 nm combined with a splitting into two separate maxima. This second process stops immediately when 1:1 stoichiometry is reached indicating the smooth formation of a 1:1 complex. The fact that the spectrum of the $Cu(tpy)_2^{2+}$ and the $Cu(tpy)^{2+}$ species are not identical suggests two different terpyridine coordination modes in the two species. This hypothesis is supported by the results of ITC titrations and a model will be discussed in the respective paragraph.
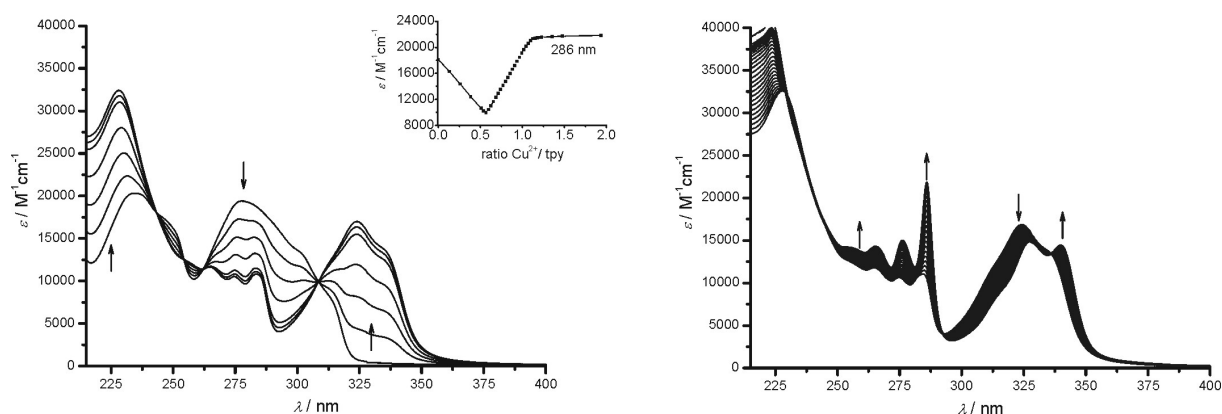
Figure 5. Constant-host titration of tpy (0.05 mM in acetonitrile) with copper(II) perchlorate hexahydrate (0.5 mM) up to a metal/ligand ratio of 0.5 (left) and at higher ratios (right). Inset shows the titration curve at 286 nm.

^{1}H NMR Titrations of tpy with Iron(II) and Zinc(II) Salts.

To assess the reversibility of terpyridine-metal complex formation, ^{1}H NMR titrations of terpyridine have been performed with iron(II) and zinc(II) perchlorate. Only these two metals afford diamagnetic complexes and therefore allow the straightforward measurement of ^{1}H NMR spectra, whereas the respective cobalt(II), nickel(II) and copper(II) complexes are paramagnetic high-spin complexes and therefore not suitable for standard NMR spectroscopy.[21] ^{1}H NMR proved to be an ideal method for the investigation of reversibility in the $Zn(tpy)_2^{2+}$ complex as all species present during a titration can be identified by their characteristic changes of the chemical shifts. This is possible because ligand exchange processes are slow on the NMR timescale.

Figure 6 shows the NMR spectra at different metal/ligand ratios, whereas figure 7 gives a titration curve presenting the amount of the three species against the Zn^{2+}/tpy ratio. The signals of the protons H6 (*) and H3' (#) are highlighted, since they are sensitive to the coordination mode of the tpy complex. H6, which is positioned next to the nitrogen atom of the lateral pyridine ring, is of particular importance, since its chemical shift exhibits a drastic change when the complex species is changed from the uncomplexed species to the 2:1 and subsequently to the 1:1 species. In the 2:1 complex H6 is positioned directly above of the central pyridine unit of the second tpy and experiences shielding by the aromatic ring current. Therefore the signal is shifted to high field by approximately 1 ppm. Consequently, the absence of a second tpy unit in the 1:1 complex leads to a downfield shift. A significant change is also observed for the signal of H3', which is shifted downfield upon the complexation. This signal shift is even more characteristic in 4'-substituted terpyridine derivatives where it appears as a sharp singlet whose change can easily be monitored.[22] H5 (δ = 7.4 ppm), which does not undergo a significant change upon complexation from the free

ligand to the 2:1 complex, is shifted by +0.51 ppm upon transition from the 2:1 to the 1:1 complex and can therefore also be used as a probe for the complexation state of the tpy unit. The chemical shifts of all tpy proton signals and their changes by transformation from the free tpy ligand to the 2:1 and subsequently to the 1:1 complex are summarized in tables 2 and 3.
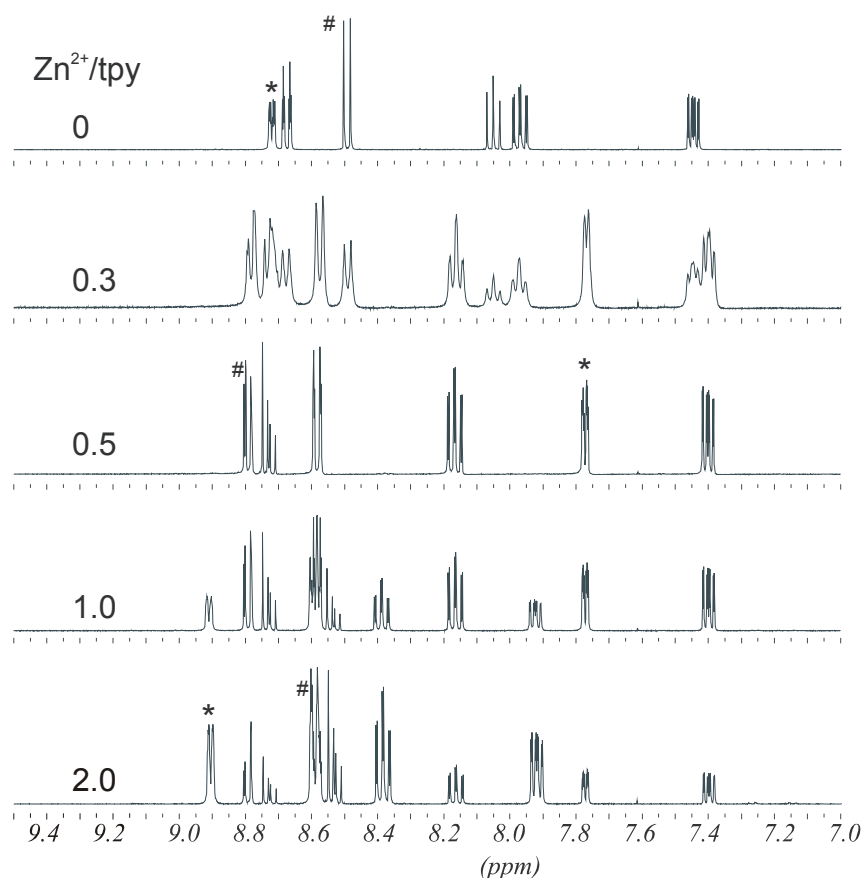
Figure 6. ^{1}H NMR titration of tpy (31 mM in *D3*-acetonitrile) with zinc perchlorate hexahydrate (62 mM in *D3*-acetonitrile). The change of the signals attributed to H6 (*) and H3' (#) are marked.
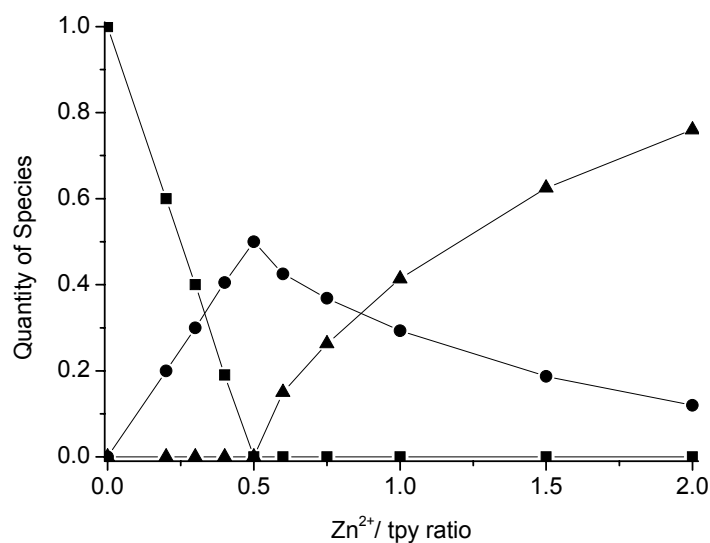
Figure 7. Different species during the NMR titration experiment with tpy and $Zn(ClO_4)_2 \cdot 6H_2O$ in *D3*-acetonitrile as shown in figure 6 (31 mM tpy; tpy = squares, $Zn(tpy)_2^{2+}$ = circles, $Zn(tpy)^{2+}$ = triangles).

The spectra in figure 6 and the corresponding titration curve in figure 7 show that at a Zn^{2+}:tpy ratio >0.5 an equilibrium between 2:1 and 1:1 complex is present. At a metal/ligand ratio of 2, still 25 % of the tpy units are bound in a 2:1 complex. This equilibrium is found to be dependent on the nature of the counterion and the solvent. For an identical titration applying zinc trifluoromethane sulfonate (triflate, OTf), the percentage of 2:1 complex present at a molar ratio of 2 was only 10 % compared to 25 % in the case of the perchlorate complex. Che and coworkers[23] could not observe reversibility for zinc terpyridine complexes when applying zinc acetate and zinc chloride in related ^{1}H NMR titrations in *D6*-dmso, but observed reversible complexation when zinc nitrate hexahydrate was applied. In conclusion, the complexation behavior of tpy with Zn^{2+} is strongly dependent on the interplay between the metal-tpy interaction, the coordination ability of the counter ion and the nature of the solvent, which can act as a competitive ligand or, if alcohols are applied, can interact with the counterions and tpy ligands as hydrogen bond donors.
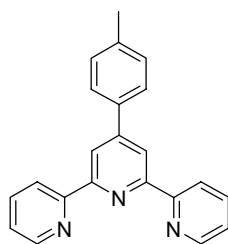
Chart 1.

Table 1. Chemical shift δ (d3-acetonitrile) of the protons in tpy and its zinc(II) complexes.

δ / ppm[a]	H3	H4	H5	H6	H3'	H4'
tpy	8.67	7.97	7.44	8.71	8.49	8.05
$Zn(tpy)_2^{2+}$	8.58	8.16	7.40	7.77	8.78	8.72
$Zn(tpy)^{2+}$	8.58	8.38	7.91	8.91	8.58	8.53

a) all chemical shifts centered and calibrated on the acetonitrile signal (1.96 ppm).

Table 1. Changes of the chemical shift δ (*d3*-acetonitrile) upon transition from tpy to $Zn(tpy)_2^{2+}$ and from $Zn(tpy)_2^{2+}$ to $Zn(tpy)^{2+}$.[a]

$\Delta\delta$ / ppm	H3	H4	H5	H6	H3'	H4'
tpy → $Zn(tpy)_2^{2+}$	-0.09	+0.19	-0.03	**-0.94**	+0.29	+0.67
$Zn(tpy)_2^{2+}$ → $Zn(tpy)^{2+}$	± 0	+0.22	**+0.51**	**+1.14**	-0.20	-0.19

a) all chemical shifts centered and calibrated on the acetonitrile signal (1.96 ppm).

The spectra in figure 6 can also give qualitative information on the exchange dynamics during the titration. The signal broadening at a metal/ligand ratio of 0.3 is an indication that exchange between the three species is present with a rate reaching NMR timescale, which is in the millisecond range. During the whole titration all compounds remained homogeneously dissolved so that aggregation or precipitation can be ruled out as a reason for the observed

line broadening. At a ratio of 1, where both 2:1 and 1:1 complexes are present in solution, the signals remain sharp indicating an exchange kinetics which is significantly slower than the NMR timescale. Exchange experiments with 4'-(*p*-methylphenyl)-2,2':6',2''-terpyridine (chart 1) reveal that after this competitive ligand is added to a $Zn(tpy)_2^{2+}$ complex, equilibration takes place within the timescale between addition and the recording of the NMR spectrum and no further change can be found afterwards.

The complexation of iron(II) perchlorate hexahydrate has been studied by ^{1}H NMR titration experiments as well. In clear contrast to the zinc(II) titrations, no formation of $Fe(tpy)^{2+}$ was observed even at high excess of Fe^{2+} and the $Fe(tpy)_2^{2+}$ complex remained the exclusively formed species. In a mixture of $Fe(tpy)_2^{2+}$ and one equivalent of *p*-methylphenylterpyridine, a detectable amount of a mixed ligand species could only be observed after one day at room temperature in *d3*-acetonitrile solution. The amount could be determined to 26 % after two weeks, pointing at a slow exchange kinetics.

The very slow reversibility in the case of iron(II) complex and the comparably fast reversibility for the zinc complex is in agreement with kinetic data determined by Hogg and Wilkins,[24] which investigated the exchange rate for several tpy complexes in aqueous solution with tpy excess. The half-life $t_½$ of the $M(tpy)_2^{2+}$ species was determined as 8400 min for Fe^{2+}, 610 min for Ni^{2+} and 50 min for Co^{2+}, whereas values < 0.1 min were determined for Cu^{2+} and Zn^{2+}. Accordingly $Zn(tpy)_2^{2+}$ complexes are kinetically the most labile species and therefore mist useful for reversible supramolecular polymerization.

Isothermal Titration Calorimetry (ITC)

Introduction. Isothermal titration calorimetry[25,26,27] is a method which can provide full thermodynamic characterization of a binding event (ΔH^0, ΔG^0, ΔS^0 and stoichiometry). The measurement is based on the electric compensation of the heat which is released or taken up by the system as a result of a binding process induced by the titration of a guest molecule into a solution of host molecules. Figure 8 shows a schematic representation of the instrumental setup. The host solution is filled into a coin-shaped cell which is positioned in an adiabatic housing together with the reference cell which only contains the solvent or buffer applied in the experiment. Both cells are brought to a constant identical temperature or are subjected to an identical temperature gradient, both of which are monitored electronically. During the titration, an automatic computer controlled step motor adds defined amounts of the guest solution into the sample cell through a stirred μl-syringe. The resulting binding event effects a temperature difference between the sample cell and the reference cell, which is compensated by electrical heating or cooling. The electrical current needed for the readjustment of the temperature equilibrium is proportional to the heat taken up or released by the binding event.
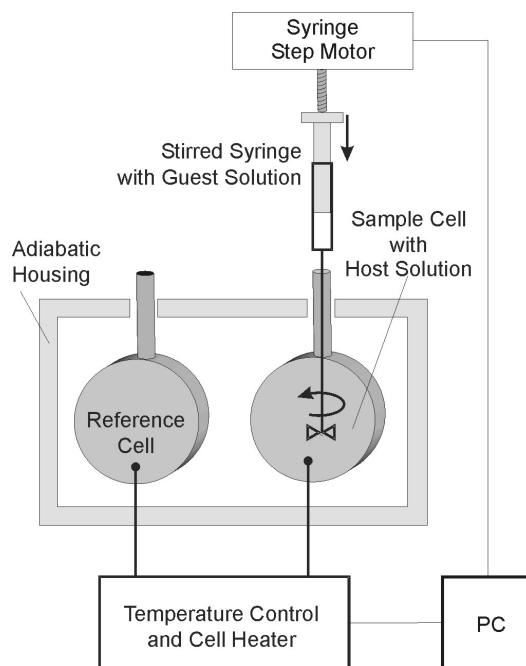
Figure 8. Schematic representation of a isothermal titration calorimeter system.

In the ideal case no reaction heat will be monitored after all host molecules are complexed and the integration over all peaks gives the binding enthalpy ΔH^0. The binding constant and the stoichiometry can be obtained from the titration curve by nonlinear curve fitting. If enthalpy *ΔH* and binding constant *K* can both be determined with good precision, a full

thermodynamic characterization of the binding event including values for the Gibbs free energy ΔG and the entropy S is possible by employing the equations:

$$\Delta G^0 = -R\,T\ln(K) = \Delta H^0 - T\,\Delta S^0$$

A characteristic output of an ITC experiment can be found in figure 9. The upper section represents the raw data as supplied by the instrument and shows the progression of the experiment in time. The peaks correspond to the individual aliquots of added guest solution and the current applied for the compensation of the reaction heat is plotted in energy units against time. The lower part shows the titration curve, resulting from the integration of the individual peaks and plotted as ΔH^0 in kcal/mol against the guest/host ratio. From this curve the stoichiometry and the binding constant can be determined by nonlinear curve fit.
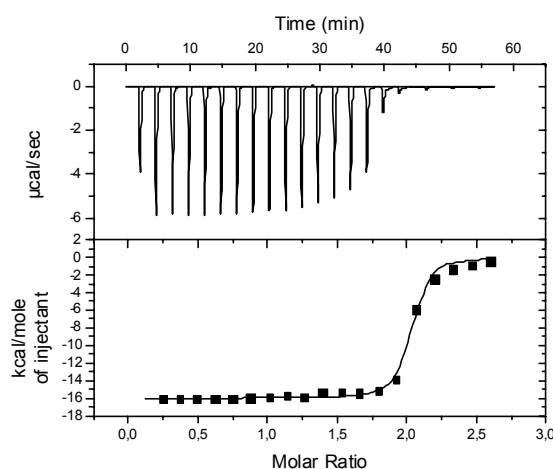
Figure 9. Characteristic output of an ITC titration showing the raw data in the upper section, plotted against the time of the experiment, and the enthalpy in the lower section, both plotted against the molar ratio of guest/host.

Titration experiments with tpy. To further investigate the binding process of tpy, ITC titrations were performed with the same series of metal ions, which have been already characterized by UV-vis spectroscopy. Again, all experiments were performed with the perchlorate hexahydrate salts in acetonitrile solution to ensure comparability. The interesting advantage of ITC titrations is that the titration direction is not restricted to the addition of metal ions to a tpy solution. The latter is the case for ^{1}H NMR and UV-vis spectroscopy, as the metal ions do not show NMR signals or UV-vis absorption, which could be monitored during the titration. In contrast, ITC is only sensitive to the heat of reaction, independent on which compound is present in the cell and which is added in aliquots through the syringe.

ITC results for the zinc/tpy system in acetonitrile are presented in figure 10. The addition of tpy to a zinc perchlorate solution (figure 10A) yields a constant reaction heat of -14.5 kcal/mol up to a molar ratio of 2. This stoichiometry is anticipated for the formation of a 2:1 complex. The fact that no difference in ΔH^0 can be detected between the areas from 0 to 1

and from 1 to 2 allows two interpretations: either only 2:1 complexes are formed and no 1:1 species are present in considerable amounts throughout both experiments, or the enthalpy detected for the complexation is identical independent if tpy is attached to a free Zn^{2+} or to an already formed 1:1 complex. ^{1}H NMR titrations indicate an equilibrium between 2:1 and 1:1 species. If this information is considered, ΔH^0 of -14.5 kcal/mol represents the enthalpy ofor the first and the second process as well.
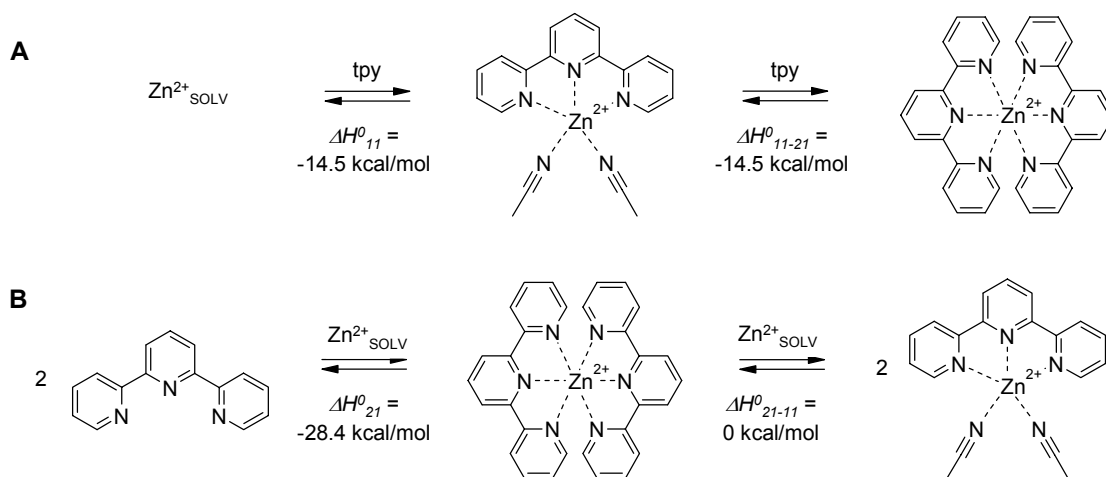
Scheme 1. Proposed thermodynamic scheme for the titration of zinc perchlorate with tpy in acetonitrile and the corresponding ΔH values determined by ITC for addition of tpy to the Zn^{2+} solution (A) and vice versa (B).

Figure 10B shows the inverted situation, with Zn^{2+} being added to a tpy solution. As expected based on our UV-vis studies, the endpoint of the titration is reached at a molar ratio of Zn^{2+}/tpy = 0.5. In this case, the resulting ΔH^0 gives the sum of the values for the first and the second binding event. A ΔH^0 of -28.4 kcal/mol corresponds to two tpy-Zn^{2+} coordination events of -14.2 kcal/mol in good accordance with the former results. As the identical titration was also done by ^{1}H NMR, it is known that after the ratio of 0.5 is exceeded, the $Zn(tpy)_2^{2+}$ complex is opened to form the 1:1 species. ITC results indicate that this process is not connected with any calorimetric signal. Therefore, the only process yielding a detectable enthalpy change is the terpyridine complexation, independent if this process takes place with a free Zn^{2+} ion or a monocomplexed $Zn(tpy)^{2+}$ species. From these results the absence of a special thermodynamic stabilization of the octahedral $Zn(tpy)_2^{2+}$ complex can be concluded.

Figure 10. Left: ITC titration curves for the addition of tpy (10 mM) to a Zn^{2+} solution (0.5 mM). Right: Reversed titration of Zn^{2+} (5 mM) into a tpy solution (0.5 mM).

The titrations with iron(II), cobalt(II) and nickel(II) perchlorates give similar curves which only differ in the absolute values for ΔH^0 (cf. appendix on page 51 for figures). In all titrations, the first and the second binding event can not be distinguished. As the concentration of the solutions was optimized for an acceptable signal/noise ratio and therefore had to be kept in the order of 0.5 mM, it is not possible to determine the exact binding constants for the systems under investigation. Comparison with the UV-vis titrations (figure 4), which have been performed with tenfold dilute solutions, show that also in this concentration range the binding strength is too high to determine K precisely. Curve-fitting tests with different binding constants could be used to estimate a lower limit for the binding constant, which is in the order of $> 10^8$ M^{-1}. Tables 3 and 4 summarize the resulting enthalpies and binding constant estimates for all metal ions studied.

Table 3. Summary of the ITC results for the titration of tpy to the metal perchlorate hexahydrate solutions in acetonitrile. The indices of the ΔH^0 values refer to the previous schemes.[a]

	$M^{2+} + tpy \rightarrow M(tpy)^{2+}$			$M(tpy)^{2+} + tpy \rightarrow M(tpy)_2^{2+}$		
	ΔH^0_{11}		K_{11}	ΔH^0_{11-21}		K_{11-21}
	[kcal/mol]	[kJ/mol]	$[M^{-1}]$	[kcal/mol]	[kJ/mol]	$[M^{-1}]$
Fe^{2+}	-19.1	-79.9	$>10^8$	-19.1	-79.9	$>10^8$
Co^{2+}	-14.7	-61.5	$>10^8$	-14.7	-61.5	$>10^8$
Ni^{2+}	-16.0	-66.9	$>10^8$	-16.0	-66.9	$>10^8$
Cu^{2+}	-22.2	-92.2	$>10^8$	**-13.0**	**-54.4**	**$\approx 10^8$**
Zn^{2+}	-14.5	-60.7	$>10^8$	-14.5	-60.7	$>10^8$

[a] Errors for ΔH^0 values are ±0.5 kcal/mol.

Table 4. Summary of the ITC results for the titration of metal perchlorate hexahydrates to a tpy solution in acetonitrile. The indices of the ΔH^0 values refer to the previous schemes.[a]

	2 tpy + M^{2+} → M(tpy)$_2$$^{2+}$			M(tpy)$_2$$^{2+}$ + M^{2+} → 2 M(tpy)$^{2+}$		
	ΔH^0_{21}		K_{21}	$\Delta H^0_{21\text{-}11}$		$K_{21\text{-}11}$
	[kcal mol^{-1}]	[kJ/mol]	[M^{-2}]	[kcal mol^{-1}]	[kJ/mol]	
Fe^{2+}	-38.4	-160.7	>10^8	± 0	± 0	0
Co^{2+}	-28.2	-118.0	>10^8	± 0	± 0	0
Ni^{2+}	-31.2	-130.5	>10^8	± 0	± 0	0
Cu^{2+}	-33.8	-141.4	>10^8	**-8.7**	**-36.4**	**3.5·10^6 ± 10^6**
Zn^{2+}	-28.4	-118.8	>10^8	± 0	± 0	0

a Errors for ΔH^0 values are ±0.5 kcal/mol.

ITC study with copper perchlorate. The UV-vis titration of copper perchlorate in acetonitrile (figure 5) revealed that the copper-tpy bond exhibits pronounced reversibility and that the UV-vis spectra of the 1:1 and the 2:1 species are different. ITC studies have been used in order to obtain a deeper insight into the Cu-tpy binding process. In analogy to the previously discussed ITC studies, figure 11 (left) shows the result of the titration of terpyridine to a copper(II) solution. In this curve, two different binding events can be distinguished, one with saturation occurring at a molar ratio of 1, the second at a molar ratio of 2 with a decreased ΔH^0. Since the stoichiometries fit to the binding of the first and the second tpy unit, the released enthalpy for the binding of the second tpy is smaller.

A complementary result is obtained for the reversed titration, the addition of tpy to a copper(II) solution. For all other metal ions, only a residual baseline signal was detected after exceeding the ratio of 0.5 in this type of titration, meaning that in the case of a reversible complexation there is no enthalpy change when the 2:1 species is changed into the 1:1 complex. For copper, exactly this is the case: when the 2:1 complex, which is present in solution at the molar ratio of 0.5, is opened to form two 1:1 species, this process is exothermic, indicating that a thermodynamically more favorable binding event takes place.
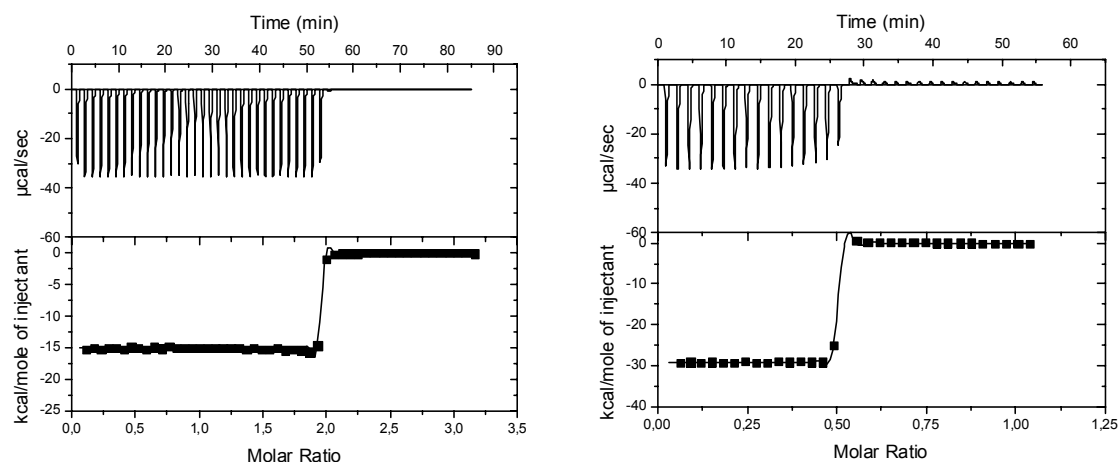
Figure 11. Left: ITC titration curves for the addition of tpy (10 mM) to a Cu^{2+} solution (0.5 mM). Right: Reversed titration of Cu^{2+} (5 mM) into a tpy solution (0.5 mM).

The observation that the copper-terpyridine system exhibits special features which are not observed for other first row transition metals has also been made by Moore and coworkers,[28] who investigated the kinetics of tpy complexation with Cu^{2+} in aqueous buffered solution and proposed the explanation that in the 2:1 copper-tpy complex only one of the tpy ligands acts as a tridentate ligand, whereas the second ligand is attached by only two pyridine units and therefore acts as a bidentate ligand like 2,2'-bipyridine. This interpretation can be supported by the ΔH^0 values measured in this work (scheme 2). The attachment of the second tpy unit to the $Cu(tpy)^{2+}$ species (scheme 2A, molar ratio 1-2) produces only a decreased enthalpy compared to the first step since one pyridine unit remains uncomplexed. Thus -22.2 kcal/mol are measured for the coordination of the first tpy unit (corresponding to -7.4 kcal/mol for each pyridine), but only -13.4 kcal/mol for the second tpy unit (corresponding to -6.7 kcal/mol for each of two coordinating units). On the other hand, for the reversed titration, the additional exothermic calorimetric signal detected for the addition of copper to the $Cu(tpy)_2^{2+}$ solution (scheme 2B, molar ratio 0.5-1) is explained by the coordination of the last uncomplexed pyridine unit (ΔH^0 = -8.7 kcal/mol).
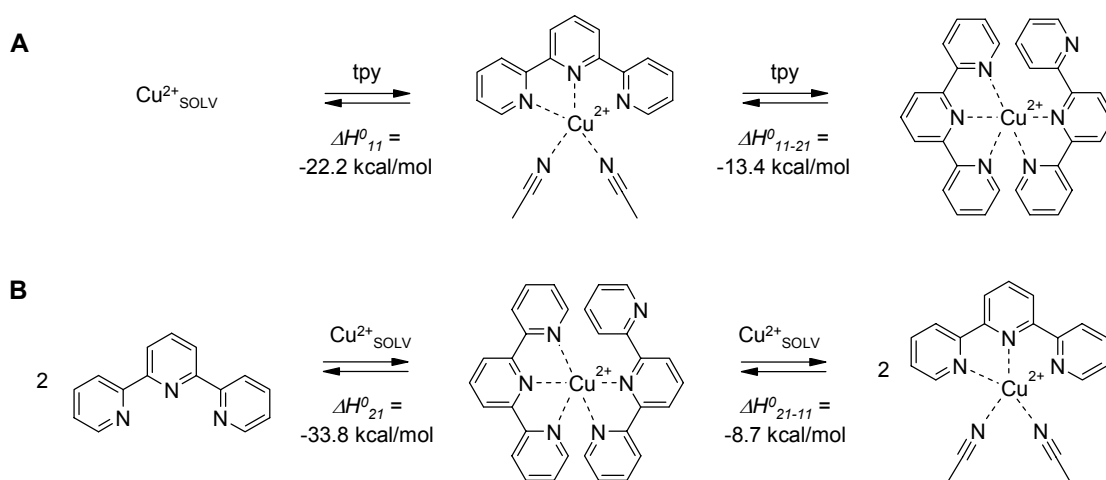
Scheme 2. Proposed mechanism for the titration of copper perchlorate with tpy in acetonitrile and the corresponding ΔH values determined by ITC for addition of tpy to the Cu^{2+} solution (A) and vice versa (B). The values suggest that the second tpy ligand in the 2:1 complex merely acts as a bidentate ligand.

All results of the ITC titrations are summarized in tables 3 and 4 for the two titration modes respectively. The attachment of the first tpy unit to the copper(II) ion gives the largest binding enthalpy with a ΔH^0 of -22.2 kcal/mol, followed by iron(II) with -19.1 kcal/mol. The value for nickel(II) is situated in between with -16.0 kcal/mol, whereas the measured enthalpies of cobalt(II) and zinc(II) are the lowest with <15 kcal/mol. With the exception of copper(II), all values determined by the addition of metal to the tpy solution, meaning an immediate formation of the 2:1 complex, are approximately twice the value for the sequential measurement by titration of tpy to the metal ion solution.

Conclusion

In conclusion, the complexation of terpyridine with a series of transition metal ions has been studied in acetonitrile as a nonaqueous solvent. A collection of the UV-vis spectra is available for all investigated metal complexes. The characteristic changes in the ^{1}H NMR spectrum have been discussed in detail for the Zn^{2+}-terpyridine system showing reversible ligand exchange in acetonitrile at room temperature. ITC studies provided binding enthalpies which could be determined for both titration directions, i.e. also the addition of tpy to the metal ion solution, which is not possible in UV-vis and NMR studies. This knowledge of the basic binding processes, i.e. binding constants, enthalpy and reversibility is essential for the rational construction of more elaborate supramolecular architectures, which are discussed in the following chapters.

Experimental Section

General. Solvents were purified and dried according to standard procedures.[29] Spectroscopy grade solvents were used for UV-vis. 2,2':6',2''-Terpyridine, zinc trifluoromethane sulfonate and the metal perchlorate hexahydrate salts are commercially available and were used without further purification. ^{1}H NMR spectra were recorded on a Bruker AMX400 spectrometer (400 MHz) in $d3$-acetonitrile and chemical shifts δ (ppm) are calibrated against the residual CH_3CN signal ($\delta = 2.96$ ppm). 4'-(p-Methylphenyl)-2,2':6',2''-terpyridine was synthesized according to a literature procedure.[30]

Isothermal Titration Calorimetry (ITC). Experiments were performed using a MicroCal isothermal titration calorimeter system and analyzed using the software supplied with the instrument. Titrations were done in both directions either by addition of metal salt solution (5 mM) into terpyridine solution (0.5 mM) or by addition of terpyridine solution (10 mM) into metal salt solution (0.5 mM). Solutions were prepared in HPLC grade acetonitrile (Scharlau Chemical Comp.). Measurements were conducted at 25.3–25.5 °C, added volume was 4 µl per addition using a 250 µl syringe, injection duration was 5 s, the interval between injections was 100 s. All ΔH values are corrected against the heat of dilution and the concentration changes during the titration.

^{1}H NMR Titration Experiments with tpy. Aliquots of a zinc perchlorate hexahydrate solution (62 mM in d_3-acetonitrile) were added to a tpy solution (31 mM in d_3-acetonitrile) and ^{1}H NMR spectra were recorded after each addition (Bruker AMX400, 400 MHz). The quantities of the different species were calculated from the integrated areas of NMR signals.

UV-vis Titration Experiments with tpy and Metal Perchlorates. Titrations were performed as constant host titrations (0.05 mM in acetonitrile) at 25.0 °C (Perkin Elmer PTP1 peltier thermostat unit) by addition of aliquots of the respective metal perchlorate hexahydrate solution (0.5 mM in tpy solution). UV-vis spectra were recorded after each addition on a Perkin Elmer Lambda 40P instrument in 1 cm cells.
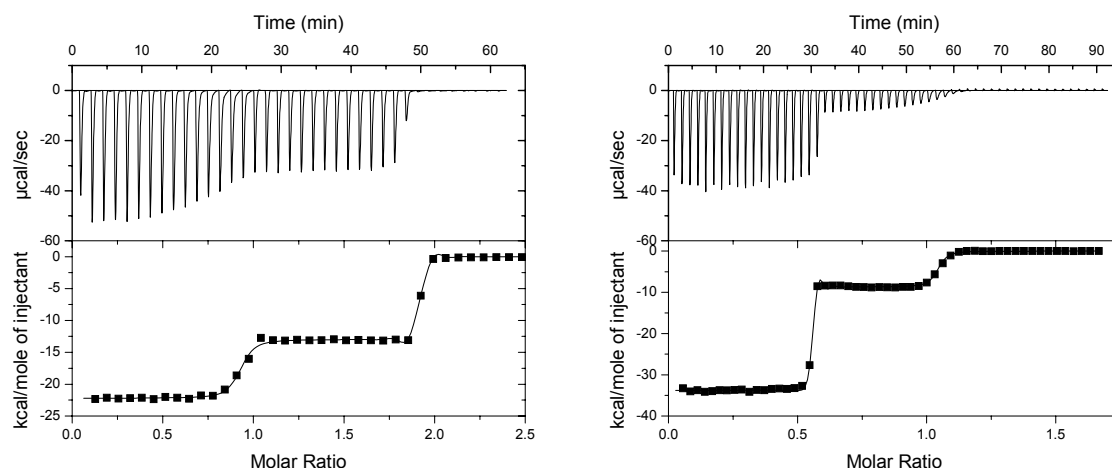
Appendix. ITC Titration Figures
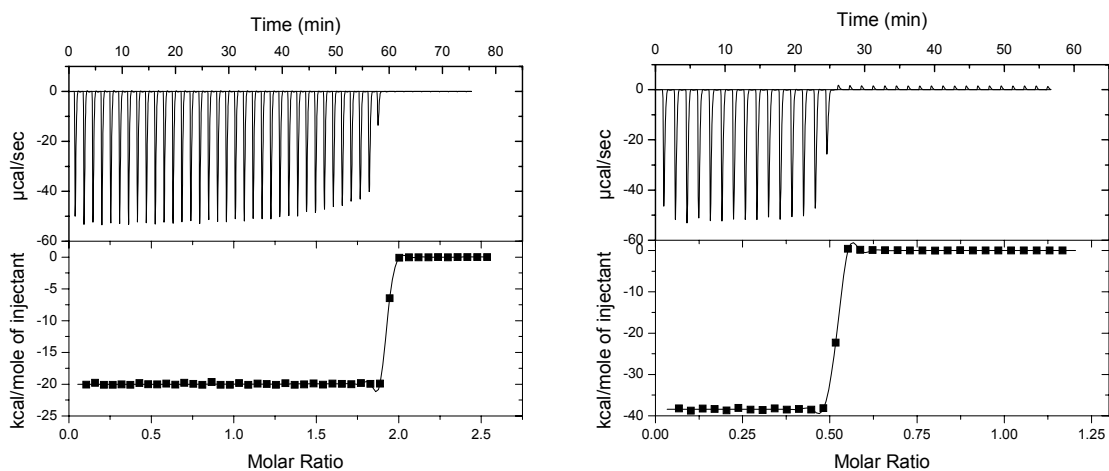
Figure 12. Left: ITC titration curves for the addition of tpy (10 mM) to a Fe^{2+} solution (0.5 mM). Right: Reversed titration of Fe^{2+} (5 mM) into a tpy solution (0.5 mM).
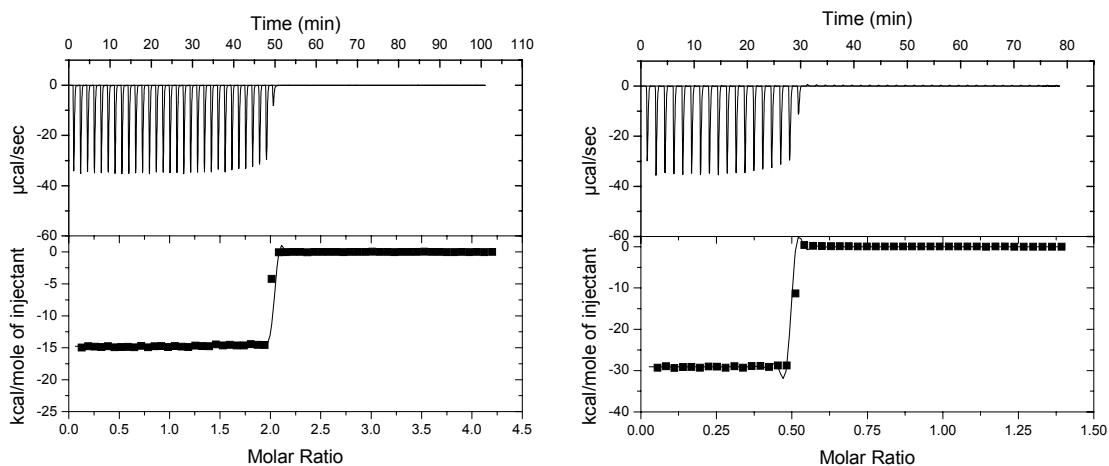
Figure 13. Left: ITC titration curves for the addition of tpy (10 mM) to a Co^{2+} solution (0.5 mM). Right: Reversed titration of Co^{2+} (5 mM) into a tpy solution (0.5 mM)
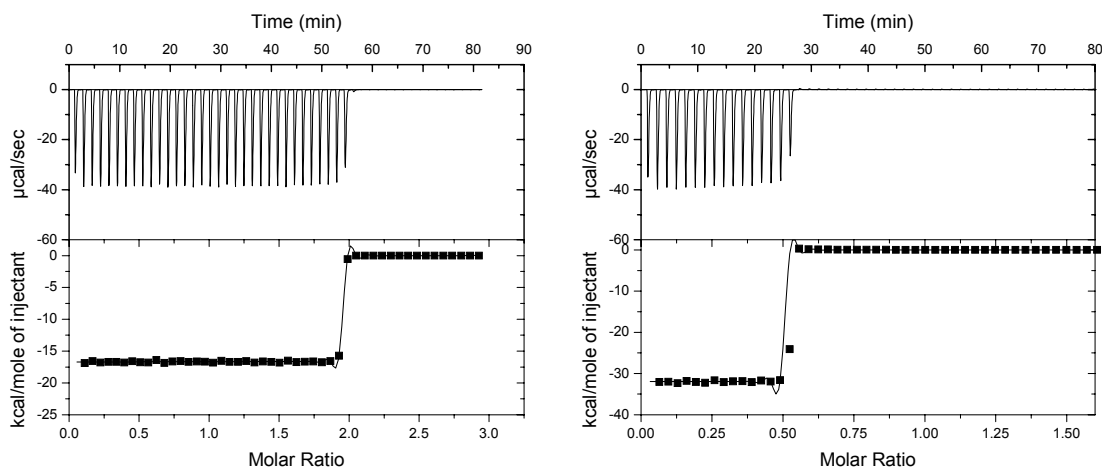
Figure 14. Left: ITC titration curves for the addition of tpy (10 mM) to a Ni^{2+} solution (0.5 mM). Right: Reversed titration of Ni^{2+} (5 mM) into a tpy solution (0.5 mM)

References

(1)   Lehn, J.-P. *Supramolecular Chemistry: Concepts and Perspectives*; VCH: Weinheim, **1995**.

(2)   Steed, J. W.; Atwood, J. L. *Supramolecular Chemistry: a concise introduction*; John Wiley & Sons, Ltd.: Chichester, **2000**.

(3)   Swiegers, G. F.; Malefetse, T. J. *Chem. Rev.* **2000**, 100, 3483-3537.

(4)   Würthner, F.; You, C.-C.; Saha-Möller, C. *Chem. Soc. Rev.* **2004**, 33, 133-146.

(5)   Newkome, G. R.; Cho, T. J.; Moorefield, C. N.; Mohapatra, P. P.; Godinez, L. A. *Chem. Eur. J.* **2004**, 10, 1493-1500; Newkome, G. R.; Cho, T. J.; Moorefield, C. N.; Cush, R.; Russo, P. S.; Godinez, L. A.; Saunders, M. J.; Mohapatra, P. *Chem. Eur. J.* **2002**, 8, 2946-2954.

(6)   Constable, E. C.; Cargill Thompson, A. M. W. *J. Chem. Soc., Dalton Trans.* **1992**, 3467-3475.

(7)   (a) Schütte, M.; Kurth, D. G.; Linford, M. R.; Cölfen, H.; Möhwald, H. *Angew. Chem. Int. Ed.* **1998**, 37, 2891-2893; (b) S. Kelch, M. Rehahn, *Macromolecules* **1999**, 32, 5818-5828; (c) Schubert, U. S.; Eschbaumer, S. *Angew. Chem. Int. Ed.* **2002**, 41, 2829-2926.

(8)   Newkome, G. R.; He, E.; Moorefield, C. N. *Chem. Rev.***1999**, 99, 1689-1746.

(9)   Ziener, U.; Lehn, J.-M.; Mourran, A.; Möller, M. *Chem. Eur. J.* **2002**, 8, 951-957.

(10) Piguet, C.; Bernardinelli, G.; Hopfgartner, G. *Chem. Rev.* **1997**, 97, 2005-2062.

(11) Reviews: (a) Baranoff, E.; Collin, J.-P.; Flamigni, L.; Sauvage, J.-P. *Chem. Soc. Rev.* **2004**, 33, 147-155; (b) J.-P. Sauvage, J.-P. Collin, J.-C. Chambron, S. Guillerez, C. Coudret, V. Balzani, F. Barigelletti, L. De Cola, L. Flamigni *Chem. Rev.* **1994**, 94, 993-1019; (c) Ziessel, R.; Hissler, M.; El-Ghayoury, A.; Harriman, A. Coord. *Chem. Rev.* **1998**, 178-180, 1251-1298.

(12) Zakeeruddin, S. M.; Nazeeruddin, M. K.; Pechy, P.; Rotzinger , F. P.; Humphry-Baker, R.; Kalyanasundaram, K.; Graetzel, M.; Shklover, V.; Haibach, T. *Inorg. Chem.* **1997**, 36, 5937-5946.

(13) Goze, C.; Ulrich, G.; Charbonniere, L.; Cesario, M.; Prange, T.; Ziessel, R. *Chem. Eur. J.* **2003**, 9, 3748-3755.

(14) Barigelletti, F.; Flamigni, L.; Calogero, G.; Hammarstrom, L.; Sauvage, J.-P.; Collin, J.-P. *Chem. Commun.* **1998**, 2333-2334.

(15) Aiet-Haddou, H.; Wiskur, S. L.; Lynch, V. M.; Anslyn, E. V. *J. Am. Chem. Soc.* **2001**, 123, 11296-11297.

(16) Wong, W.-L; Huang, K.-H.; Teng, P.-F.; Lee, D.-S.; Kwong. H.-L. *Chem. Commun.* **2004**, 384-385.

(17) Jimenez-Molero, M. C.; Dietrich-Buchecker, C.; Sauvage, J.-P. *Chem. Commun.* **2003**, 1613-1616.

(18) Drew, M. G. B.; Hudson, M. J.; Iveson, P. B.; Russell, M. L.; Liljenzin, J.-O.; Skålberg, M.; Spjuth, L.; Madic, C. *J. Chem. Soc., Dalton Trans.* **1998**, 2973-2980.

(19) Molecular modeling was performed with the Fujitsu Quantum CAChe 5.2 program; MM3 force field is used unless otherwise stated.

(20) Nakamoto, K. *J. Phys. Chem.* **1960**, 64, 1420-1425.

(21) (a) Rao, J. M.; Macero, D. J. *Inorg. Chim. Acta* **1980**, *41*, 221-226; (b) Waldmann, O.; Hassmann, J.; Müller, P.; Volkmer, D.; Schubert, U. S.; Lehn, J. M. *Phys. Rev. B.* **1998**, *58*, 3277-3285.

(22) Refer to chapter 3 for a NMR titration applying a 4'-substituted terpyridine derivative.

(23) Yu, S.-C.; Kwok, C.-C.; Chan, W. K.; Che, C.-M. *Adv. Mater.* **2003**, 15, 1643-1647.

(24) Hogg, R.; Wilkins, R. G. *J. Chem. Soc.* **1962**, 341-350.

(25) Freire, E.; Mayorga, O. L.; Straume, M. *Anal. Chem.* **1990**, 62, 950 A – 959 A.

(26) Blandamer, M. J.; Cullins, P. M.; Engberts, J. B. F. N. *J. Chem. Soc., Faraday Trans.* **1998**, 94, 2261-2267.

(27) Jelesarov, I.; Bosshard, H. R. *J. Mol. Recognit.* **1999**, 12, 3-18.

(28) Priimov, G. U.; Moore, P.; Helm, L.; Merbach, A. E. *Inorg. React. Mech.* **2001**, 3, 1-23.

(29) Perrin, D. D.; Armarego, W. L. F. *Purification of Laboratory Chemicals*, 2nd ed., Pergamon Press: Oxford, **1980**.

(30) Chemchoumis, C.; Potvin, P. G. *J. Chem. Research (M)* **1998**, 870-875.

3

Synthesis and Optical Properties of Perylene Bisimide – Terpyridine Compounds and their Metal Complexes

Abstract: Building blocks for metallosupramolecular organization of fluorophores have been synthesized by equipping perylene bisimide derivatives with one or two 2,2':6',2''-terpyridine ligand units. Subsequent supramolecular coordination polymerization of those building blocks has been investigated by using Zn^{2+} as metal ion. The formation of the dimeric complexes in the case of monotopic model compounds **5** and coordination polymerization of ditopic functional building blocks **3** have been confirmed by ^{1}H NMR studies. Optical properties of dimeric and polymeric complexes have been investigated by UV-vis and fluorescence spectroscopy and fluorescence quenching has been studied with a series of metal ions. Only coordination of Zn^{2+} to the terpyridine unit was found not to affect the advantageous fluorescence properties of perylene bisimide moieties. Furthermore, Zn^{2+} complexation offers reversible formation of dimer complexes and coordination polymers, which has been established by ^{1}H NMR.

Introduction

Perylene-3,4:9,10-tetracarboxylic acid bisimide ("perylene bisimide") compounds have been used for a long time as pigments[1,2] due to their intense color and high photostability. Since the large aromatic system causes a high tendency to aggregate, soluble dyes can only be prepared by introduction of sterically demanding residues. Langhals[3] solved this problem by the introduction of long branched alkyl chains, the so-called swallowtails, in the imide positions. Soluble perylene bisimide dyes show intense fluorescence with fluorescence quantum yields of almost unity and can be reversibly oxidized and reduced. Both properties have obtained significant attention only after soluble compounds had been accessible.
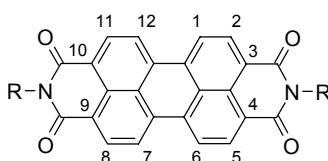
Chart 1. Perlene-3,4:9,10-tetracarboxylic acid bisimide (R = H, Ar, Alk)

The chlorination reaction of perylene bisanhydride can be controlled in a way that tetrachlorination takes place in the "bay-positions" 1, 6, 7 and 12. This functionalization offers the possibility for a second way to modify the perylene bisimide scaffold in addition to the imide positions. Nucleophilic displacement of the chlorine substituents by phenolates can be used to introduce phenoxy residues, which was first accomplished by Seybold and coworkers at BASF.[4] Perylene bisimide compounds with phenoxy substituents in the bay positions offer considerably increased solubility due to the effectively reduced aggregation of the π-system, and additionally by the introduction of a twist between the two naphthalene units with respect to each other, caused by the steric repulsion of the bay substituents. Since solubility is provided by the bay-substituents, the imide positions are free for further functionalization of the fluorophore.

Several examples for the construction of functional systems with perylene bisimide units used as building blocks have been published. Müllen and coworkers reported a number of different photoactive systems built from perylene bisimide units incorporated into covalent polymers for application in light emitting diodes[5] or functional dendrimers for energy[6] and electron transfer.[7] Covalently linked perylene bisimide – porphyrin systems have been published by the group of Wasielewski.[8]

Supramolecular organization of functional units is an attractive alternative to covalent synthesis. If the molecular interactions are well balanced and the design of the molecules and

receptor units is optimized, systems of high complexity can be formed in a self-assembly process without extensive synthetic effort. Perylene bisimide building blocks are suitable candidates for the construction of such systems[9] as they offer remarkable functional properties in combination with the possibility for orthogonal synthetic variation making use of the imide groups and the residues in the bay-positions. Several examples for supramolecular perylene bisimide systems have already been published by our group using a wide range of noncovalent interactions.[9] Van der Waals forces between alkyl chains and π-π-interactions have been used for the fabrication of liquid crystalline dye aggregates.[10] The construction of polymeric aggregates was achieved by combining π-π-interaction with the directional interaction of hydrogen bonds between a perylene bisimide (chart1, R = H) and a complementary melamine unit.[11,12] Stronger and highly defined interaction can be obtained through metal-ligand bonds, which can be varied in a wide range depending on the number of individual metal-ligand interactions and on the properties of the applied metals and ligand systems. With the use of pyridine receptor units and geometrically apt metal-corners coordinating in a 90° angle, molecular squares could be obtained.[13]

The construction of coordination polymers (Chapter 1) composed of perylene bisimide units is an attractive alternative to classical polymerization methods. In many cases, classical monomers are highly reactive and therefore not suited for extensive purification. Often also the resulting polymers are not well defined, suffering from defective connections. Supramolecular polymers can offer a solution to some of these problems, as the interaction which builds up the polymer can be controlled externally through solvent, temperature or the stoichiometry of the building blocks. Therefore the units can be synthesized in high purity and the resulting polymers can offer advantageous properties like self-healing and reversibility due to their supramolecular nature.

As discussed in Chapter 2, the 2,2':6',2''-terpyridine ligand is an interesting receptor unit for the construction of functional coordination polymers, especially in combination with Zn^{2+}, since the complex is not photoactive and is therefore not expected to interact with the perylene bisimide fluorescence, and it offers the advantage of reversible complexation. In this chapter, the synthesis of terpyridine-functionalized perylene bisimide building blocks is reported and their self-assembly with Zn^{2+} as well as the effect of complexation on the optical properties of the chromophore is investigated.

Results and Discussion

Synthesis of tpy-functionalized perylene bisimides: Ditopic terpyridine–functionalized perylene bisimide ligands **3a,b** were prepared by condensation of 4'-*p*-aminophenyl-2,2':6',2"-terpyridine **2** with the respective bisanhydrides **1a,b**[11,13,14] in quinoline with zinc acetate as catalyst in isolated yields of 37% (for **3a**) and 12% (for **3b**). The aminophenylterpyridine compound was synthesized by reduction of the respective nitrophenylterpyridine with hydrazine hydrate and palladium/charcoal catalyst in ethanol in 75 % yield.[15]
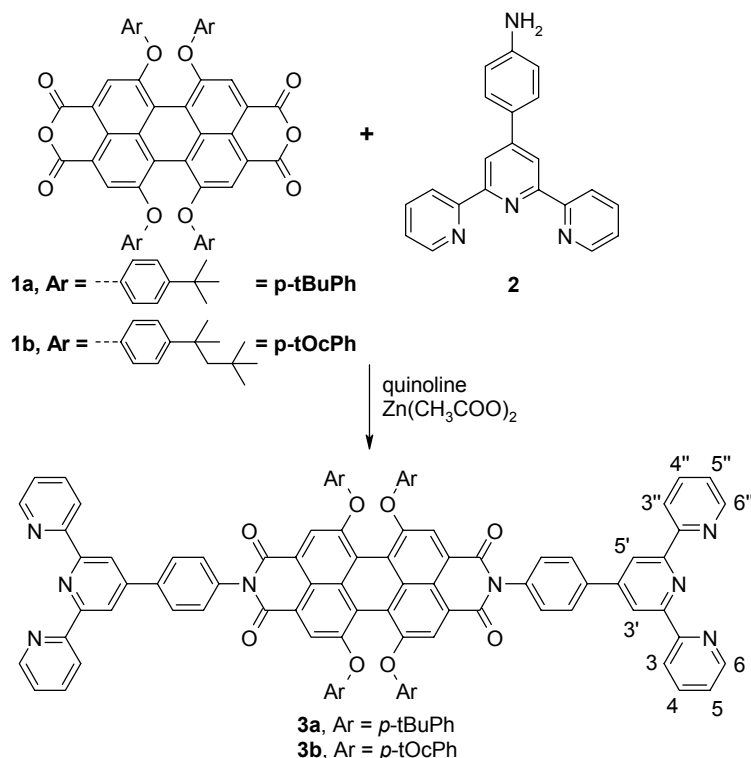
Scheme 1.

As the monotopic ligands **5** are valuable model compounds for complexation studies, the condensation reaction of **2** was carried out with a mixture of the bisanhydride **1** and imide anhydride **4**, the latter is accessible via partial saponificaion of the corresponding *n*-butyl bisimide.[16] The mixture of products **3** and **5** was separated by repetitive column chromatography on basic alumina of activity II. Due to strong adsorption of the tpy units to alumina, the isolated yields of the products are only moderate. Despite f their extended π-systems all terpyridine functionalized perylene bisimide compounds **3a,b** and **5a,b** exhibit good solubility in halogenated organic solvents due to the bulky phenoxy substituents bearing *tert*-butyl or 1,1,3,3-tetramethylbutyl (*tert*-octyl) groups.

4a, Ar = *p*-tBuPh
4b, Ar = *p*-tOcPh

5a, Ar = *p*-tBuPh
5b, Ar = *p*-tOcPh
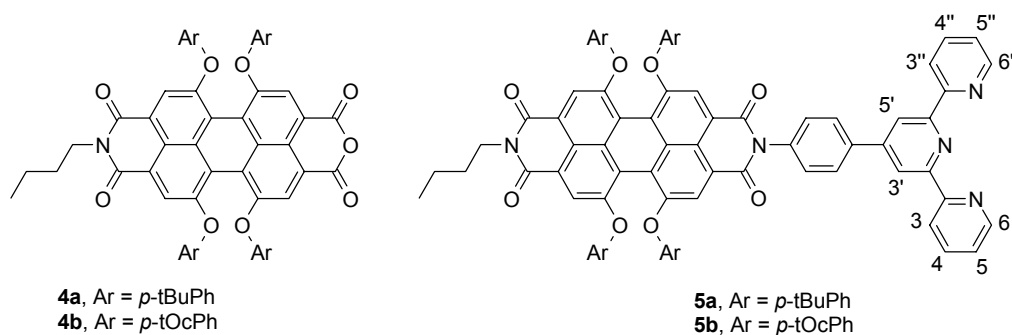
Chart 2.

Dimer complex formation with zinc triflate: Complexation of the monotopic model ligand **5**, which forms the dimer complex **6** upon addition of Zn^{2+}, was used to test the influence and suitability of solvent systems and counterions. Especially with respect to the coordination polymer formation, the counterions and the solvent have to facilitate smooth and fast complexation and offer high solubility. The solvent system has to be well balanced to provide enough polarity to solubilize the metal salt and the ionic $Zn(tpy)_2^{2+}$ unit but still keep the extended aromatic system of the perylene bisimide in solution. Best results were achieved by application of zinc trifuoromethane sulfonate (triflate, OTf) in mixtures of chloroform–methanol (60/40 or 80/20) and chloroform–acetonitrile (80/20). The complexation reaction was monitored by ^{1}H NMR.

6a, Ar = *p*-tBuPh
6b, Ar = *p*-tOcPh

7a, Ar = *p*-tBuPh
7b, Ar = *p*-tOcPh
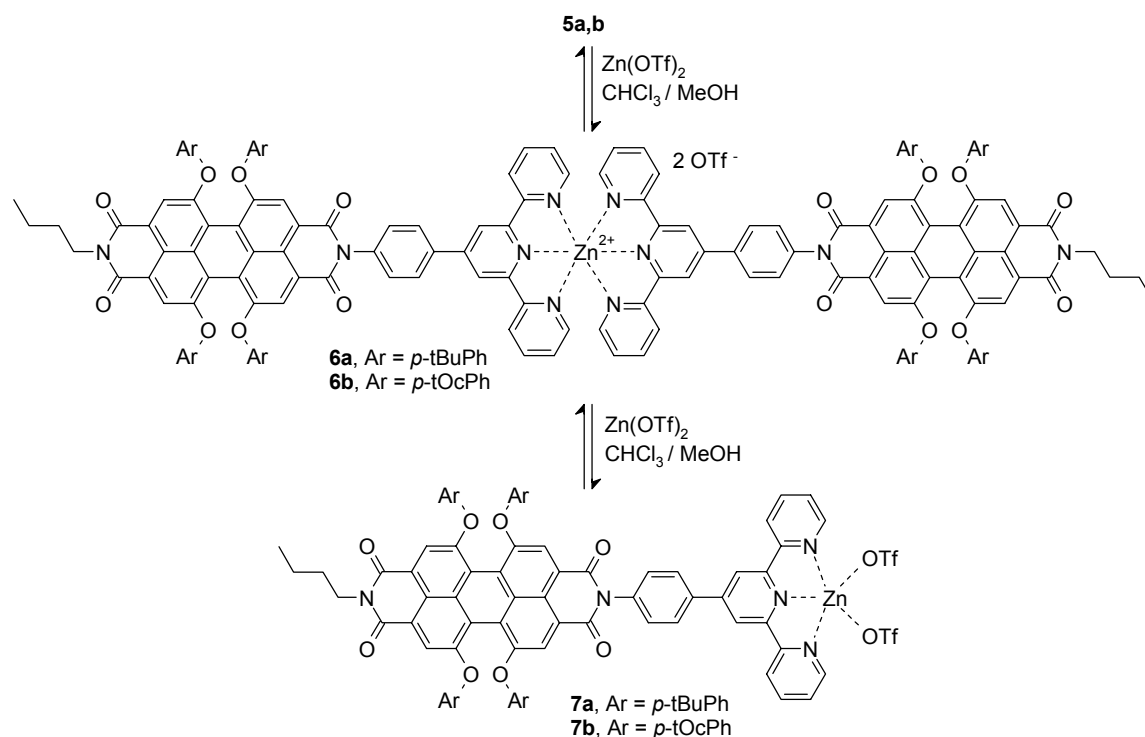
Scheme 2.

Figure 1 shows the characteristic ^{1}H NMR signals of the aromatic region during the titration at different ligand/metal ratios. The formation of dimer **6a** is clearly indicated by the disappearance of the original set of signals which belongs to the uncomplexed ligand **5a** and the rise of a second set of signals, exemplified by the downfield shift of the singlet of the central pyridine unit (3', marked with *) from 8.75 ppm to 9.1 ppm and the drastic highfield shift of the proton H6 and H6" (marked with #) from 8.74 ppm to 7.80 ppm, which is due to the shielding effect of the second metal-bound tpy unit. At a ratio of 2:1 only the dimer **6a** is present in solution and the ^{1}H NMR signals can be clearly assigned. Once this ratio is exceeded by addition of more Zn^{2+} ions, the dimer signals decrease in intensity again and a third set of signals evolves demonstrating the reversible binding of the $Zn(tpy)_2$ unit under the given conditions. The newly formed species may be assigned to a 1:1 complex like **7a** with the additional coordination sites of the metal center saturated either by acetonitrile molecules or the triflate counterions (see scheme 2). This assumption is supported by the significant downfield shift of H6 signal (#) owing to the removal of the second tpy unit (figure 1). Also here, as in the case of unsubstituted tpy, the exchange kinetics is slow on the NMR timescale, but equilibrium has been reached within a few seconds after addition of zinc triflate. The chemical shift data and the characteristic changes of the signals assigned to the tpy unit within the ligand **5a**, the dimer complex **6a** and the corresponding 1:1 species **7a** are summarized in Table and Table . The respective *t*octylphenoxy substituted compounds **6b** and **7b** show similar behavior in the ^{1}H NMR titration study (data not shown). Despite its labile nature, dimer **6a** could be characterized by MALDI-TOF mass spectrometry (figure 2) revealing the mass of the dimer cation with one triflate counterion and the resulting fragments.

Table 1. Chemical shift δ (CDCl$_3$–CD$_3$CN, 80:20) of the tpy protons in **5a** and its Zn^{2+} complexes.

δ / ppm[a]	H3	H4	H5	H6	H3'
Ligand **5a**	8.68	7.94	7.39	8.74	8.79
Dimer **6a**	8.72	8.12	7.44	**7.80**	**9.00**
Complex **7a**	8.59	8.27	**7.84**	8.93	8.68

Table 2. Characteristic changes of the chemical shift δ (CDCl$_3$–CD$_3$CN, 80:20) upon transition from ligand **5a** to the 2:1 complex **6a** and subsequently to the 1:1 species **7a**.

$\Delta\delta$ / ppm	H3	H4	H5	H6	H3'
Ligand **5a** $\rightarrow$ Dimer **6a**	+0.04	+0.18	+0.05	**-0.94**	+0.21
Dimer **6a** $\rightarrow$ Complex **7a**	-0.13	+0.15	**+0.40**	**+1.13**	-0.32
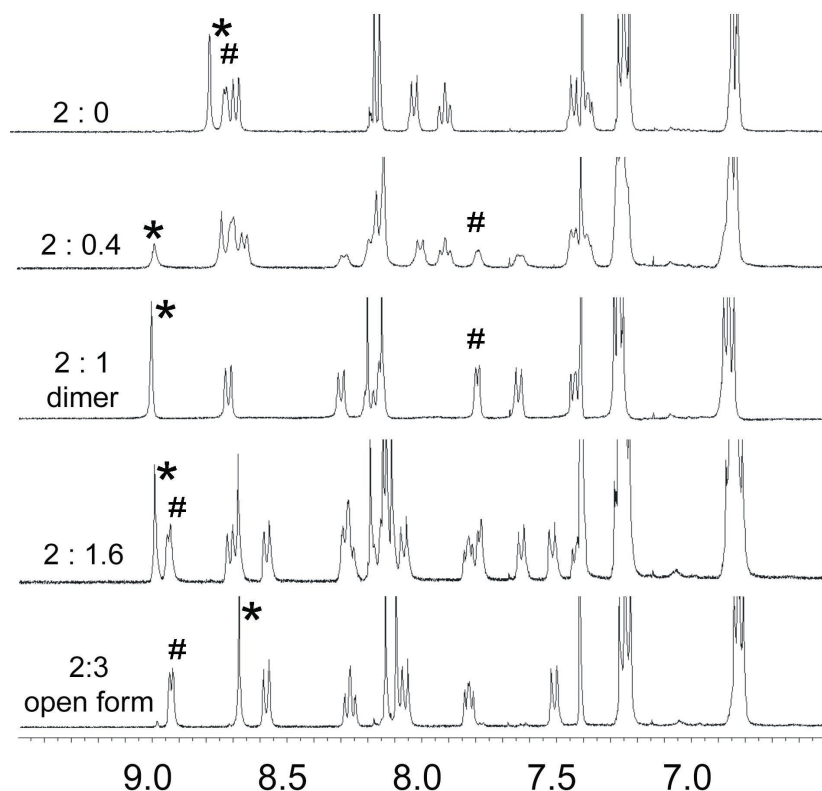
Figure 1. ^{1}H NMR titration of the monotopic ligand **5a** with zinc triflate in CDCl$_3$–CD$_3$CN (80:20, 5 mM) depending on the ligand / metal ratio ranging from free **5a** (upper spectrum, 2:0) to dimer **6a** (middle, 2:1) and the opened form **7a** (bottom, 2:3). The marked signals correspond to proton 3' (*) of the central pyridine unit and proton 6 (#) adjacent to the lateral pyridine atoms.
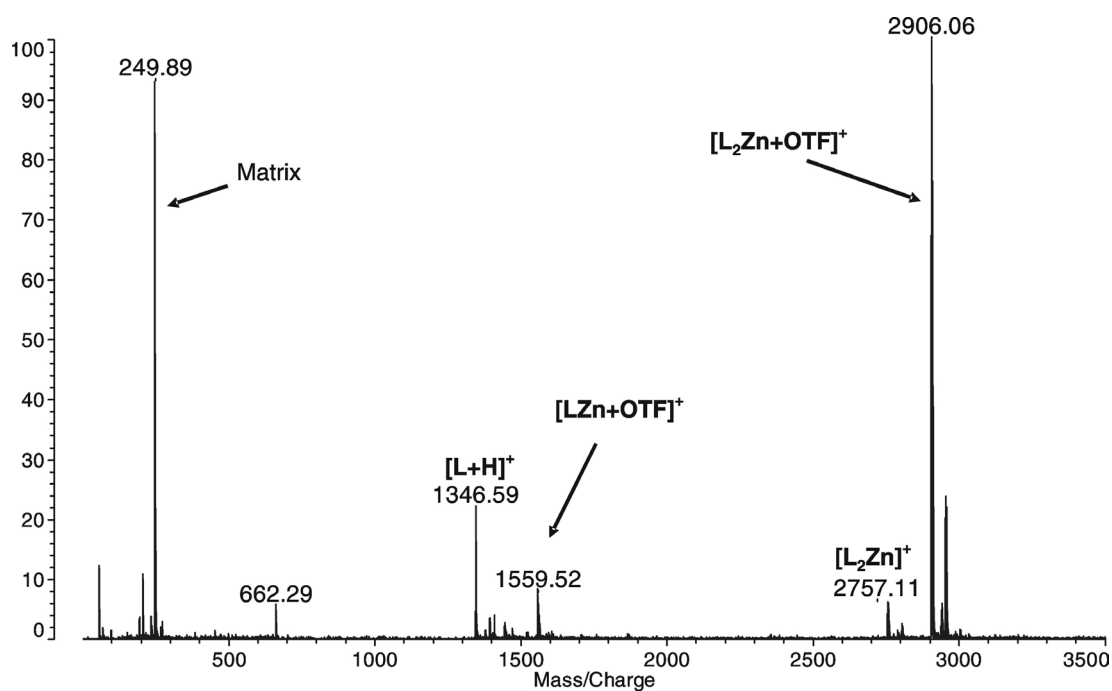
Figure 2. MALDI TOF mass spectrum (DTCB[17] matrix) of the dimeric zinc(II) complex **6a** showing the species with one triflate counterion as the main species together with the further fragments.

Polymer formation from ditopic ligands 3a,b with zinc triflate. In analogy to the dimer formation of the monotopic ligands **5a,b**, the ditopic ligand **3a,b** should lead to an extended $(AA–BB)_n$-type coordination polymer when mixed with exactly one equivalent of Zn^{2+}. Accordingly, a similar titration as in the case of ligand **5a,b** was performed with the ditopic ligands **3a,b**. As can be seen from Figure , the ^{1}H NMR titration resembles the situation observed for the formation of dimer **6a** and the characteristic proton chemical shifts of different species can be found in the same regions. The formation of a coordination polymer can be concluded from the following indications: Upon addition of zinc triflate broadening is observed for the first upcoming set of signals which becomes the only set of signals present in the spectrum when 1:1 stoichiometry is reached. Since the solution remains clear and no precipitation or aggregation can be observed, this signal broadening can be attributed to the formation of a polymeric species **8**. Comparison of the ^{1}H NMR spectra of polymer **8a** (figure 3, 1:1) and the model dimer **6a** (figure 1, 2:1) shows the identical set of signals but significantly broadened in the case of the polymer. Again, reversible complexation is observed when excess Zn^{2+} is added to the coordination polymer solution which results in the shortening of the polymer strands to form a distribution of oligomeric and monomeric fragments such as **9a** with two monocomplexed Zn^{2+} units at the ends.

The polymer length at a 1:1 ratio can be estimated from the ^{1}H NMR signals of the endgroups to a minimum of 10 repeat units corresponding to a chain length of 30 nm and a minimum molecular weight of ~16600 g/mol. Since the coordination polymer is a $(AA–BB)_n$ type, its chain length depends crucially on the exact 1:1 stoichiometry and even small deviations cause a drastic decrease in polymer length. This fact, together with the very hygroscopic nature of the zinc triflate is the reason why all coordination compounds have not been prepared in a classical synthetic manner but by a titration method using ^{1}H NMR to ensure the precise 1:1 stoichiometry. Despite several attempts, mass spectrometric characterization of the coordination polymers by MALDI-TOF MS was not successful as only fragments showing the ligand with one Zn^{2+} ion could be observed due to fragmentation during the ionization process.
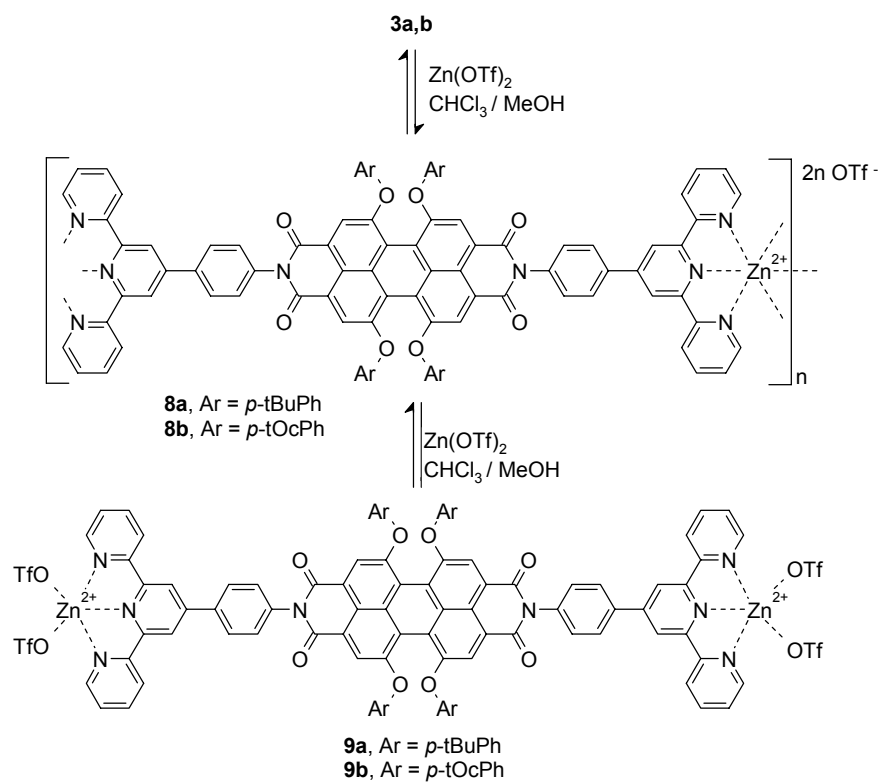
Scheme 3.
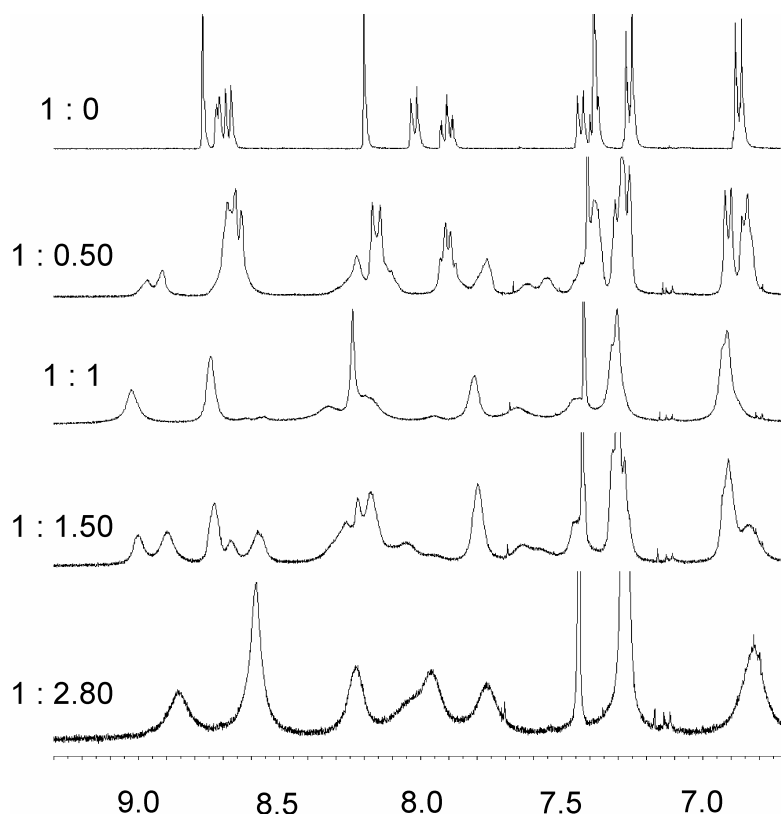
Figure 3. ^{1}H NMR titration of the ditopic ligand **3a** with zinc triflate in CDCl$_3$–CD$_3$CN (80:20) depending on the ligand/metal ratio ranging from free **3a** (upper spectrum) to polymer **8a** (middle, 1:1) and the fragmented dicomplexed form **9a** (bottom).

Interestingly, if the zinc(II) salt is changed from zinc triflate to zinc acetate in the same solvent (chloroform–acetonitrile mixture), the titration does not show the formation of a polymeric species. The respective ^{1}H NMR signals (figure 4) show only the transition from the free ligand **5a** to a twofold complexed species, which results from the obtained metal/ligand ratio of 2:1.
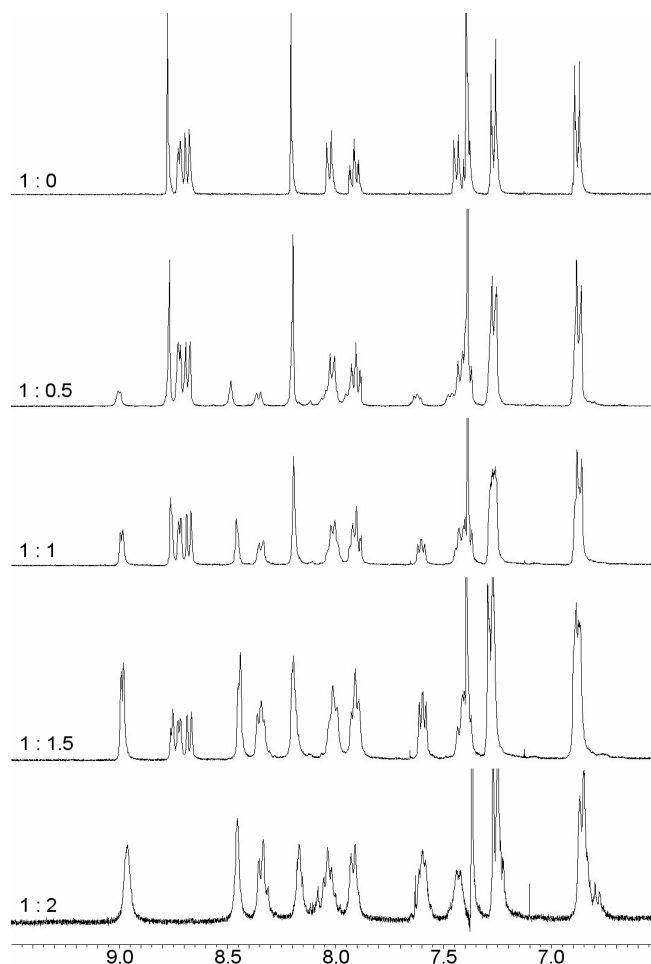
Figure 4. Titration of ditopic ligand **3a** with zinc acetate dihydrate in CDCl$_3$–CD$_3$CN (80:20, 5 mM). The fact that only two species are observed and that the titration ends at a molar ration of **3a**/Zn^{2+} = 1:2 suggests that no coordination polymer comparable to **8a** is formed.

Although the solubility of both coordination polymers **8a,b** is good in chloroform–methanol and chloroform-acetonitrile mixtures, differences are observed in regard to long-term solubility. Whereas polymer **8a** with the *tert*-butylphenoxy residues at the perylene bisimide core slowly starts to precipitate within one day after preparation, polymer **8b** is solubilized sufficiently by the bulky *tert*-octylphenoxy residues to form stable, clear solutions for weeks. Both coordination polymers are also highly soluble in *N,N*-dimethylformamide (DMF) and ^{1}H NMR spectra recorded in deuterated DMF reveal that the coordination remains unchanged. The spectra are arranged in figure 5 to illustrate the similarity of the chemical shift of the

monotopic ligand and the resulting dimeric complex in comparison to the ditopic ligand and the resulting coordination polymer. Also the change in chemical shift due to complex formation can clearly be seen.

Several attempts have been made to assess the polymer length by gel permeation chromatography (GPC). Using different solvents under varying conditions, only the signal corresponding to the molecular mass of the monomer has been found. This observation can be explained in terms of the reversible nature of the complex bond. Due to the non-equilibrium conditions during a GPC run, the constant dilution and shear forces cause fragmentation of the coordination polymers. A further explanation for the exclusive detection of monomers may be that the charged polymer chains adsorb to the stationary phase.
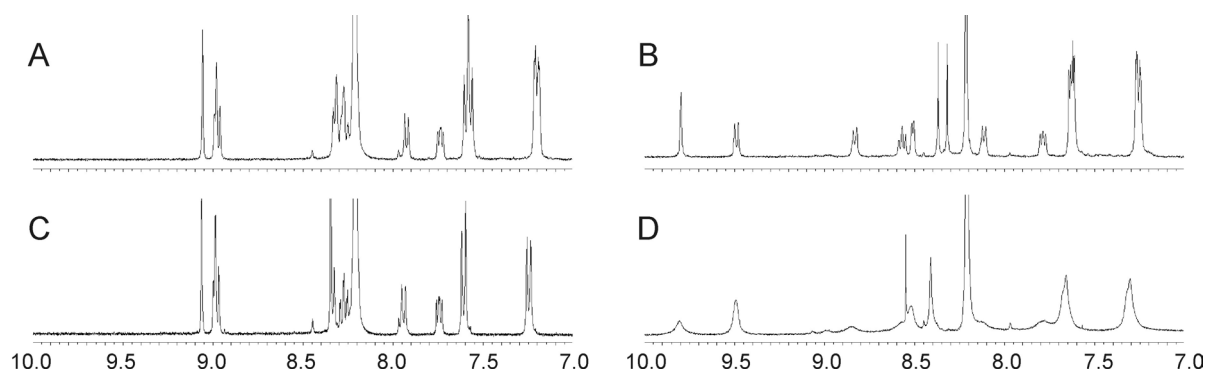
Figure 5. Comparison of the ^{1}H NMR spectra in DMF of the ligands and respective complexes to show the similarity of the chemical shifts in the dimer and coordination polymer: A) monotopic ligand **5a**, B) dimer complex **6a**, C) ditopic ligand **3a** and D) coordination polymer **8a**.

UV-vis Absorption Properties: All uncomplexed monotopic (**5a,b**) and ditopic (**3a,b**) ligands show the characteristic absorption bands of the tetraphenoxy substituted perylene bisimide chromophore between 500–650 nm ($S_0 \rightarrow S_1$, ε = 50.000–55.000 l mol^{-1} cm^{-1}) and 400-500 nm ($S_0 \rightarrow S_2$), whereas at wavelengths below 350 nm both the perylene bisimide and the terpyridine units absorb. UV-vis titrations of the monotopic and ditopic building blocks were performed to assess the ground state interaction of the perylene bisimide chromophore with the terpyridine unit, the latter should act purely as the structure determining part. Figure shows the UV-vis titration of the mono- and ditopic *tert*-butylphenoxy substituted ligands **5a** and **3a** with zinc triflate. As expected from the studies with the parent terpyridine ligand, complexation does not have any significant influence on the absorption of the perylene bisimide chromophore. However, an increase in absorbance between 300-350 nm and a decrease at wavelengths below 300 nm was observed corresponding to the change in tpy absorption (cf. spectra in Chapter 2). These changes can be assigned to the complexation of

the tpy unit which fixes the three pyridine units in an all-*cis* conformation. The dimer **6a** does not show any significant change in the perylene bisimide absorption band compared to the uncomplexed form (see figure 6A), while the polymer exhibits a small increase in absorption and small red-shift of the absorption maximum from 591 nm to 594 nm.
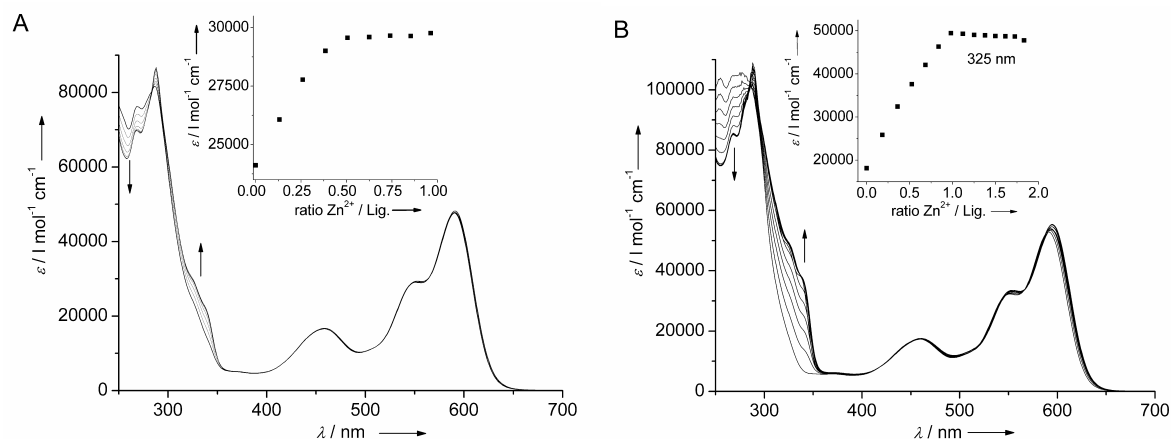
Figure 6. UV-vis titration of monotopic (A, **5a**) and ditopic (B, **3a**) perylene bisimide ligands with zinc triflate in $CHCl_3$–MeOH (60:40); insets show extinction coefficient (at 325 nm) as a function of the Zn^{2+}/ligand ratio.

Fluorescence Properties: All tpy substituted perylene bisimide compounds exhibit intense red fluorescence (λ_{max} = 620 nm) with fluorescence quantum yields around Φ_{fl} = 0.9 in halogenated solvents such as chloroform or dichloromethane. The effect of metal complexation on the fluorescence properties of the perylene bisimide fluorophore unit was investigated by steady state fluorescence spectroscopy. Figure depicts the fluorescence titrations of monotopic perylene ligand **5a** with both zinc(II) triflate and iron(II) perchlorate hexahydrate. The fluorescence of **5a** is drastically quenched upon addition of Fe^{2+} ions (figure 7A) and the fluorescence quantum yield decreases from > 0.9 for the uncomplexed ligand **5a** to < 0.1 for the iron(II) complex (figure 7B, triangles). The fluorescence quenching is likely to be caused by electron transfer from the $Fe(tpy)_2^{2+}$ complex to the excited perylene bisimide unit to form the $Fe(tpy)_2^{3+}$ species and the perylene bisimide radical anion. In contrast, complexation with zinc(II) (figure 7B, circles) has virtually no effect on the fluorescence quantum yield of the perylene bisimide unit.
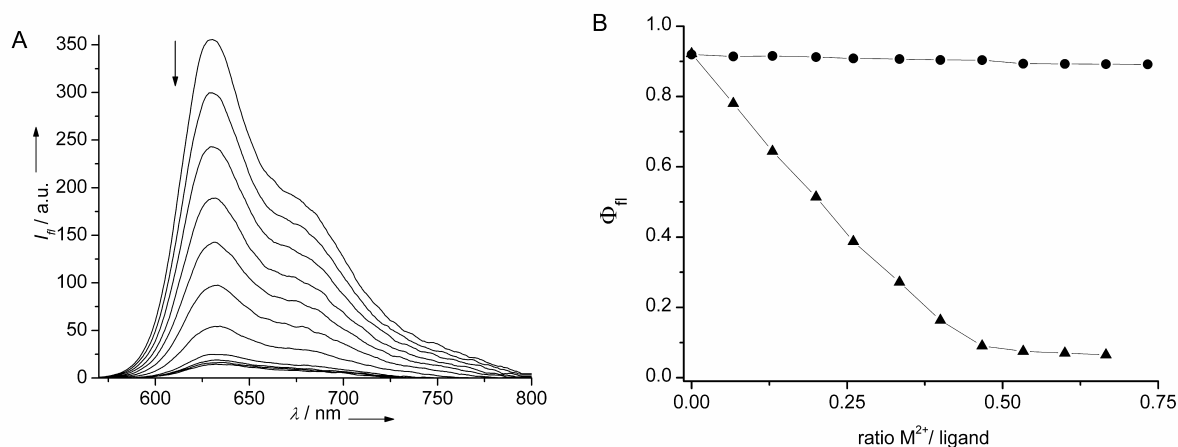
Figure 7. Fluorescence quenching (A) of monotopic perylene bisimide ligand **5a** on addition of iron(II) perchlorate hexahydrate and fluorescence quantum yields (B) as a function of iron(II)/**5a** ratio (triangles) and zinc(II)/**5a** ratio (circles). All measurements in CHCl$_3$–MeOH (60:40) at 10^{-5} M concentration of **5a**.

The results of a detailed investigation of fluorescence quantum yields and lifetimes are summarized in Table . The compounds have been investigated in chloroform and additionally in DMF to ensure complete dissolution and to avoid possible aggregation of the complexed species, which may occur in chloroform. The coordination polymer **8a** is insoluble in chloroform and therefore only characterized in DMF. Comparison of the quantum yields of confirms the result of the titration that there is no influence on Zn^{2+} complexation in the case of the dimer **6a** compared to the ligand **5a** and only a small decrease in the case of the polymer **8a** compared to the ditopic ligand **3a**. All fluorescence quantum yields are reduced by approx. 0.14 when determined in DMF instead of chloroform independent on the complexation state. This moderate decrease is apparently an effect of the increased polarity of DMF. This effect can also be observed for the fluorescence lifetimes, which are decreased by approx. 1 ns when determined in DMF. Interestingly, a minor increase of fluorescence lifetime is observed when the complexed species are compared with their parent ligands.

Table 3. Emission properties of uncomplexed ligands and the respective Zn^{2+} complexes in CHCl$_3$ and DMF.[a]

	CHCl$_3$		DMF	
	Φ_{fl}	τ / ns	Φ_{fl}	τ / ns
Monotopic ligand **5a**	0.93	5.7	0.80	4.8
Ditopic ligand **3a**	0.92	6.1	0.75	4.8
Dimer **6a**	0.90	6.3	0.74	5.5
Polymer **8a**	–	–	0.61	4.9

[a] Errors for quantum yields are ±0.04, errors for lifetimes are ±0.2 ns except for **8a**: ±0.4 ns

Further fluorescence quenching experiments have been done with the metal salts that have already been investigated by UV-vis titrations and ITC (cf. Chapter 2). As expected from their

paramagnetic properties, the $M(tpy)_2^{2+}$ complex units of Co^{2+}, Ni^{2+} and Cu^{2+} cause partials or , for copper, nearly complete quenching of the perylene fluorescence by effective deactivation of the perylene bisimide excited state by the paramagnetic metal centers.
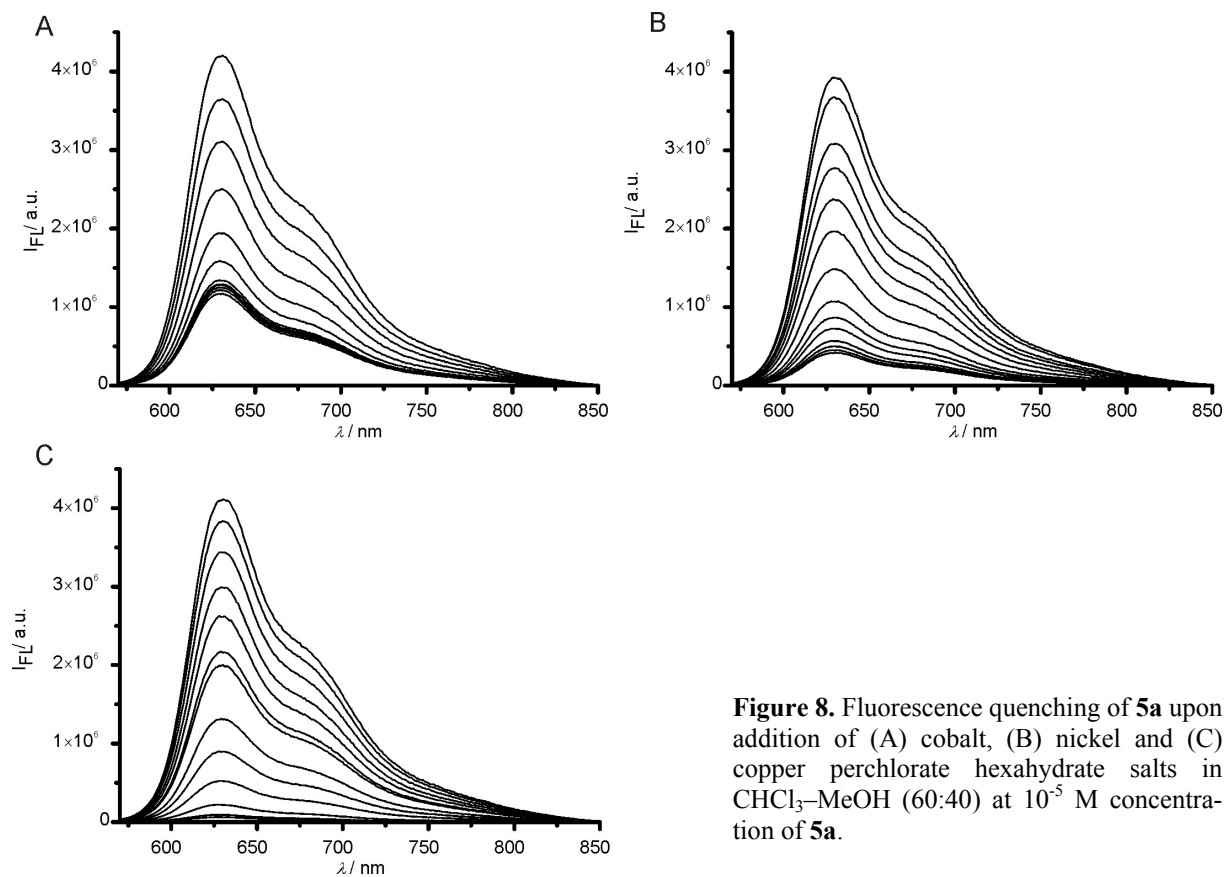
Figure 8. Fluorescence quenching of **5a** upon addition of (A) cobalt, (B) nickel and (C) copper perchlorate hexahydrate salts in $CHCl_3$–MeOH (60:40) at 10^{-5} M concentration of **5a**.

Conclusion

In conclusion, the synthesis of well-soluble perylene bisimide fluorophores equipped with one or two terpyridine complex ligands was described in this chapter and the complexation of these units with Zn^{2+} ions was studied. The formation of a dimer complex from the monotopic ligands and the formation of a coordination polymer from the respective ditopic ligands have been investigated by ^{1}H NMR titration experiments. Due to the reversibility of the $Zn(tpy)_2^{2+}$ unit, a long-chain polymer is only possible at an exact 1:1 ration between ditopic building block and Zn^{2+}. The coordination polymers are found to be well soluble in organic solvents and the high fluorescence quantum yield of the perylene bisimide units is retained also in the coordinated form.

Since the polymer is constituted by a reversible bond, it can not be characterized by GPC. In contrast, characterization methods are required which retain equilibrium between the solvent and the dissolved polymer. Such methods will be used in Chapter 4 to further prove the reversible polymer formation, which was introduced in the present chapter.

Experimental Section

General: Solvents were purified and dried according to standard procedures.[18] Chromatography is performed with silica gel (0.035-0.070 mm) and basic alumina, which was deactivated with 4 weight% of water to activity II. Perylene bisanhydrides applied in this work are accessible by literature procedures.[11,13,14] Zinc trifluoromethane sulfonate and all applied metal perchlorate hexahydrate salts are commercially available. ^{1}H NMR spectra were recorded on a Bruker Avance 400 spectrometer (400 MHz) and chemical shifts δ (ppm) are calibrated against tetramethylsilane (TMS) as internal reference. MALDI-TOF-MS were measured using a Bruker-Franzen ReflexII spectrometer in reflector mode. Fluorescence spectra are measured on a PTI QM-4/2003 spectrometer. All fluorescence spectra are corrected against photomultiplier sensitivity and lamp intensity. Fluorescence quantum yields were determined by the optical dilute method[19] (A < 0.05) using N,N'-di(2,6-diisopropyl-phenyl)-1,6,7,12-tetraphenoxyperylene-3,4:9,10-tetracarboxylic acid bisimide ($\Phi_{fl} = 0.96$ in chloroform)[20] as standard. Fluorescence lifetimes are determined with a fluorescence lifetime system using a PTI GL330 nitrogen laser (337 nm) and a PTI GL302 dye laser. Fluorescence decay curves were evaluated using the software supplied with the instrument. Merck Uvasol® grade solvents were used for UV-vis and fluorescence studies.

4'-*p*-Aminophenyl-2,2':6',2''-terpyridine[15] **2:** A slurry of 4'-*p*-nitrophenyl-2,2':6',2''-terpyridine[21] (1.25 g, 3.5 mmol) and palladium/charcoal catalyst (10% Pd content, 0.125 g) in dry ethanol (200 ml) is heated to reflux under argon atmosphere and a solution of hydrazine hydrate (0.85 ml, 0.87 g, 17,5 mmol) in ethanol (ca. 50 ml) is added over a period of 15 min. The mixture is refluxed for 5 h and then filtered hot through celite. The solution is kept over night at 4 °C to yield a precipitate, which is filtered and dried in vacuum. The celite material is extracted thoroughly with dichloromethane (ca. 200 ml), the extract is filtered over another batch of celite to completely remove catalyst material, and evaporated to give further product. The fractions are combined to give 0.85 g (2.62 mmol, 75 %) of a white, crystalline product.

m.p.: 256-275 °C, white needles; ^{1}H NMR (400 MHz, CDCl$_3$, TMS): δ = 8.74 (m, 2H; H6, H6''), 8.63 (d, J = 8.0 Hz, 2H; H3, H3''), 8.61 (s, 2H; H3', H5'), 8.01 (td, J = 8.0, 2.0 Hz, 2H; H4, H4''), 7.65 (d, J = 8.5 Hz, 2H; H2'', H6''), 7.49 (ddd, J = 8.0, 5.0, 1.0 Hz, 2H; H5, H5''), 6.73 (d, J = 8.5 Hz, 2H, H3''', H5'''), 5.58 (s, 2H; NH$_2$); ^{13}C-NMR (100 MHz, *d6*-DMSO) δ = 155.34, 155.33, 150.50, 149.56, 149.24, 137.33, 127.57, 124.28, 123.71, 120.80, 116.12, 114.25; MS (MALDI-TOF, dithranol[17]): *m/z*: 325.21 [M+H]$^+$ calcd. for C$_{21}$H$_{16}$N$_4$: 324.14; elemental analysis calcd (%) for C$_{21}$H$_{16}$N$_4$ (324.38): C 77.76, H 4.97, N 17.27; found: C 77.28, H 5.11, N 17.09.

***N,N'*-Di-*(p*-4'-phenyl-2,2':6',2''-terpyridyl)-1,6,7,12-tetra(4-*t*-butylphenoxy)perylene-3,4:6,10-tetracarboxylic acid bisimide 3a:** 1,6,7,12-Tetra(4-*t*-butylphenoxy)perylene-3,4:6,10-tetracarboxylic acid bisanhydride (1a) (0.70 g, 0.71 mmol) was reacted with 4'-*p*-aminophenyl-2,2':6',2''-terpyridine (2) (0.58 g, 1.79 mmol) and anhydrous zinc acetate as catalyst (70 mg) in quinoline (20 ml) for 5 h at 180 °C under argon. After cooling to room temperature, the mixture was poured on aqueous HCl (200 ml, 1 M), the resulting precipitate was allowed to settle over night and isolated by filtration and subsequently washed with water and methanol. The crude product was redissolved in a minimum amount of dichloromethane and precipitated by addition of methanol. Purification was achieved by repetitive column chromatography on aluminium oxide (basic, activity II) with a gradient from CHCl$_3$ to CHCl$_3$/MeOH (90:10) to yield 3a (415 mg, 37 %) as a dark-blue microcrystalline powder.

m.p. > 350 °C; ^{1}H NMR (400 MHz, CDCl$_3$, TMS): δ = 8.78 (s, 4H; H3', H5'), 8.73 (ddd, J = 5.0, 2.0, 1.0 Hz, 4H; H6, H6''), 8.67 (d, J = 8.0 Hz, 4H; H3, H3''), 8.29 (s, 4H; H$_{Pery}$), 8.05 (d, J = 8.5 Hz, 4H; H$_{Ar}$), 7.87 (td, J = 8.0, 2.0 Hz, 4H; H4, H4''), 7.42 (d, J = 8.5 Hz, 4H; H$_{Ar}$), 7.35 (m, 4H; H5, H5''), 7.24 (d, J = 9.0 Hz, 4H; H$_{Ar}$), 6.87 (d, J = 9.0 Hz, 4H; H$_{Ar}$), 1.27 (s, 36H; CH$_3$); UV-vis (CHCl$_3$): λ_{max} (ε) = 590 (54500), 549 (32800), 458 nm (17500 M^{-1}cm^{-1});

fluorescence (CHCl$_3$): λ_{max} = 620 nm, quantum yield (CHCl$_3$): Φ_{fl} = 0.91, lifetime (λ_{ex} = 520 nm, λ_{em} = 645 nm): τ = 6.1 ns (CHCl$_3$), 4.8 ns (DMF); MS (MALDI-TOF, dithranol): m/z 1597.51 [M+H]$^+$ (calcd for C$_{106}$H$_{84}$N$_8$O$_8$: 1596.64); elemental analysis calcd (%) for C$_{106}$H$_{84}$N$_8$O$_8$ (1597.9): C 79.68, H 5.30, N 7.01; found C 79.48; H 5.31, N 6.96.

N,N'-Di-*(p*-4'-phenyl-2,2':6',2''-terpyridyl)-1,6,7,12-tetra(4-*(1,1,3,3-tetramethylbutyl)*-phenoxy)perylene-3,4:6,10-tetracarboxylic acid bisimide 3b: The compound was synthesized and purified in the same way as described for **7a** starting from the respective 1,6,7,12-tetra(4-1,1,3,3-tetramethylbutylphenoxy)perylene-3,4:6,10-tetracarboxylic acid bisanhydride (**1b**) (400 mg, 0.33 mmol) and 4'-*p*-aminophenyl-2,2':6',2''-terpyridine (**6**) (320 mg, 1 mmol) to yield **3b** (72.3 mg, 0.04 mmol, 12%) as a bright-red powder: m.p. >350 °C; ^{1}H NMR (400 MHz, CDCl$_3$, TMS): δ = 8.78 (s, 4H; H3', H5'), 8.72 (d, J = 4.0 Hz, 4H; H6, H6''), 8.66 (d, J = 8.0 Hz, 4H; H3, H3''), 8.22 (s, 4H; H$_{Pery}$), 8.03 (d, J = 8.5 Hz, 4H; H3''', H5'''), 7.86 (td, J = 7.5 , 2.0 Hz, 4H; H4, H4''), 7.40 (d, 2H, J = 5.5 Hz, 4H; H2''', H6'''), 7.35 (dd, J = 7.0, 5.0 Hz, 4H; H5, H5''), 7.17 (d, J = 8.5 Hz, 8H; H$_{Ar}$), 6.85 (d, J = 8.5 Hz, 8H; H$_{Ar}$), 1.71 (s, 8H; CH$_2$), 1.34 (s, 24H; CH$_3$); 0.75 (s, 36H; CH$_3$); UV-vis (CH$_2$Cl$_2$): λ_{max} (ε) = 586 (54800), 548 (33800), 453 nm (18100 M^{-1}cm^{-1}); fluorescence (CH$_2$Cl$_2$): λ_{max} = 620 nm, quantum yield (CH$_2$Cl$_2$): Φ_{fl} = 0.95; MS (MALDI-TOF, DHB^{17}): m/z 1821.74 [M+H]$^+$ (calcd for C$_{122}$H$_{116}$N$_8$O$_8$: 1820.89); elemental analysis calcd (%) for C$_{122}$H$_{116}$N$_8$O$_8$·H$_2$O (1840.3): C 79.62, H 6.46, N 6.09; found: C 79.89, H 6.42, N 5.94.

Monotopic Ligands 5a,b: The respective mixtures of mono- (**4a,b**) and bisanhydrides (**1a,b**) (20% content of monoanhydrides) were reacted with 4'-*p*-aminophenyl-2,2':6',2''-terpyridine **2** and purified under the same conditions as described above. Monotopic *tert*-butylphenoxy ligand **5a**: (353 mg, 0.26 mmol, 40% calcd on monoanhydride content), blue powder: m.p. > 350 °C; ^{1}H NMR (400 MHz, CDCl$_3$, TMS): δ = 8.76 (s, 2H; H3', H5'), 8.72 (ddd, J = 5.0, 2.0, 1.0 Hz, 2H; H6, H6'), 8.66 (dt, J((H,H) = 8.0, 1.0 Hz, 2H; H3, H3'), 8.26 (s, 2H; H$_{Pery}$), 8.25 (s, 2H; H$_{Pery}$), 8.04 (d, J = 8.5 Hz, 2H; H$_{Ar}$), 7.87 (td, J = 7.5, 2.0 Hz, 2H; H4, H4'), 7.41 (d, J = 8.5 Hz, 2H; H$_{Ar}$), 7.35 (m,2H; H5, H5'), 7.26-7.22 + CHCl$_3$ (m; H$_{Ar}$), 7.87-6.83 (m, 8H; H$_{Ar}$), 4.12 (t, J = 7.5 Hz, 2H; NCH$_2$), 1.67 (m, 2H; CH$_2$), 1,43 (m, 2H; CH$_2$), 1.30 (s,18H; CH$_3$), 1.26 (s, 18H; CH$_3$), 0.94 (t, J = 7.5 Hz, 3H; CH$_3$); UV-vis (CHCl$_3$): λ_{max} (ε) = 587 (52100), 547 (31000), 455 nm (17700 M^{-1}cm^{-1}); fluorescence (CHCl$_3$): λ_{em} = 622 nm, quantum yield (CHCl$_3$): Φ_{fl} = 0.89; MS (MALDI-TOF, dithranol): m/z 1346.50 [M+H]$^+$ (calcd for C$_{89}$H$_{79}$N$_5$O$_8$: 1345.59); elemental analysis calcd (%) for

$C_{89}H_{79}N_5O_8$ (1346.61): C 79.38, H 5.91, N 5.20; found C 79.18; H 6.08, N 5.12.

Monotopic *tert*-octylphenoxy-ligand **5b**: (10 mg, 0.06 mmol, 7% calcd on monoanhydride content), bright-red powder: m.p. > 350 °C; ^{1}H NMR (400 MHz, CDCl$_3$, TMS): δ = 8.77 (s, 2H; H3', H5'), 8.72 (d, J = 4.0 Hz, 2H; H6, H6''), 8.66 (d, J = 8.0 Hz, 2H; H3, H3''), 8.19 (s, 2H; H$_{Pery}$), 8.18 (s, 2H; H$_{Pery}$), 8.03 (d, J = 8.5 Hz, 2H; H3''', H5'''), 7.86 (td, J = 7.5, 2.0 Hz, 2H; H4, H4''), 7.40 (d, 2H, J = 5.5 Hz, 2H; H2''', H6'''), 7.35 (dd, J = 7.0, 5.0 Hz, 2H; H5, H5''), 7.29-7.25 (m, 8H; H$_{Ar}$), 6.89-6.85 (m, 8H; H$_{Ar}$), 4.11 (t, J = 7.5 Hz, 2H; NCH$_2$), 1.73 (s, 4H; CH$_2$), 1.70 (s, 4H; CH$_2$), 1.65 (m, 2H; CH$_2$); 1.43 - 1.33 (m, 26H; CH$_3$), 0.94 (t, J = 7.0 Hz, 3H; CH$_3$), 0.79 (s, 18H; CH$_3$), 0.75 (s, 18H; CH$_3$); UV-vis (CHCl$_3$): λ_{max} (ε) = 590 (49000), 549 (29400), 454 nm (17500 M^{-1}cm^{-1}); fluorescence (CHCl$_3$): λ_{max} = 620 nm, quantum yield (CHCl$_3$): Φ_{fl} = 0.90; MS (MALDI-TOF, dithranol): *m/z* 1570.58 [M+H]$^+$ (calcd for $C_{105}H_{111}N_5O_8$: 1569.84); elemental analysis calcd (%) for $C_{105}H_{111}N_5O_8$ (1571.0): C 80.27, H 7.12, N 4.46; found: C 79.72, H 7.13, N 4.24.

Model Complex [(5a)$_2$Zn][OTf]$_2$ 6a: To a solution of the monotopic ligand **5a** (13.3 mg, 9.8 µmol) in CHCl$_3$–CH$_3$CN (80:20, 4 ml) a stock solution of zinc triflate (10 mM, 490 µl, 4.9 µmol) was added and the solution was stirred for one hour at room temperature. Exact 2:1 stoichiometry is confirmed by ^{1}H NMR and, if necessary, is adjusted until no residual signals of the uncomplexed ligand is present. The solution was condensed, the product was precipitated by addition of more acetonitrile (10 ml) and isolated quantitatively by centrifugation.

^{1}H NMR (400 MHz, CDCl$_3$ / CD$_3$CN (80:20), TMS): δ = 9.00 (s, 4H; H3', H5'), 8.72 (d, J = 8.5 Hz, 4H; H3, H3''), 8.31 (d, J = 8.5 Hz, 4H; H$_{Ar}$), 8.24–8.12 (12H; H$_{Pery}$, H4, H4''), 7.80 (d, J = 5.0 Hz, 4H; H6, H6''), 7.65 (d, J = 8.5 Hz, 4H; H$_{Ar}$), 7.44 + CHCl$_3$ (m, 4H; H5, H5''), 7.28 (m, 16H; H$_{Ar}$), 6.87 (m, 16H; H$_{Ar}$), 4.10 (t, J = 6.5 Hz, 4H; NCH$_2$), 1.66 (m, 4H; CH$_2$), 1.41 (m, 4H; CH$_2$), 1.31 (s, 32H; CH$_3$), 1.29 (s, 32H; CH$_3$), 0.95 (t, J = 7.5 Hz, 6H; CH$_3$); UV-vis (CHCl$_3$): λ_{max} (ε) = 589 (103500), 548 (60700), 457 nm (34000 M^{-1}cm^{-1}); fluorescence (CHCl$_3$): λ_{max} = 623 nm, quantum yield: Φ_{fl} = 0.90 (CHCl$_3$), 0.75 (DMF), lifetime (λ_{ex} = 520 nm, λ_{em} = 645 nm): τ = 6.3 ns (CHCl$_3$), 5.5 ns (DMF); MS (MALDI-TOF, DCTB[17]): *m/z* (%) 2904.05 (100) [M+OTf]$^+$, 2755.15 (10) [M]$^+$, 1554.52 (10) [**5a**+Zn+OTf]$^+$, 1345.59 (20) [**5a**+H]$^+$ (calcd for $C_{178}H_{158}N_{10}O_{16}Zn$: 2755.11).

Coordination Polymer 8a: To a solution of the ditopic ligand **3a** (19.6 mg, 12.3 µmol) in CHCl$_3$–CH$_3$CN (80:20, 4 ml) a stock solution of zinc triflate (10 mM, 1.23 ml, 12.3 µmol)

was added and the solution was stirred for one hour at room temperature. The exact 1:1 stoichiometry is checked by ^{1}H NMR and, if necessary, was adjusted until no residual signals of uncomplexed ligand was observed. The solution was condensed, the product is precipitated by addition of more acetonitrile (10 ml) and isolated quantitatively by centrifugation.

^{1}H NMR (400 MHz, CDCl$_3$ / CD$_3$CN (80:20), TMS): δ = 9.03 (br, 4H; H3'), 8.75 (br, 4H), 8.4–8.1 (br, 8H), 7.82 (br, 4H), 7.66 (br, 4H), 7.43+CHCl$_3$ (br, 4H), 7.31 (br, 8H; H$_{Ar}$), 6.92 (br, 8H; H$_{Ar}$), 1.31 (br, 36 H; CH$_3$); UV-vis (DMF): λ_{max} (ε) = 575 (45500), 537 (28600), 446 nm (14750 M^{-1}cm^{-1}); fluorescence (DMF): λ_{max} = 613 nm, quantum yield (DMF): Φ_{fl} = 0.61, lifetime (DMF, λ_{ex} = 520 nm, λ_{em} = 645 nm): τ = 4.9 ns.

^{1}H NMR Titration Experiments for Dimer 6a and Polymer 8a: To a solution of the monotopic (**5a**) or ditopic (**3a**) perylene bisimide ligand (5 mM in CDCl$_3$-CD$_3$CN, 80:20) were added aliquots of zinc triflate (10 mM in CDCl$_3$-CD$_3$CN, 80:20) and ^{1}H NMR spectra were recorded after each addition.

UV-vis Titration Experiments for Dimer 6a and Polymer 8a: The titrations were performed as constant host titrations using a solution of the respective monotopic (**5a**) or ditopic (**3a**) ligand (2.5×10^{-5} M in CHCl$_3$-MeOH, 60:40) to which aliquots of a zinc triflate solution (2.5×10^{-4} M in the respective ligand solution) are added and the UV-vis spectra (Perkin Elmer Lambda 40P, 1 cm quartz cuvettes) were recorded after each addition.

Fluorescence Titrations for Dimer 6a with Iron Perchlorate and Zinc Triflate: The titrations were performed as constant host titrations using a 10^{-5} M solution of the monotopic ligand **5a** in chloroform-methanol (60:40) and the solution of the respective metal salt (10^{-4} M in the ligand solution). Aliquots of the metal salt solution were added and the fluorescence spectrum was recorded (λ_{ex} = 550 nm, λ_{em} = 560-800nm, 1cm quartz fluorescence cuvettes, PTI QM-4/2003 spectrometer).

References

(^{1}) Herbst, W.; Hunger, K. *Industial Organic Pigments : Production, Properties, Applications*, 2nd Ed.; VCH: Weinheim **1997**.

(^{2}) Zollinger, H. *Color Chemistry : Synthesis, Properties and Application of Organic Dyes and Pigments*, 2nd Ed.; VCH: Weinheim **1991**.

(^{3}) Langhals, H. *Heterocycles* **1995**, *40*, 477-500

(^{4}) G. Seybold and G. Wagenblast, *Dyes Pigm.*, 1989, **11**, 303-317; G. Seybold and A. Stange (BASF AG), *German Pat.*, DE 35 45 004, 1987, *Chem. Abstr.*, 1988, **108**, 77134c.

(^{5}) Ego, C.; Marsitzky, D.; Becker, S.; Zhang, J.; Grimsdale, A. C.; Müllen, K.; MacKenzie, J. D.; Silva. C; Friend, R. H. *J. Am. Chem. Soc.* **2003**, *125*, 437-443.

(^{6}) Qu, J.; Pschirer, N. G.; Liu, D.; Stefan, A.; De Schryver, F. C.; Müllen, K. *Chem. Eur. J.* **2004**, *10*, 528-537.

(^{7}) Weil, T.; Reuther, E.; Müllen, K. *Angew. Chem. Int. Ed.* **2002**, *41*, 1900-1904.

(^{8}) van der Boom, T.; Hayes, R. T.; Zhao, Y.; Bushard, P. J.; Weiss, E. A.; Wasielewski, M. R. *J. Am. Chem. Soc.* **2002**, *124*, 9582-9590.

(^{9}) Würthner, F. *Chem. Commun.* **2004**, 1564-1579.

(^{10}) (a) Sautter, A.; Thalacker, C.; Würthner, F. *Angew. Chem. Int. Ed.* **2001**, *40*, 4425-4428; (b) Würthner, F.; Thalacker, C.; Diele, S.; Tschierske, C. *Chem. Eur. J.* **2001**, *7*, 2245-2253.

(^{11}) Würthner, F.; Thalacker, C.; Sautter, A.; Schärtl, W.; Ibach, W.; Hollricher, O. *Chem. Eur. J.* **2000**, *6*, 3871-3886.

(^{12}) Thalacker, C.; Würthner, F. *Adv. Funct. Mater.* **2002**, *12*, 209-218.

(^{13}) Würthner, F.; Sautter, A.; Schmid, D.; Weber, P. J. A. *Chem. Eur. J.* **2001**, *7*, 894-902.

(^{14}) Dotcheva, D.; Klapper, M.; Müllen, K. *Macromol. Chem. Phys.* **1994**, *195*, 1905-1911;

(^{15}) A similar procedure has been published recently: Laine, P.; Bedioui, F.; Ochsenbein, P.; Marvaud, V.; Bonin, M.; Amouyal, E. *J. Am. Chem. Soc.* **2002**, *124*; 1364-1377.

(^{16}) Würthner, F.; Sautter, A.; Schmid, D.; Weber, P. J. A. *Chem. Eur. J.* **2001**, *7*, 894-902.

(^{17}) Matrices for MALDI-MS: dithranol = 1,8,9-anthracenetriol, DHB = 2,5-dihydroxybenzoic acid, DCTB = trans-2-(3-4-*tert*-butylphenyl)-2-methyl-2-propenylidene)malonitrile

([18]) Perrin, D. D.; Armarego, W. L. F. *Purification of Laboratory Chemicals*, 2nd ed., Pergamon Press, Oxford, **1980**.

([19]) Lakowicz, J. R. *Principles of Fluorescence Spectroscopy*, 2nd ed., Kluwer Academic/Plenum, New York, **1999**.

([20]) Gvishi, R.; Reisfeld, R.; Burshtein, Z. *Chem. Phys. Lett.* **1993**, *213*, 338-344.

([21]) Mukkala, V.-M.; Helenius, M.; Hemmilae, I.; Kankare, J.; Takalo, H. *Helv. Chim. Acta* **1993**, *76*, 1361-1378.

4

Perylene Bisimide – Terpyridine Coordination Polymer

Abstract: In this chapter, the reversible formation of coordination polymers from perylene bisimide fluorophores equipped with terpyridine ligands is proven by two diffusion based methods, i.e. DOSY NMR spectroscopy and fluorescence anisotropy measurements. Both methods revealed that the diffusion coefficient of the coordination polymer is significantly lower than the monomer from which it is constructed, presenting clear evidence for the presence of an assembly of significantly increased size. The reversibility of the complexation could be observed by the significant increase of the diffusion coefficients if the 1:1 ratio of Zn^{2+} and ditopic ligand is exceeded. Additionally, AFM micrographs of the uncomplexed monomers and the coordination polymers could be obtained which clearly show the presence of polymeric chains.

Introduction

The average number of repeat units that are incorporated in a single polymer chain is the most important quantity for polymer characterization. This degree of polymerization X can be expressed by the ratio of polymer molecular weight against the molecular weight of the monomers. As polymers do not exhibit a uniform, exact molecular weight, but a more or less broad distribution of chain lengths with individual statistical weights, the average of a molecular weight distribution is determined.[1,2] Depending on the characterization method, different types of average values are detected. The number average molecular weight M_n is defined as

$$\overline{M}_n = \frac{\sum\limits_i N_i M_i}{\sum\limits_i N_i} \qquad \textbf{Equation 1}$$

where N_i are the number of molecules with the molecular weight M_i. determination of M_i is possible by end group analysis or experiments based on colligative properties like osmometry. The second important value is the weight average molecular weight M_w, which is defined as

$$\overline{M}_w = \frac{\sum\limits_i m_i M_i}{\sum\limits_i m_i} \qquad \textbf{Equation 2}$$

where m_i is the mass of material of molecular weight M_i. As the compounds with higher mass contribute relatively more to the average when mass fractions instead of number fractions are used, the value for M_w will always be higher than M_n. The weight fraction can for example be determined by light scattering methods. Gel permeation chromatography (GPC) can be used to determine both types of values. Further methods for molecular weight determination are viscosimetry or sedimentation methods like ultracentrifugation.

For supramolecular polymers the situation is more complicated since the monomer units are not connected by covalent bonds but by weaker, noncovalent interactions like for example hydrogen bonding[3] or metal-ligand interactions.[4] These interactions span a wide range of binding strengths and can be influenced by a number of parameters like the nature of the solvent, temperature and concentration or external influences like shear forces. As a consequence, characterization methods must not influence the interaction that forms the supramolecular polymeric species. This requirement implies that for many systems only indirect, noninvasive characterization methods can be applied, which do not disturb the equilibrium of the sample with the surrounding solvent.

Since the increase in molecular weight is always connected with an increase in the size of the particle, the latter is a significant change during any polymer formation and a number of methods, like for example light-scattering, are based on the direct or indirect determination of the polymer size. The increase in size is further correlated with a decrease of the diffusion coefficient, so that the determination of the latter gives an indirect inference on the molecular size and weight. The measurement of diffusion phenomena is done under equilibrium conditions and any disturbance like flow or convection is excluded, which makes the method ideally suited for the characterization of noncovalently bound supramolecular systems. Terpyridine based coordination polymers have been characterized by various methods. Since most of the reported tpy polymer systems are constructed from $M(tpy)_2^{2+}$ units which show no or only negligible reversibility by application of Ru^{2+} or Fe^{2+}, the methods were not as restricted as for reversible systems. In addition to standard NMR techniques, viscosimetric studies[5,6] and ultracentrifugation[7] was used for the characterization of terpyridine-based coordination polymers.

The perylene bisimide coordination polymers which are constructed by the zinc(II) terpyridine metal-ligand interaction (Chapter 3) show the aforementioned problems with standard polymer characterization methods because the zinc-terpyridine interaction is strong from the supramolecular point of view, but anyhow exhibits reversibility, resulting for example in the fragmentation of the coordination polymer when eluted through a GPC column caused by the continuous dilution. Therefore, DOSY NMR spectroscopy has been employed to determine translational diffusion under equilibrium conditions. The fluorescence properties of the coordination polymers can be used for the observation of rotational diffusion by applying fluorescence anisotropy measurements.

With the evolution of scanning probe techniques like scanning tunneling microscopy (STM) or atomic force microscopy (AFM) and their possibility to resolve images on the atomic scale, also the direct visualization of polymer chains became possible, allowing the length measurement of individual strands without an intrinsic averaging effect of the method. The advantage of the microscopic methods for the investigation of supramolecular species is that the systems have to be adsorbed on a solid substrate, for example by a spin-coating process. As most supramolecular systems are irreversibly fixed in the absence of solvent, their stability is sufficient for imaging with the scanning probe tip. However, it has to be kept in mind that the substrate can exert an influence on the system by adsorption interactions so that the structure visualized by scanning probe methods does not necessarily reflect the structure in solution.

Results and Discussion

DOSY NMR Studies on Coordination Polymer Formation

Introduction. The mobility of molecules in liquid solution can be divided into rotational and translational motion. The latter, also known as Brownian molecular motion, is often simplified as diffusion or self-diffusion. It depends on a number of physical parameters like the size and shape of the molecule, temperature and solvent viscosity. The relation between the translational diffusion coefficient D (at infinite dilution) and the size of a molecule (represented by its radius r) is described by the Stokes-Einstein equation[8] for spherical compounds:

$$D = \frac{k_B T}{6\pi \cdot \eta \cdot r} \qquad \textbf{Equation 3}$$

where k_B is the Boltzmann constant, T the temperature, η the viscosity of the solvent and r the hydrodynamic radius of the molecule. In the case of nonspherical molecules, the equation gives the radius of a so-called "hydrodynamically equivalent sphere", i.e. the respective radius if the molecule was a impermeable sphere of the same volume. DOSY NMR (diffusion ordered spectroscopy)[9] is an extremely useful technique for the determination of translational diffusion coefficients as it is noninvasive allowing the measurement under equilibrium conditions. Since in this two-dimensional NMR technique the ^{1}H NMR spectrum is plotted against the diffusion coefficient D, the structural information given by the chemical shift can be clearly assigned to the diffusion coefficient of the corresponding species. Thus the size as well as the size distribution (in the slow exchange limit) can be assigned by this technique. The method has recently been successfully applied to characterize supramolecular coordination polymers.[10,11]

The method is based on the spatial labeling of molecules by using a magnetic field gradient along the z-direction of the spectrometer, i.e. the position of a molecule within the sample tube is marked. After a diffusion time Δ, in which the molecules change their position due to translational diffusion, their new positions can be resolved by application of a second gradient. The measured signal is attenuated depending on the length of the diffusion time Δ and the parameters of the applied field gradient (g = gradient strength, δ = gradient length) following the following relation:

$$I = I_0 \cdot e^{-D\gamma^2 g^2 \delta^2 (\Delta - \frac{\delta}{3})} = I_0 \cdot e^{-Dg^2 \cdot const} \qquad \textbf{Equation 4}$$

where I is the observed signal intensity, I_0 is the unattenuated signal intensity, D is the diffusion coefficient, γ the gyromagnetic ratio of the observed nucleus. If all experimental parameters are kept constant, the observed intensity I only depends on the diffusion coefficient. In the DOSY experiment, the signal intensity is measured repeatedly with varying field gradients g and the diffusion coefficient is determined by curve fitting of the resulting Gauss curve. The pulse sequence used for DOSY experiments is a modified spin echo sequence using a bipolar field gradient.[12]
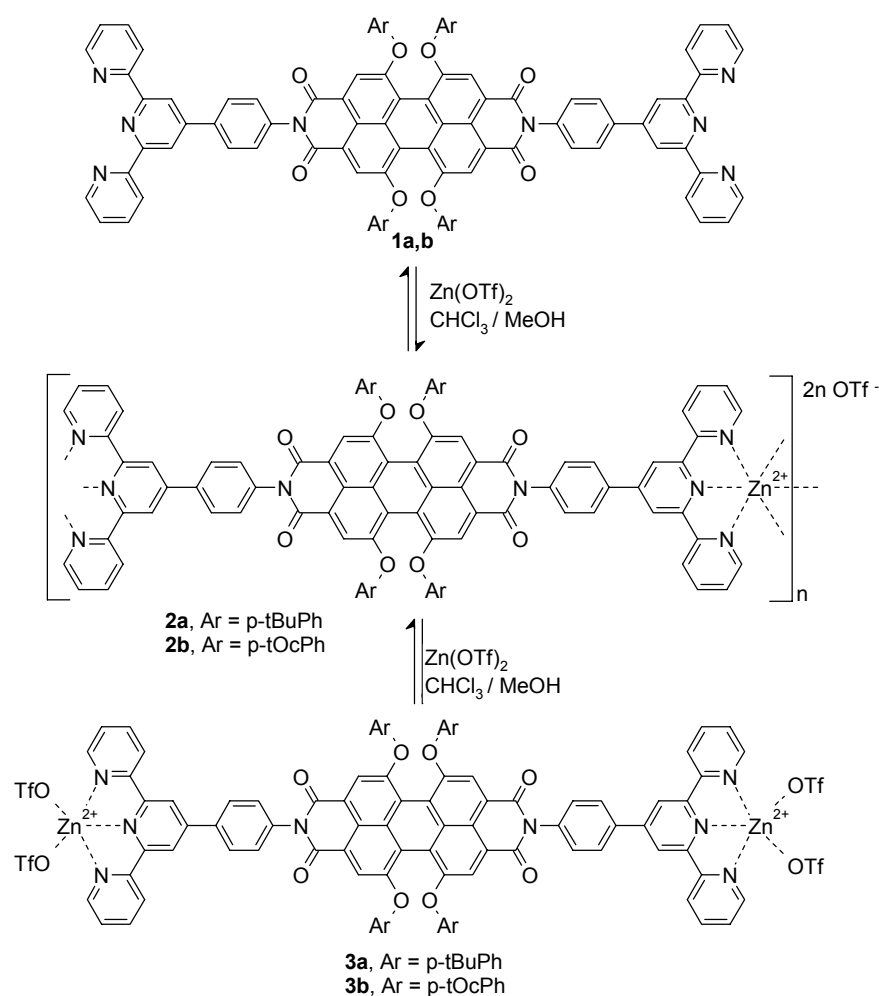
Scheme 1

Application of DOSY NMR for the characterization of the coordination polymer. To further substantiate the reversibility in polymer formation observed by ^{1}H NMR spectroscopy, DOSY (diffusion ordered spectroscopy)[13] NMR experiments were carried out. This two-dimensional NMR technique correlates the ^{1}H NMR signals with the diffusion coefficient of the respective species in solution and has recently been successfully applied to characterize supramolecular coordination polymers.[11,14] The DOSY spectra were recorded in chloroform-

methanol (80:20) first for the monomeric ligand **1b** alone, then after addition of one equivalent of Zn^{2+}, to form coordination polymer **2b**, and subsequently after addition of two more equivalents of Zn^{2+}, which should lead to fragmentation of polymer **2b** to low molecular weight species like **3b**. Figure 1 shows the aromatic region of the DOSY NMR spectra for monomer **1b** (A), polymer **2b** (C) and fragments (D) with the corresponding ^{1}H NMR spectrum plotted against the normalized logarithm of the diffusion coefficient. As the monomer **1b** is itself a large molecule with a molecular weight of $M = 1822$ g/mol, it appears at a significantly smaller diffusion coefficient (log D = -9.45) in comparison to the chloroform molecule (log D = -8.66). The diffusion coefficient of the coordination polymer **2b** in the range of log D = -10.45 is one order of magnitude smaller than that of the monomer **1b**. The strong decrease of diffusion coefficient upon addition of one equivalent of Zn^{2+} ion to monomer **1b** clearly indicates the formation of an extended, high molecular weight polymer structure with the corresponding ^{1}H NMR signals characteristic for the complexed form of the tpy unit. Upon addition of more than one equivalent of Zn^{2+} to monomer **1b**, the diffusion coefficient drops drastically to a value in the range of log D = -9.5 – -9.7, which is slightly higher than that of the monomer, indicating fragmentation of the coordination polymer to low molecular weight oligomers. For comparison, also the DOSY result of the dimer model compound **4b** is depicted in figure 1 (B). The diffusion coefficient of the model complex, which exhibits nearly twice the volume compared to the uncomplexed ditopic ligand **1b**, is virtually identical. This indicates that a significantly larger number of units is necessary to cause a tenfold decreased diffusion coefficient as found for the polymer **2b**.

4a, Ar = *p*-tBuPh
4b, Ar = *p*-tOcPh
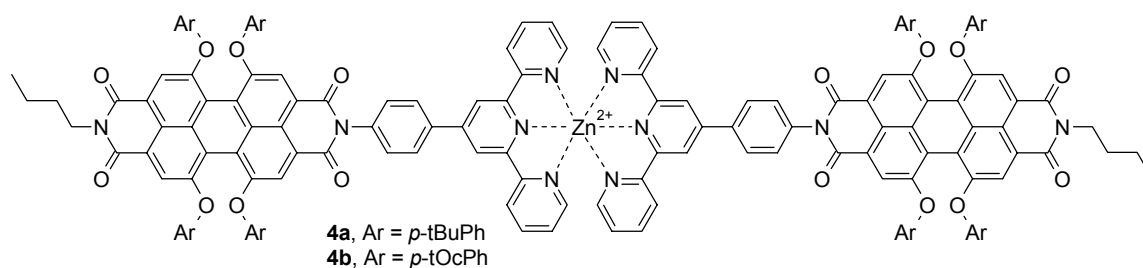
Chart 1
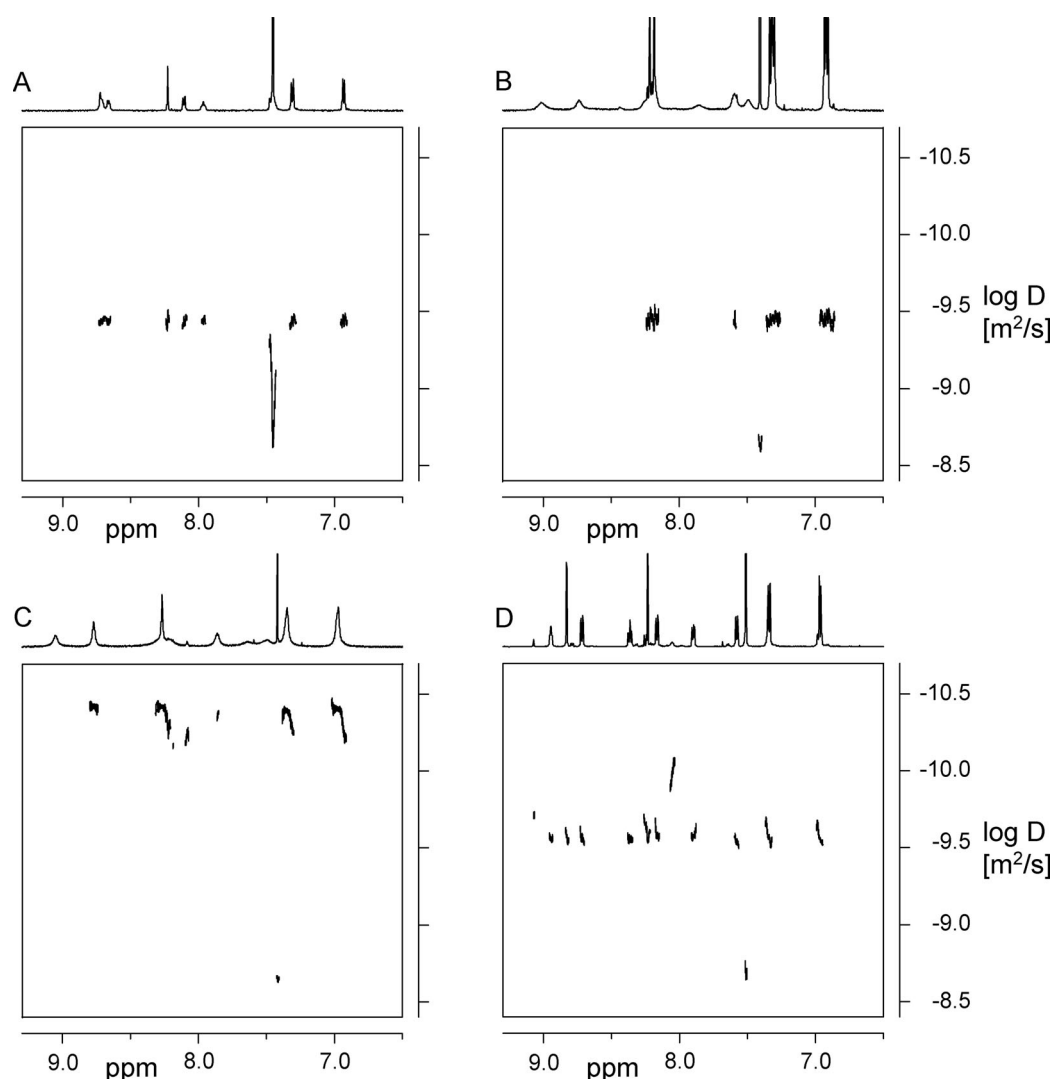
Figure 1. Aromatic region of the DOSY NMR spectra of monomer **1b** (A), dimer **4b** (B), polymer **2b** and the fragmented species **3b** (C) in chloroform–methanol (80:20). The diffusion coefficients D are plotted in a logarithmic scale against the chemical shift δ.

Solving of the Stokes-Einstein equation for the hydrodynamic radius r indicates that the there is a linear reciprocal relationship between the hydrodynamic radius and the diffusion coefficient D:

$$r = \frac{k_B T}{6\pi \cdot \eta \cdot D} \qquad \textbf{Equation 5}$$

This implies that a tenfold decrease of the diffusion coefficient, as observed when transforming the monomer **1b** into the coordination polymer **2b**, is caused by a tenfold increase of the hydrodynamic radius of the hydrodynamically equivalent sphere. Although these equations only apply for spherical molecules, the basic result still holds for elliptical or rod-like molecules and proves the formation of an extended coordination polymer.

Fluorescence Anisotropy Titration

Introduction. Fluorescence can be employed to study changes in the size of fluorophores, for example during a titration experiment, by determination of the fluorescence anisotropy.[15] The method is widespread in biology, biochemistry and medicinal chemistry to detect binding events between fluorescence-labeled ligands and biomacromolecules. The measurement of fluorescence anisotropy is based on the excitation of the fluorophore with vertically polarized light. This leads to the preferential excitation of fluorophores, whose excitation transition dipoles are collinear with the polarization direction of the excitation light, a process which is called photoselection. The emitted light will also be polarized vertically, if three prerequisites are given: (a) the molecules are fixed in their position within the duration of their fluorescence lifetime without rotational of translational diffusion or flow effects, (b) other depolarization processes like energy transfer are absent, and (c) the transition dipole moments for absorption and emission are collinear. The photoselection by excitation of a fluorophore with polarized light therefore offers the same possibility for encoding the orientation of a molecule like the application of the field gradient in DOSY NMR encodes its position in the sample. The difference is that depolarization is not caused by translational diffusion but by rotational diffusion. If the fluorophores are not fixed but are subject to rotation, then depolarization of the emitted light will be observed. As the timescales for rotational diffusion and for fluorescence (i.e. the fluorescence lifetime) are often in the same order of magnitude, polarized fluorescence measurements are sensitive for rotational processes and offer a measure of the molecular volume through the rotational diffusion coefficient.

The relevant quantity for the fluorescence depolarization is the anisotropy r. Anisotropy measurements are done by exciting the sample with vertically polarized light and detecting the fluorescence intensities with the emission polarizer in both vertical and horizontal alignment, and r is then calculated using the equation:

$$r = \frac{I_{VV} - I_{VH}}{I_{VV} + 2I_{VH}} \qquad \textbf{Equation 6}$$

The terms I_{VV} and I_{VH} represent the fluorescence intensities at vertical (V) or horizontal (H) orientation of the excitation (first subscript) and the emission (second subscript) polarizer with respect to the excitation/emission plane. The anisotropy can range between +0.4 and -0.2 with 0 indicating totally depolarized emission. The Perrin equation connects the anisotropy with external parameters:

$$\frac{r_0}{r} = 1 + \frac{\tau}{\theta} = 1 + 6D_R\tau \qquad \textbf{Equation 7}$$

$$\theta = \frac{\eta \cdot V}{RT} \qquad \textbf{Equation 8}$$

In this equation, r_0 represents the limiting anisotropy in the absence of diffusion effects, which can be determined at low temperatures in highly viscous solution, τ is the fluorescence lifetime of the fluorophore and D_R is the rotational diffusion coefficient. The term θ is the rotational correlation time, which depends on the molecular volume V, the viscosity η of the solvent and the temperature T. If the correlation time is significantly higher than the fluorescence lifetime ($\theta \gg \tau$), then the anisotropy r will be equal to r_0, since no movement of the excited fluorophore is possible. In the inverse case, when $\theta \ll \tau$ the anisotropy will be zero and the fluorescence will be totally depolarized. It has to be noted that the abovementioned equations only hold for spherical chromophores. The (oblate or prolate) shape of fluorophores can be judged from time dependent anisotropy measurements, which resolve the contributions of various individual correlation times.

Application to coordination polymer formation. In a titration experiment of stepwise addition of zinc triflate to the ditopic perylene bisimide ligand **1b**, which transforms the monomer **1b** to the coordination polymer **2b** and subsequently fragments the latter into short oligomeric species like **3b**, all involved species exhibit the strong red perylene bisimide fluorescence. This offers, in addition to DOSY NMR, a second diffusion based method for proving the model of reversible coordination polymer formation as the three species involved should exhibit significantly different diffusion behavior. Fluorescence anisotropy measurements have already been applied successfully to characterize supramolecular perylene bisimide aggregates.[16]

Figure 2 shows a plot of the fluorescence anisotropy r of the perylene bisimide ligand **1b** against the Zn^{2+}/**1b** ratio. The chromophore was excited in the $S_0 \rightarrow S_1$ transition at 550 nm and the fluorescence was detected at 610 nm, to ensure the highest possible anisotropy value, since the $S_0 \rightarrow S_1$ absorption dipole moment is expected to be collinear with the respective fluorescence dipole moment. The titration was performed in a chloroform-methanol mixture to ensure comparability with the UV-vis and fluorescence titration experiments (c.f. Chapter 3). For the monomer **1b**, an anisotropy value of $r = 0.045$ was observed which increased nearly linearly to a maximum of $r = 0.133$ at a 1:1 ratio of Zn^{2+} and **1b**. These results confirm the formation of a larger species **2b**. Due to the fact that in the rigid coordination polymer all chromophores are aligned in the direction of their fluorescence transition dipole moments, which are located along the *N,N*-axis of the perylene bisimide unit, potential energy transfer

within the perylene bisimide units along the strands should not decrease anisotropy. As expected, the anisotropy decreases again upon exceeding the 1:1 stoichiometry due to the fragmentation of the polymer into oligomeric units. The value saturates at $r = 0.091$, indicating that these fragments are significantly smaller than the polymer but still larger than the monomeric unit. These results are consistent with that of the DOSY NMR experiments. A similar titration with ligand **1a** showed the same characteristics, only differing in the absolute r-values, which were $r = 0.048$ for the monomer, $r = 0.096$ for the polymer (**2a**) and $r = 0.062$ for the oligomeric fragments **3a**. The smaller values for **2a** may be explained in terms of the less steric demand of the *tert*-butyl groups compared to the very bulky *tert*-octyl residues in **2b**. The smaller steric demand lowers the molecular volume of **2a** and consequently increases the diffusion coefficient to decline anisotropy value.
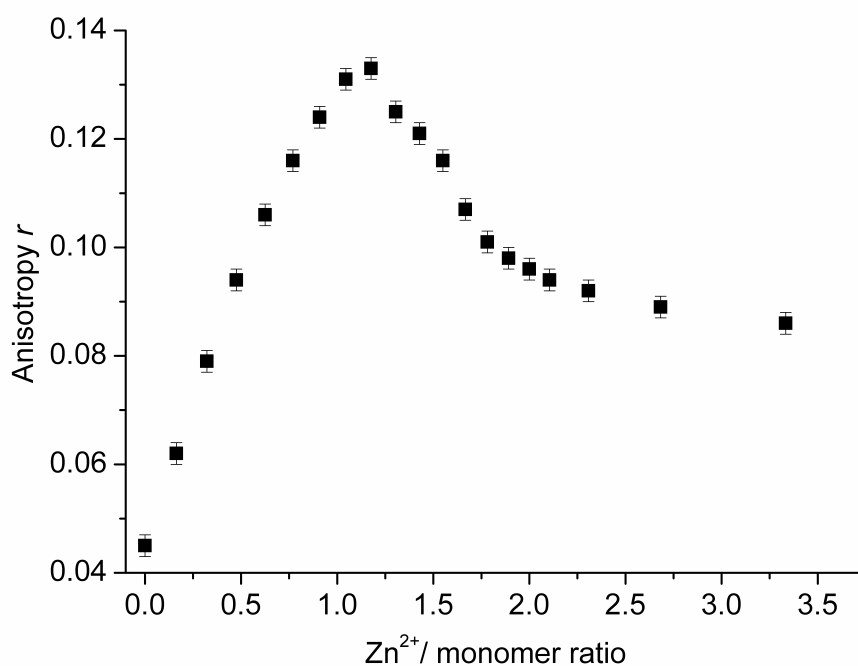

Figure 2. Fluorescence anisotropy titration of monomer **1b** with zinc triflate in chloroform-methanol (60:40, [**1b**] = 2.5×10^{-5} M, λ_{ex} = 550 nm, λ_{em} = 610 nm, 20.0±0.1 °C), error bars are ±0.005.

Atomic Force Microscopy (AFM)

The aim of atomic force microscopy experiments was to determine the shape and size of the single polymer strands as well as their two-dimensional organization on a surface. The uncomplexed ligand molecules **1a**, which were deposited via spin-coating of DMF solution onto freshly cleaved mica, appeared as isolated dots (figure 3, A). The height of these globular objects was found to be quite homogeneous with a mean value of 1.6±0.1 nm. Due to the tip broadening effect, a rather high value of 9.2±1.2 nm was obtained for the mean diameter of the particles. Samples of the coordination polymers **2a,b** were prepared by spin-coating of DMF solutions of different concentration on both mica and HOPG (highly ordered pyrolytic graphite) substrates. AFM images of the polymers **2a,b** (figure 3, B, F-H) clearly show the linear appearance of the polymers on both types of substrates. Mean heights of the strands reveal the same value of 1.6±0.1 nm for both polymers **2a,b**. However, in comparison to the very uniform heights, the apparent length of the rods shows a broad distribution. For both polymers long filaments up to 400 nm in length as well as very small globular objects, similar to the ligand molecules, can be observed. The apparent length of the polymers measured by AFM revealed a mean value of 50.1±5.3 nm. Molecular modeling of the ligand and the coordination polymer (figure 4, MM3 force field) reveals a length of 3 nm for each repeat unit. Comparison of the measured mean length with the calculated model suggests that a single rod is formed from approximately 15 repeat units corresponding to a molecular weight of ~25000. The diameter of the polymer strand determined from molecular modeling is 1–2 nm and depends on the conformation of the phenoxy residues. This is in very good agreement with the measured height of 1.6 nm suggesting that no vertical aggregation of the strands takes place. Another information which can be extracted from molecular modeling studies is the relative flexibility of the polymer strand. Although the $M(tpy)_2$ unit represents a very rigid linkage, the two single bonds of the phenyl rings connecting perylene bisimide and tpy provide some flexibility which has also been observed by in AFM showing curvature of the individual strands.
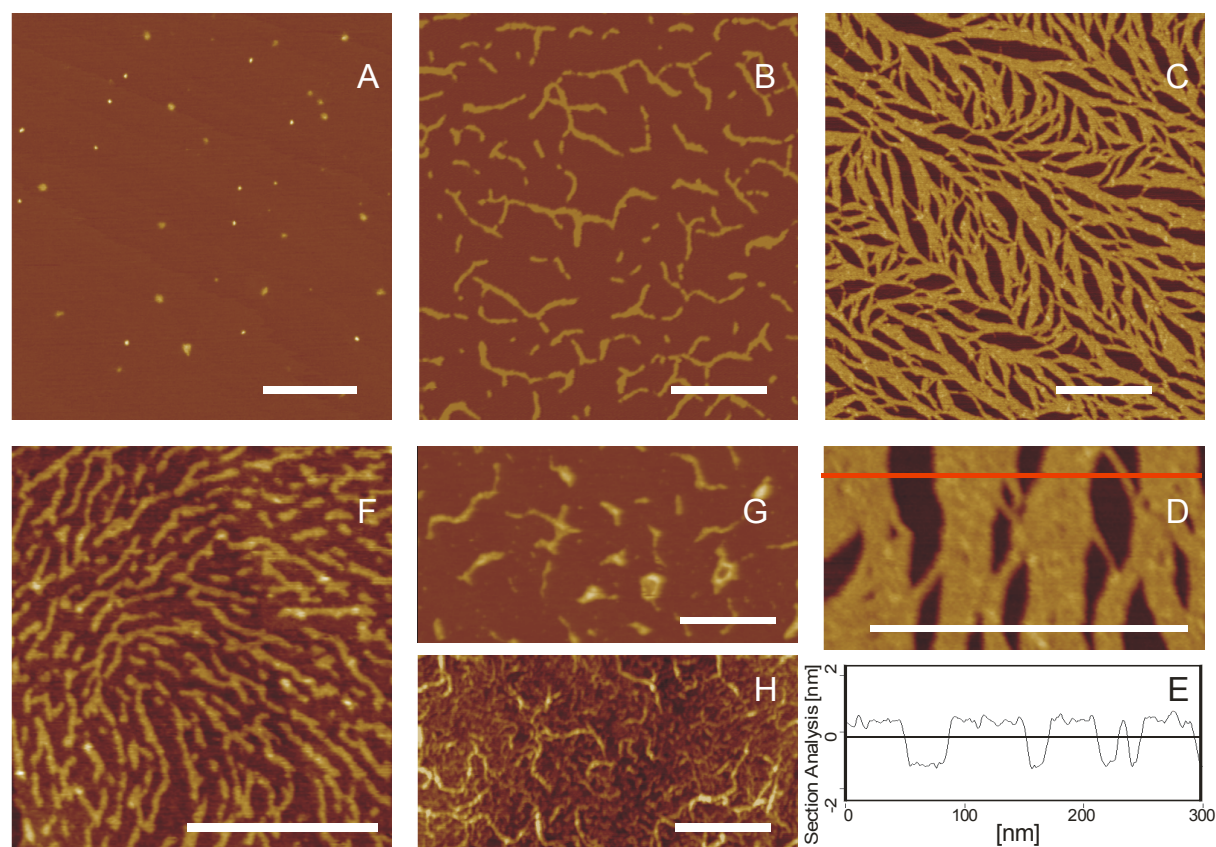
Figure 3. (A) AFM image of ligand **1a** on mica and the corresponding coordination polymer **1a** prepared from dilute (B, 0.1 mM) and concentrated (C, 1 mM) DMF solution on mica; (D) high resolution AFM image with feather-like structures, a cross-section along red line is presented in (E); (F) coordination polymer **2a** (0.1 mM) on HOPG; coordination polymer **2b** (0.05 mM) on mica (G) and HOPG (H). In all AFM images the scale bar corresponds to 250 nm, z data scale is 5 nm. All samples were prepared by spin-coating.
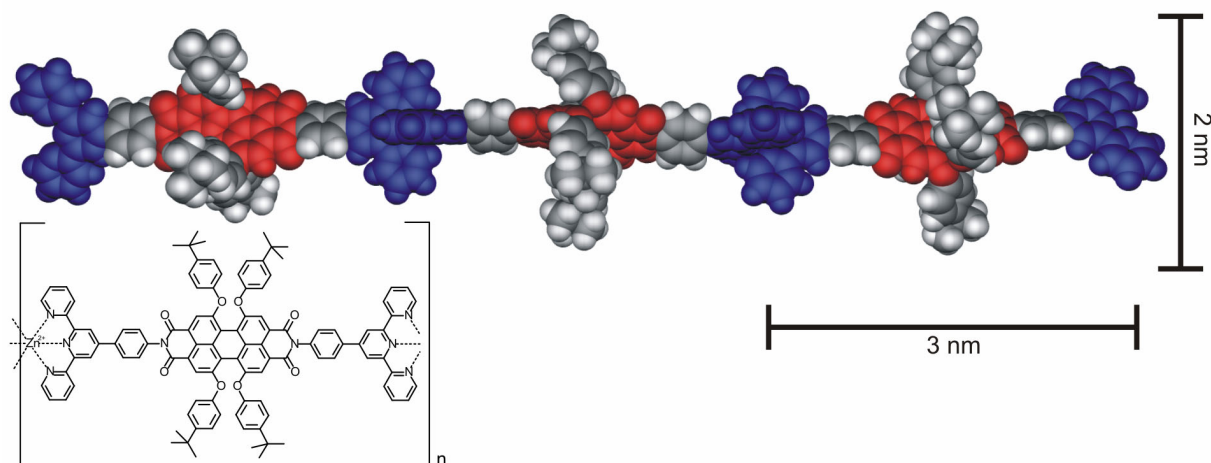
Figure 4. Molecular modeling (Fujitsu Quantum CAChe 5.2, MM3 force field) and schematic representation of coordination polymer **8a**; three repeat units are shown, perylene bisimide units are represented in red, $Zn(tpy)_2$ units in blue.

Investigation of more concentrated solutions (1 mM) reveal the formation of a dense film over large areas in the µm range for both types of substrates (figure 3, C and D). Also in this case analysis of the apparent height measured from the AFM images revealed a value of 1.5±0.1 nm (figure 3, D, E). From the AFM images it is evident that the neighboring strands

tend to interact with each other, forming 2D layers. Because of the spreading of the polymer samples in the surface plane, probably caused by the spin-coating process, defects in the packing of the polymer chains are observed, enabling the visualization of the some single chains. Lateral dimensions of single chains were measured to be approximately 4 nm. Definitely, under higher concentration the polymer tends to aggregate by contacting terminally and laterally to form a network of strands. As the surface of freshly cleaved mica bears negative charges, the interaction with the coordination polymer, being a polycation, is expected to be very strong, thus explaining the formation of dense monolayers.

Conclusion

The reversible complexation of ditopic terpyridine functionalized perylene bisimide chromophores with Zn^{2+} ions has been discussed in Chapter 3. Characterization of the resulting coordination polymers with standard polymer characterization methods is problematic due to the reversible nature of these structures. Therefore, methods had to be applied where the supramolecular systems remain in equilibrium or where they are adsorbed on a surface. In this chapter, the reversible coordination polymer formation, which was suggested in Chapter 3 from the results of ^{1}H NMR titration experiments, could be proven by investigation of the system with two diffusion based methods as well as by imaging the adsorbed coordination polymer on substrates.

DOSY NMR and fluorescence anisotropy measurements were conducted to examine the change of diffusion coefficient of the perylene bisimide-terpyridine system upon stepwise addition of Zn^{2+}, which leads first to the coordination polymer and subsequently to its fragmentation due to the reversible nature of the complex bond. The significantly decreased translational diffusion coefficient of the polymer species in comparison to the monomer ligand and the fragmented species could be measured by DOSY NMR. The analogous decrease of the rotational diffusion coefficient causes a significant increase in fluorescence anisotropy.

Direct observation of the polymer strands was achieved by atomic force microscopy from samples spin-coated on mica and graphite substrates. In contrast to the monomeric ligand, which shows only small circular spots, the coordination polymer could be identified by its one-dimensional linear form. Spin-coating of concentrated coordination polymer solutions results in the formation of ordered monolayers which show a clear tendency of the single polymer strands to aggregate laterally. This film formation is an interesting and promising

result with respect to the use of this system in further hierarchical self-assembly like - for example - the construction of electrostatically self-assembled polyelectrolyte film, which will be discussed in chapter 6.

Experimental Section

DOSY NMR Spectroscopy: [1]H DOSY experiments were carried out at 298 K on a Bruker DMX 600 spectrometer (Bruker BioSpin, Rheinstetten, Germany) equipped with a BGPA 10 gradient generator, a BGU II control unit and a conventional 5 mm broadband ([15]N-^{31}P)/^{1}H probe with automatic tune/match accessory and z axis gradient coil capable of producing pulsed magnetic field gradients in the z direction of 52 G cm^{-1}. Data were acquired and processed using the Bruker software XWIN-NMR 3.5, patch level 6. The longitudinal eddy current delay sequence with bipolar gradient pulse pairs for diffusion (PBB-LED)[17] and additional sinusoidal spoil gradients after the second and forth 90° pulses was used with the following acquisition parameters: duration δ of a bipolar gradient pulse: 4.4 and 20.0 ms ($2 \times$ 2.2 and 2×10.0 ms), diffusion times Δ: 50 ms, spoiler gradient duration: 1.1 ms, spoiler gradient strengths: 17.13 and 13.17 % of maximum gradient strength, eddy current delay: 5 ms. The diffusion time Δ was kept constant in each DOSY experiment whereas the sinusoidal diffusion gradients were incremented from 2 % to 95 % of maximum gradient strength in 32 linear steps. Signal averaging ranged from 16 to 288 scans per increment as required for adequate signal-to-noise ratio. The ^{1}H NMR data were recorded in $CDCl_3$-CD_3OD (80:20) solutions in 5 mm NMR tubes and referenced to interal TMS. The DOSY experiments with short bipolar gradient pulses of $\delta = 4.4$ ms length were performed for each sample to measure the diffusion coefficient of TMS to which the results were finally normalized to eliminate minor temperature and viscosity differences between the different systems. The DOSY spectra with longer diffusion gradients were recorded to determine the diffusion coefficients of the compounds of interest.

The strength of the pulsed magnetic field gradients was calibrated by ^{1}H DOY experiments with a sample of 1 % H_2O in 99 % D_2O, doped with $GdCl_3$ (0.1 mg/ml) to achieve short spin-lattice relaxation times, using the known value of the diffusion coefficient for H_2O at 298 K in this H_2O/D_2O mixture.[18]

The DOSY spectra were calculated using the Bruker software XWIN-NMR 3.5, patch level 6. For this purpose, a Levenberg-Marquardt algorithm was used for one component fittings of

the gradient strength dependence if the signal intensities according to equation 8 for each data point in the ^{1}H NMR spectrum with D and I_0 as adjustable parameters. The widths of the peaks in the diffusion correlate with the fitting error. In addition, fittings for the individual ^{1}H NMR signals according to equation 8 were performed to judge the quality of the DOSY spectrum.

$$I = I_0 e^{-D\gamma^2 g^2 \delta^2 (\Delta - \delta/3)}$$ **Equation 9**

The diffusion coefficient D in equation 8 represents the result of the fitting procedure, I_0 is the fitting signal intensity for zero gradient strength, I the observed intensity for the gradient strength g and γ the gyromagnetic ratio of the observed nuclei.

Fluorescence Anisotropy Titration of Polymers 2a,b: To a solution of the monomer **1a** or **1b** (2.5×10^{-5} M in chloroform-methanol, 60:40, 1500 µl in 1cm quartz fluorescence cuvette) aliquots of zinc triflate (2.5×10^{-4} M in monomer solution, 25 µl aliquots) were added and the polarized fluorescence intensity was recorded after 5 min equilibration time. The fluorescence anisotropy r is a measure for the depolarization of the fluorescence emission and is defined as

$$r = \frac{I_{VV} - G \cdot I_{VH}}{I_{VV} + 2 \cdot G \cdot I_{VH}} \text{ with } G = \frac{I_{HV}}{I_{HH}}.$$ **Equation 10**

I is the fluorescence intensity at a specific wavelength and the indices are related to the vertical or horizontal orientation of the excitation (first index) and the emission polarizer (second index) with respect to the excitation-emission plane. G is an instrument factor which compensates for polarization effects of the emission optics. Fluorescence anisotropy is determined on a PTI/QM4 fluorescence spectrometer equipped with a two Glan-Thomson polarizers. Correction for the G-factor was obtained automatically. Fluorescence intensities were averaged for 60 s at 2 points/s, bandpass was set to 6 nm, and all titrations are performed at 20.0±0.1 °C, with temperature control by a peltier element incorporated in the sample holder.

Atomic Force Microscopy (AFM): AFM investigations were performed under ambient conditions using a multimode scanning probe microscope (Nanoscope IIIa, Digital Instruments, Sta. Barbara, CA) operating in tapping mode. Silicon cantilevers (Olympus OMCL-AC, 160 TS) with a resonance frequency of ~300 kHz were used. Samples of both ligand **3a** and coordination polymers 3**a,b** were prepared by spin-coating of the respective solutions onto HOPG and freshly-cleaved muscovite mica at 10000 rpm (both substrates supplied by SPI Supplies).

References

(^{1})   Hiemenz, P. C. *Polymer Chemistry : The Basic Concepts* Dekker: New York **1984**.

(^{2})   Tieke, B. *Makromolekulare Chemie : Eine Einführung* VCH: Weinheim **1997**.

(^{3})   (a) Brunsveld, L.; Folmer, B. J. B.; Meijer, E. W.; Sijbesma, R. P. *Chem. Rev.* **2001**, *101*, 4071-4087; (b) ten Cate, A. T.; Sijbesma, R. P. *Macromol. Rapid Commun.* **2002**, *23*, 1094-1112.

(^{4})   (a) Rehahn, M. *Acta Polymer.* **1998**, *49*, 201-224; (b) Schubert, U. S.; Eschbaumer, C. Angew. Chem. Int. Ed. **2002**, *41*, 2892-2926.

(^{5})   Kelch, S.; Rehahn, M. *Macromolecules* **1999**, *32*, 5818-5828.

(^{6})   Schmatloch, S.; van den Berg, A.; Alexeev, A. S.; Hofmeier, H.; Schubert, U. S. *Macromolecules* **2003**, *36*, 9943.

(^{7})   Schütte, M.; Kurth, D. G.; Linford, M. R.; Cölfen, H.; Möhwald, H. *Angew . Chem., Int. Ed.* **1998**, *37*, 2891-2893

(^{8})   Elias, H.-G. *Polymere : Von Monomeren und Makromolekülen zu Werkstoffen* Hüthig & Wepf Verlag: Zug, Heidelberg, Oxford, CT/USA **1996**.

(^{9})   Johnson, C. S., Jr. *Progr. NMR Spectrosc.* **1999**, *34*, 203-256.

(^{10})   Paulusse, J. M. J.; Sijbesma, R. P. *Chem. Commun.* **2003**, 1494-1495.

(^{11})   Vermonden, T.; van der Gucht, J.; de Waard, P.; Marcelis, A. T. M.; Besseling, N. A. M.; Sudhölter, E. J. R.; Fleer, G. J.; Cohen Stuart, M. A. *Macromolecules* **2003**, *36*, 7035-7044.

(^{12})   Kerssebaum, R. *DOSY and Diffusion by NMR : Users Guide for XWinNMR 3.1 / 3.5, Version 1.03*, Bruker BioSpin GmbH, Rheinstetten, Germany **2002**.

(^{13})   Johnson, C. S., Jr. *Progr. NMR Spectrosc.* **1999**, *34*, 203-256.

(^{14})   Paulusse, J. M. J.; Sijbesma, R. P. *Chem. Commun.* **2003**, 1494-1495.

(^{15})   Lakowicz, J. R. *Principles of Fluorescence Spectroscopy*, 2nd ed., Kluwer Academic/Plenum, New York, **1999**.

(^{16})   Haas, U.; Thalacker, C.; Adams, J.; Fuhrmann, J.; Riethmüller, S.; Beginn, U.; Ziener, U.; Möller, M.; Dobrawa, R.; Würthner, F. *J. Mater. Chem.* **2003**, *13*, 767-772.

(^{17})   Wu, D.; Chen, A.; Johnson, C. S., Jr. *J. Magn. Reson. A* **1995**, *115*, 260-264.

(^{18})   Holz, M.; Weingärtner, H. *J. Magn. Reson.* **1991**, 115-125.

5

Blue-Fluorescent Ligands for Terpyridine-Based Coordination Polymers

Abstract: Two ditopic ligands bearing a rigid (**8**) and a flexible spacer (**12**) are presented in this chapter. Both show fluorescence in the blue-green region. Their complexation with Zn^{2+} ions is investigated by UV-vis and fluorescence titration. For the tetraethylene glycol spacered ligand **8** ^{1}H NMR titration and DOSY NMR reveal the formation of two coordination compounds, which are assigned to a macrocyclic and an oligomeric or polymeric chain species. UV-vis and fluorescence spectroscopic titrations show that the fluorescence of ligand **8** increases upon Zn^{2+} complexation. Investigations of mixed polymer systems consisting of ligands **8** and **12** respectively together with 5% of a perylene bisimide ligand **14** revealed that no energy transfer from the tpy-based fluorophores to the perylene bisimide units takes place.

Introduction

The construction of fluorescent coordination polymers bearing perylene bisimide fluorophores and their characterization have been presented and discussed in the two previous chapters. If the application of such self-assembled polymeric systems for devices like light-harvesting systems of organic light emitting diodes (OLEDs) is desired, there is also need for fluorescent units with emission in the blue, green and yellow wavelength range. Self-assembled fluorescent polymers are presented in this chapter with a slightly different approach compared to the functionalization of dyes with receptor groups (chapters 3 and 4): due to their extended π-system, 4'-phenyl-substituted terpyridine derivatives exhibit fluorescence itself and therefore these ligands can also act as fluorophores in addition to their application as the structure-forming units.

Investigations have been made with two ligands, one bearing a terphenyl-spacer, the other with a tetraethylene glycol spacer, which allows a large amount of flexibility in the resulting coordination compound. Since both ligands exhibit fluorescence in the complexed form, the possibility for energy transfer was investigated in mixtures with the red-fluorescent tpy-functionalized perylene bisimide units.

Results and Discussion

Fluorescence of 4'-Phenyl-2,2':6',2''-terypridine: The fluorescence properties of 4'-phenyl-substituted terpyridine ligands and their Zn^{2+} complexes have been reported only recently.[1,2] In dichloromethane, the parent 4'-phenyl-2,2':6',2''-terpyridine (ptpy) ligand exhibits an absorption maximum at 278 nm ($\varepsilon = 33000$ $M^{-1}cm^{-1}$) and an emission with a maximum at 340 nm with a fluorescence quantum yield of $\Phi_{fl} = 0.33$.[2] A quantum yield of $\Phi_{fl} = 0.28$ was determined for the respective 4'-*p*-methoxyphenyl-2,2':6',2''-terpyridine.[2]

To study the change of the absorption and fluorescence properties of the ptpy ligand upon Zn^{2+} coordination, two titration experiments have been performed using UV-vis and fluorescence spectroscopy. The reversible complexation of zinc triflate in acetonitrile and in chloroform-methanol mixtures, which was established for the unsubstituted tpy ligand (chapter 2) and the perylene bisimide-terpyridine systems (chapters 3 and 4), can also be observed with ptpy (scheme 1).
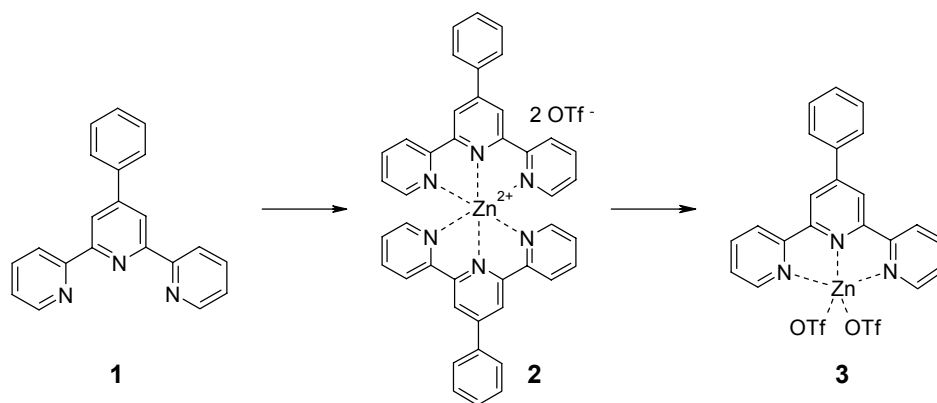
Scheme 1.

The spectra resulting from the titration experiments in acetonitrile are depicted in Figure . Comparison of the absorption spectra with those of unsubstituted tpy shows that in the area from 300 – 350 nm a broad absorption band of minor intensity can be seen already for the uncomplexed ligand, originating from the extension of the π-system at the 4'-position. Upon complexation, a structured band with two maxima evolves between 325–350 nm. The fluorescence spectra show a related behavior starting from an unstructured band and changing to a band exhibiting two maxima. The change of the absorption bands occurs linear with the addition of Zn^{2+} indicating a high binding constant. After reaching the 2:1 ratio of ligand/metal no further change is observed.

The fluorescence spectra, which were obtained by excitation of the sample at the isosbestic point at 279 nm to avoid the necessity to correct for absorption effects, show a significant increase of the fluorescence intensity upon complexation with Zn^{2+}. Interestingly, the fluorescence intensity does not remain constant after the 2:1 ratio of ligand/metal is reached but still increases further. Whereas the increase up to the 2:1 ratio is linear due to the high binding constant, the fluorescence intensity does not increase linearly any more after exceeding the 2:1 ratio.
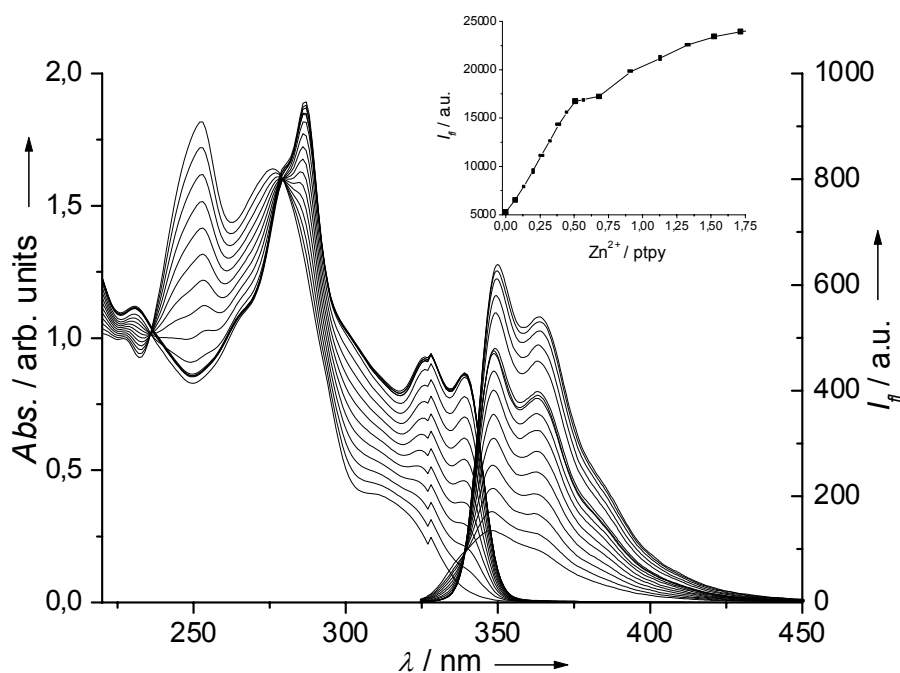
Figure 1. UV-vis and fluorescence constant-host titration experiment of 4'-phenyl-2,2':6',2''-terpyridine (ptpy) **1** with zinc triflate in acetonitrile (UV-vis: 50µM, fluorescence: 5µM). Inset: titration curve of the integrated fluorescence (325–450 nm) against the amount of added Zn^{2+}.

As a consequence of the fluorescence properties of ptpy **1**, the first attempt to synthesize Zn^{2+}/tpy coordination polymers showing blue fluorescence was started with the ditopic bis-1,4-(4'-terpyridyl)-benzene **4**. This compound has already been applied successfully for the construction of coordination polymers with Fe^{2+} and Co^{2+} by Kurth and coworkers.[3,4] Despite of several attempts and the application of a variety of Zn^{2+} salts with different counterions and in various solvents, no defined soluble coordination polymer could be obtained in a reproducible way. To circumvent the problems related with ligand **5** two alternative ligands were synthesized, which had been chosen due to the presence of solubilizing groups.
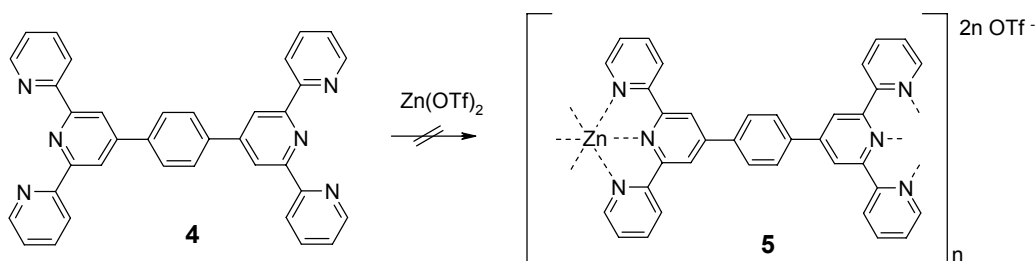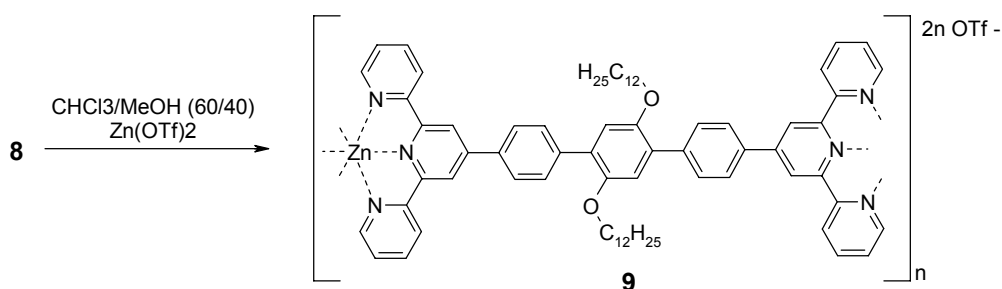

Scheme 2.

Studies on the Bis-(*n*-dodecyloxy)-terphenyl Spacered Ligand 8: The bis-*n*-dodeclyoxy-terphenyl-spacered ligand **8** has been introduced by Che and coworkers,[5] who also reported the formation of Zn^{2+} coordination polymers in DMSO. However, no synthetic procedure for this compound is given in the paper by Che et al. In the present work the ligand

8 was synthesized by palladium-catalyzed Suzuki coupling reaction between two boronic ester functionalized terpyridine units[6] and the central 1,4-dibromo-2,5-bis-*n*-dodecyloxybenzene unit[7] in 84 % yield.
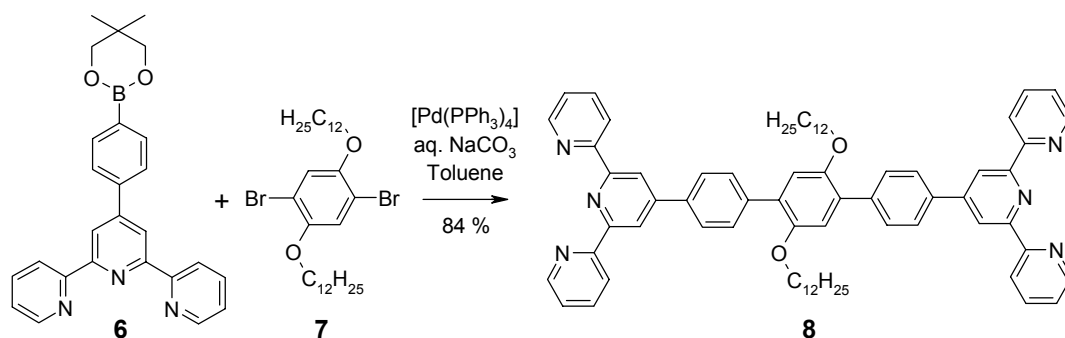
Scheme 3.

In analogy to the perylene bisimide-terpyridine systems introduced in chapters 3 and 4, also the ditopic terphenyl-spaced ligand **8** should form a coordination polymer **9** according to scheme 4. Although the ligand bears two long *n*-dodecyloxy chains, it does not exhibit high solubility in chloroform/methanol mixtures. For this reason it was not possible to conduct ^{1}H NMR titrations, which would provide an exact structural proof for the existence of a coordination polymer.

Scheme 4.

Despite of the insufficient solubility for complexation studies with NMR methods, UV-vis titration experiments could be performed. The spectra of ligand **8** upon complexation with zinc triflate show the appearance of two bands at 325 nm and 375 nm from the broad shoulder between 300–400 nm (figure 2).

Interestingly, the fluorescence band of the free ligand **8** is very broad with an emission maximum at 470 nm in chloroform/methanol (60:40). The spectra were obtained from excitation of the sample at the isosbestic point at 310 nm to avoid the necessity to correct for changing absorption during the titration. Upon addition of Zn^{2+}, the fluorescence intensity decreases and a pronounced hypsochromic shift can be observed. The fluorescence reaches a minimum at a metal/ligand ratio of 1:1 with a fluorescence maximum at 440 nm. When the equimolar ratio is exceeded, the fluorescence intensity increases again and the fluorescence

spectrum becomes sharper to form a mirror image of the highest wavelength absorption at 375 nm.
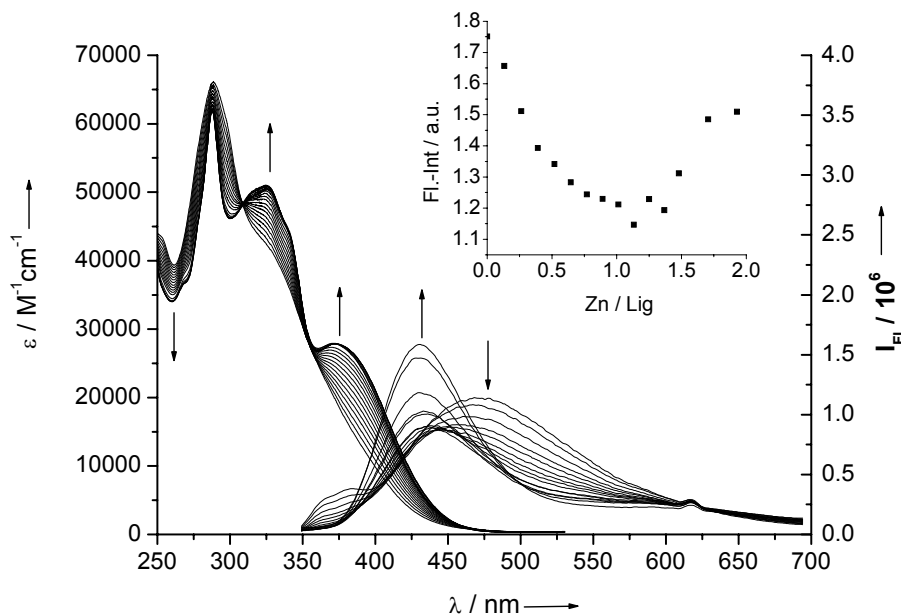

Figure 2. UV-vis and fluorescence titration of ligand **8** with zinc triflate in chloroform/methanol (60/40) (UV-vis: 50 μM, fluorescence: 5 μM). The fluorescence spectra were obtained by excitation at the isosbestic point at 310 nm. Arrows indicate the spectral change upon addition of Zn^{2+}. Inset: titration curve of the integrated fluorescence (350 – 625 nm) against the amount of added Zn^{2+}.

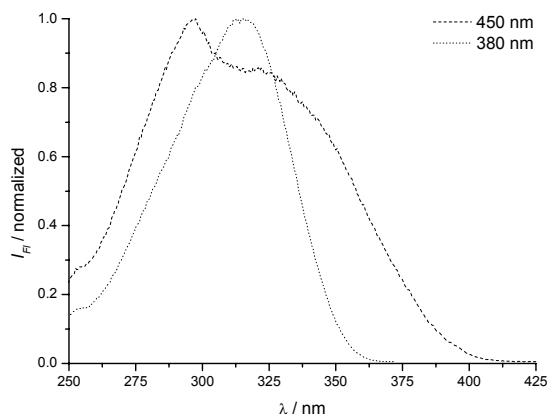In the fluorescence spectrum of the uncomplexed ligand **8** (figure 2) two fluorescence bands can be seen, one with minor intensity at 360 nm and one major band at 475 nm. Fluorescence excitation spectra look quite different depending on the wavelength of fluorescence detection (figure 3). The literature value for the fluorescence quantum yield determined for **8** by Che et al.[5] is $\Phi_{Fl} = 0.18$ (*N,N*-dimethylacetamide, $\lambda_{ex} = 330$ nm, quinine sulfate standard), the respective value for the zinc polymer **9** under the same conditions is $\Phi_{Fl} = 0.77$.

Figure 3. Fluorescence excitation spectra of the terphenly-spacered ligand 8 recorded at 380 nm (dotted line) and 450 nm (dashed line).

Investigation of the Tetraethylene Glycol Spacered Ligand 12: Since ligand **8** is not ideally suited to be used as a building block for fluorescent coordination polymers due to its low solubility and its complicated spectroscopic behavior, the focus was turned to the ditopic

ligand **12**, composed of two 4'-*p*-alkoxyphenyl-2,2':6',2"-terpyridine units linked by a tetraethylene glycol chain, which should provide good solubility in various solvents of low and medium polarity. The synthesis was achieved by alkylation of the 4'-hydroxyphenyl-2,2':6',2"-terpyridine[8] **10** with tetraethylene glycol ditosylate[9] **11** in DMF with potassium carbonate in 83 %. The ligand is isolated as colorless oil that can be transformed into a white solid by treatment with acetonitrile in an ultrasonic bath for a couple of minutes. The compound was characterized by ^{1}H and ^{13}C NMR and mass spectrometry. One drawback of this synthetic route is the presence of a terpyridine isomer, which can be observed in ^{1}H NMR and quantified to approx. 5 %. This isomer stems from the synthesis of the 4'-*p*-hydroxyphenyl-terpyridine **10** and is likely to be the 6'-*p*-hydroxyphenyl-2,2':4',2"-terpyridine derivative.[10] Attempts to isolate the isomer by chromatographic methods, recrystallization or complexation/decomplexation steps[11] were not successful.
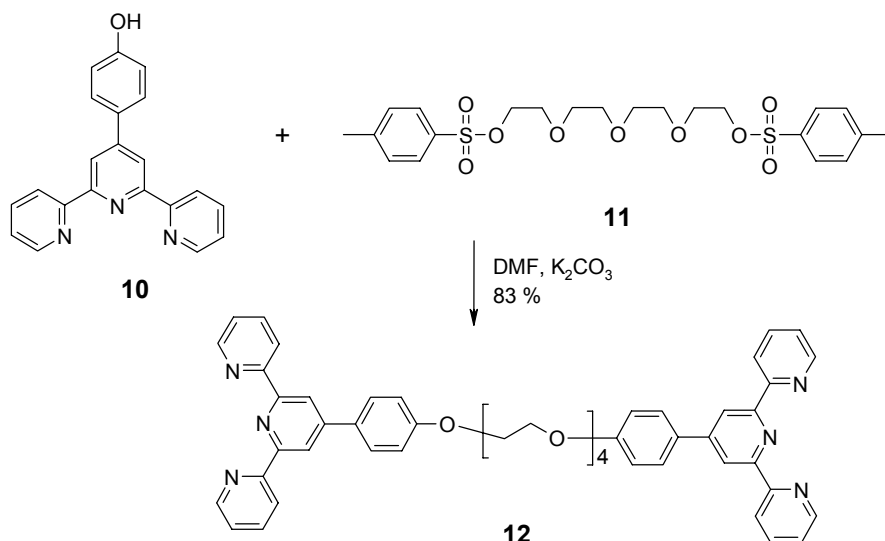
Scheme 5.

Complexation of **12** with zinc triflate was investigated by ^{1}H NMR titration. The resulting complex species **13** exhibited good solubility in chloroform/methanol mixtures (Scheme). In contrast to all other ditopic ligands in this word, the flexibility of the tetraethylene glycol bridge in the ligand **12** allows the formation of macrocycles. Molecular modeling reveales that the length of the spacer unit does not permit the intramolecular cyclization to a [1+1] cycle, but that formation of higher macrocycles like the [2+2] species is possible (figure 4). The ^{1}H NMR titration of **12** with zinc triflate in chloroform/methanol (60:40) does not only show three different species during the course of the titration (which are free ligand **12**, coordination polymer **13** and the fragment form) but indicates the presence of a further species (figure 5, approx. 20 %). In contrast to the coordination polymer species, the amount of this fourth compound is not depending significantly on the metal/ligand ratio. To illustrate

the ^{1}H NMR spectra of the titration, the presumed assignment of the NMR signals is color-coded in the figure showing blue bars for the uncomplexed ligand **12**, red bars for the assumed coordination polymer species **13** and green bars for the assumed macrocyclic compound. When the metal/ligand ratio of 1:1 is exceeded, fragmented species are formed with increasing amount of Zn^{2+}, which are marked grey in figure 5.
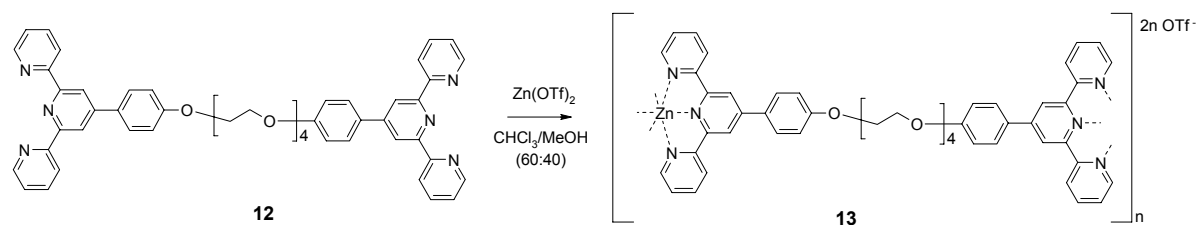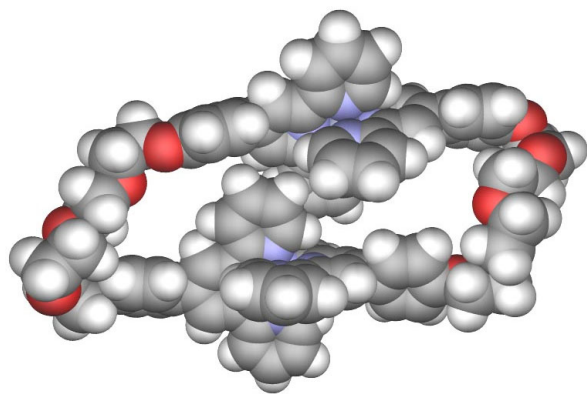

Scheme 6.

Figure 4. Molecular Modeling (Fujitsu CAChe 5.2, MM3) showing the possibility of the oligoethylene glycol spacered ligand **12** to form macrocyclic assemblies of the type [2+2]. The formation of a [1+1] cycle is not possible since the spacer is too short for complete ring formation, but larger macrocycles might also be a possibility.
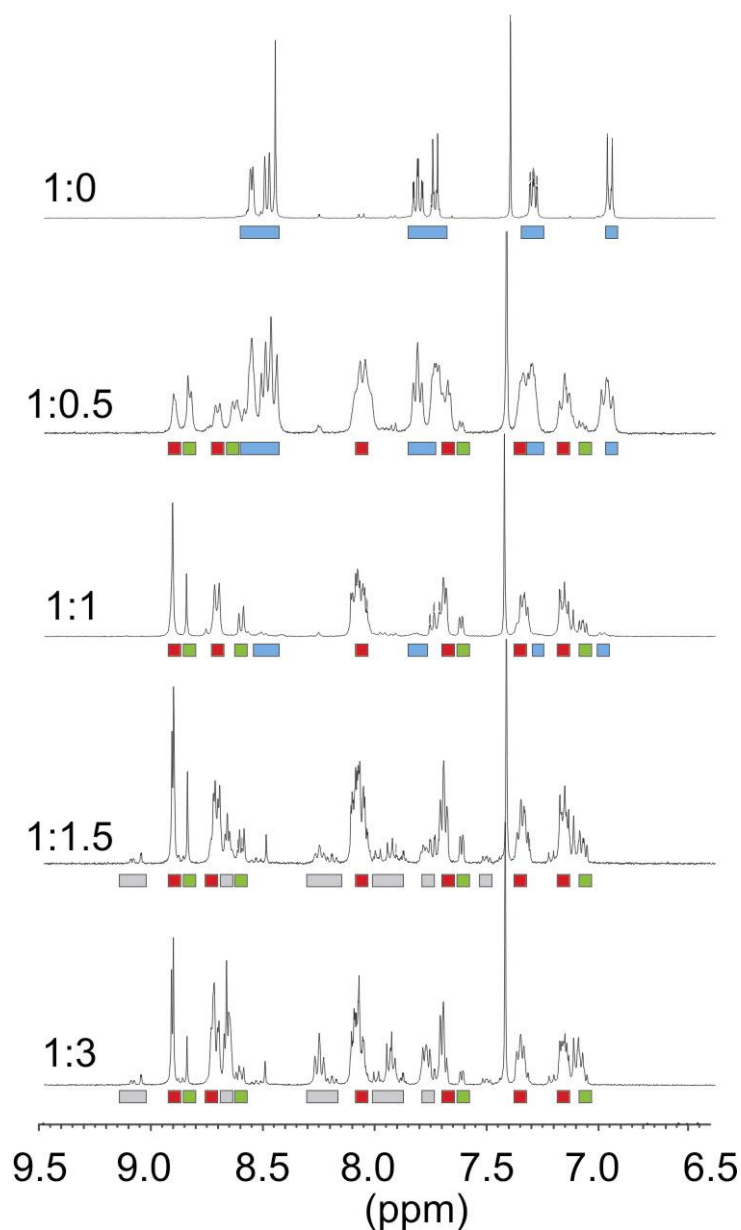

Figure 5. Constant host ^{1}H NMR titration of the tetraethylene glycol spacered ligand **12** with zinc triflate in CHCl$_3$/MeOH (60:40, 7mM) showing the formation of a number of different products. The interpretation is color-coded as: free ligand (blue), coordination polymer (red), macrocyclic species (green) and fragmented species (grey). The amount of macrocyclic species is approx. 20%.

In order to obtain further information on the nature of the system formed from compound **12** and one equivalent of Zn^{2+}, this mixture was investigated by DOSY NMR (refer to chapter 4

for detailed information on this method). The interpretation which is presented in figure 5 is supported by the DOSY results (Figure and Figure), which indicate that signals marked in red and green indeed belong to two separate species due to their different diffusion coefficient. The diffusion coefficient determined for the supposed macrocycle (marked green in figure 5) is $D = 2.8{\times}10^{-10}$ m^2 s^{-1}, whereas the respective value for the polymeric compound (marked red in figure 5) is $D = 1.8{\times}10^{-10}$ m^2 s^{-1}. Since the oligoethylene glycol spacers allow a large amount of flexibility, the decrease of diffusion coefficient upon coordination polymer formation is not expected to be as drastic as discussed in chapter 4 for the rigid rod-like polymers. Also the NMR signals and diffusion coefficients of higher macrocyclic species can not be distinguished from the respective signals of a polymer chain. Additionally, the presence of approx. 5% of the isomeric terpyridine unit which can not form defined complexes and therefore is expected to function as a chain stopper also does not give rise to the expectation of high molecular weight polymer species. To rule out changes in the composition of the sample due to slow rearrangement effects, the spectra were recorded again after 24 and 48 hours but no change could be observed. Comparison of the DOSY results for the Zn^{2+} complexes with the respective result for the free ligand (figure 8) indicates that the latter has a clearly higher diffusion coefficient.
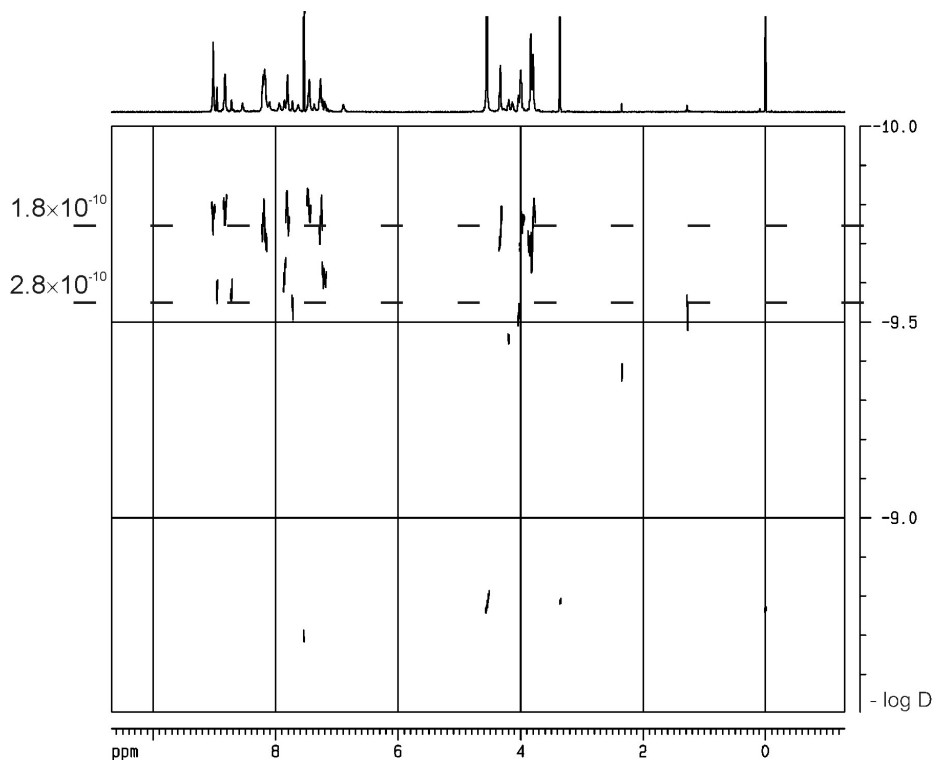

Figure 6. DOSY NMR spectrum of compound **12** when complexed with one equivalent of Zn^{2+}. The signals marked in green in figure 5 can be attributed to the diffusion coefficient of $2.8{\times}10^{-10}$ m^{2}s^{-1} and related to the macrocyclic species whereas the signals marked in red are attributed to the diffusion coefficient of $1.8{\times}10^{-10}$ m^{2}s^{-1} and related to a higher macrocyclic or a polymeric chain species.
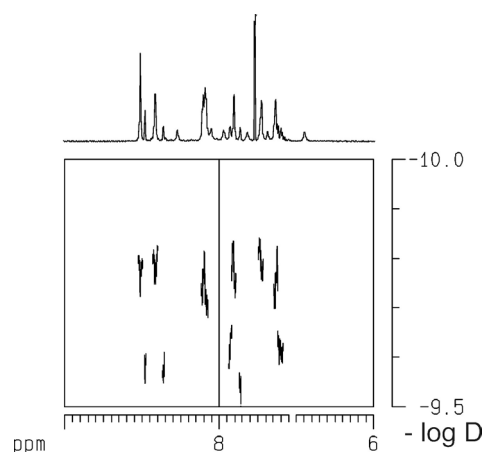
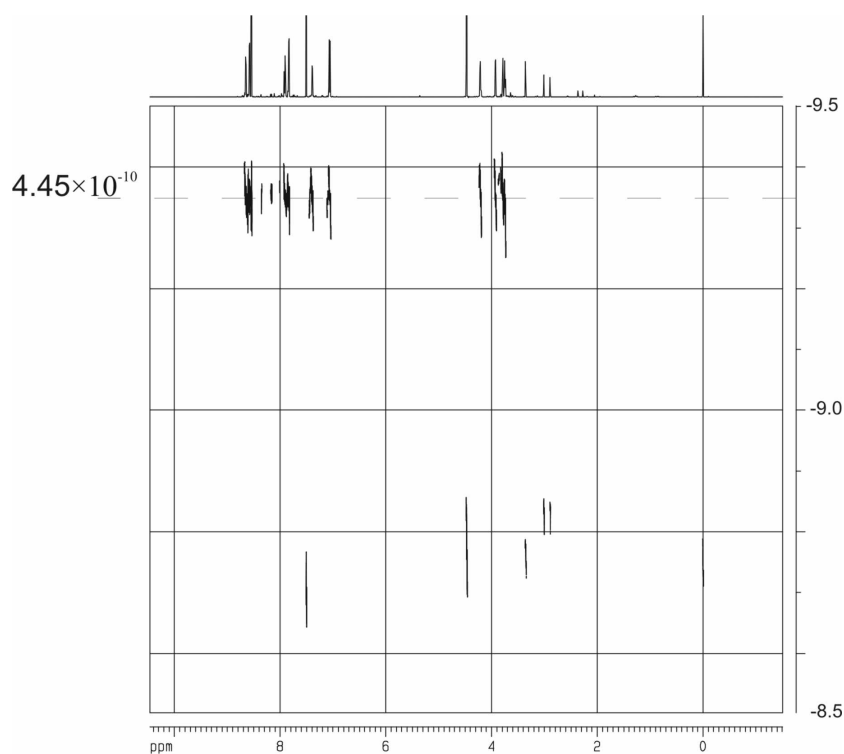**Figure 7.** Expansion of the aromatic region of the DOSY spectrum of Figure .

Figure 8. DOSY NMR of the uncomplexed ligand **12** showing a diffusion coefficient of 4.45 m^2 s^{-1} being clearly higher than that of the complexed cyclic or polymeric species.

The UV-vis and fluorescence titrations of the tetraethylene glycol spacered ligand **12** with zinc triflate can be found in figure 9. The UV-vis spectra show the characteristic appearance of an absorption band between 300–400 nm with an absorption maximum at 350 nm. Comparison with the titration of the *p*-phenyl substituted ligand **1** indicates that the electron-donating *p*-alkoxy-group causes a bathochromic shift since the absorption of complex **2** at 350 nm is almost zero.

The fluorescence spectrum of the uncomplexed ligand is broad and unstructured with an emission maximum at 390 nm. Upon stepwise addition of Zn^{2+} to the ligand solution in

chloroform/methanol (60:40), the band at 390 nm gradually decreases and a second band with an emission maximum at 460 nm appears. Again, the fluorescence spectra were obtained by excitation at the isosbestic point, in this case at 320 nm.
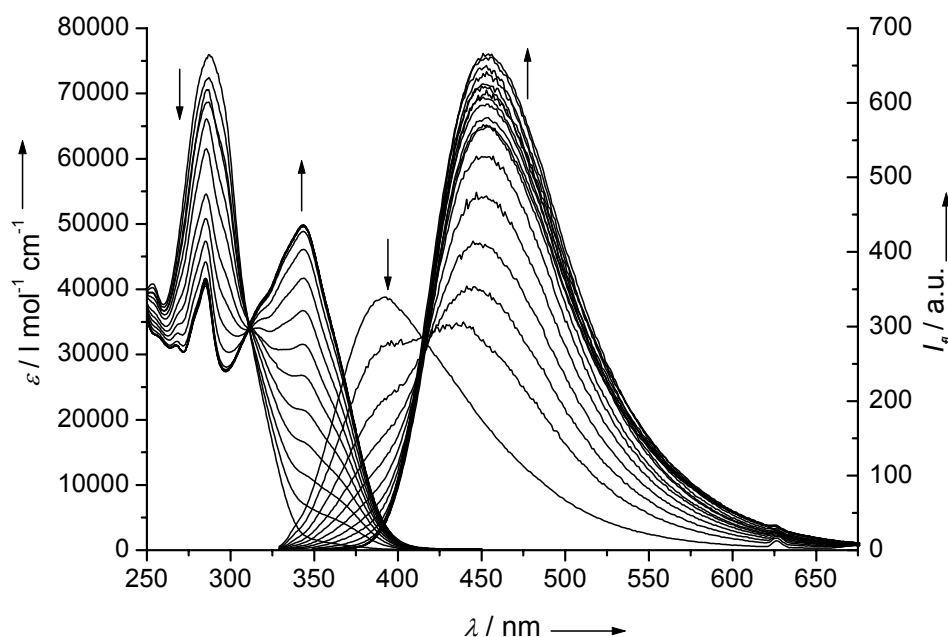

Figure 9. Constant Host UV-vis and fluorescence titration of the tetraethylene glycol spaced ligand **12** with zinc triflate to form coordination compound **13**. Titrations are performed in CHCl$_3$/MeOH (60/40, UV-vis: 50μM, Fluorescence: 5μM).

The determination of the fluorescence quantum yields turned out to be problematic because the values which were determined for different wavelengths varied significantly. The quantum yield of the uncomplexed ligand lies in the range between 0.25-0.35, which is also in agreement with the model compound *p*-methoxyphenyl-2,2':6',2"-terpyridine ($\Phi_{Fl} = 0.28$)[2]. In the complexed form, the fluorescence quantum yield increases to $\Phi_{Fl} = 0.40$-0.50.

Investigation on potential energy transfer. The fluorescence properties of the coordination polymers **9** and **13** should be generally suited to provide energy transfer from the tpy-based fluorophores to perylene bisimide units like in ligand **14**. The synthesis, characterization and polymer formation of the latter has been discussed in chapters 3 and 4. In a mixed system, the tpy-based fluorophores should act as the energy donors which could transfer their excitation energy to the perylene bisimide unit acting as an energy acceptor. To assess potential energy transfer, mixed systems have been prepared from a solution containing the respective ligands **8** or **12** (95 %) together with the ditopic *tert*-octylphenoxy-substituted perylene bisimide unit **14** (5 %). To this mixture, an equimolar amount (with respect to the total amount of tpy-units) of zinc triflate is added. This procedure is supposed to ensure the

formation of a mixed polymer from a homogeneously mixed solution of the ligands as depicted in charts 2 and **3**.
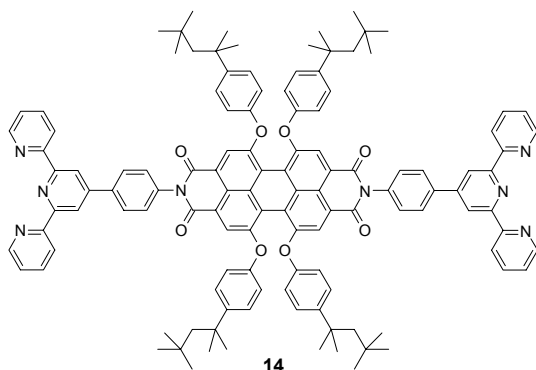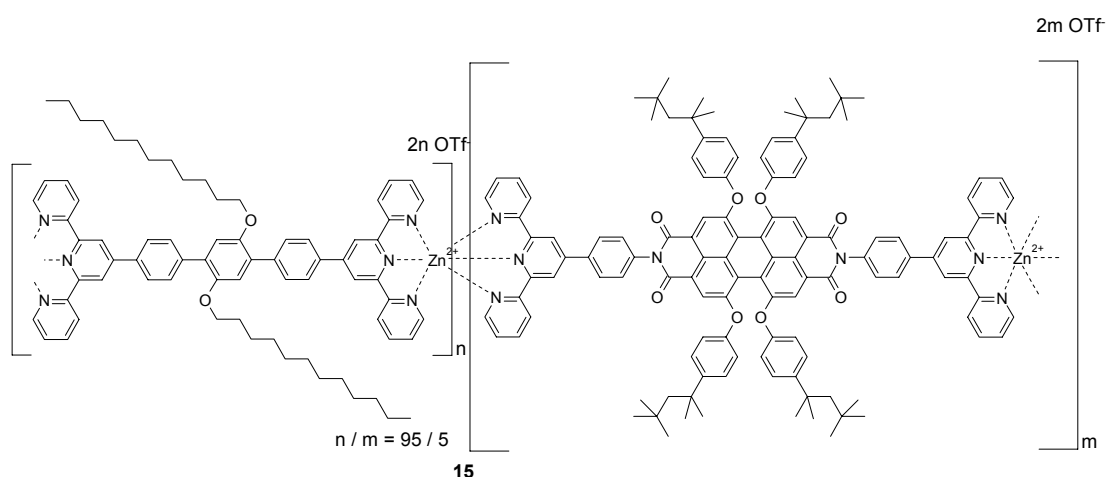

14

Chart 1

Chart 2

The result of the spectroscopic characterization of the mixed system **15** consisting of the terphenyl-spacered ligand **8** (95 %) and the perylene bisimide unit **14** (5 %) is presented in figure 10. The left spectrum shows the UV-vis (solid line) and the fluorescence (dotted line) spectra of **15**. The fluorescence spectrum shows both the fluorescence bands of ligand **8** at 450 nm and the perylene bisimide fluorescence at 630 nm. The latter is shifted about 30 nm to higher wavelengths compared to the coordination polymer consisting exclusively of the perylene bisimide ligand **14**. The system was excited at 375 nm to provide preferential excitation of the tpy-based fluorophore **8**. The fact that significant donor (**8**) fluorescence can be observed indicates that, if energy transfer is present, it is not very effective since for effective energy transfer nearly complete quenching of the donor fluorescence is expected.

The right spectrum of Figure 7 shows the fluorescence excitation spectrum of the perylene bisimide unit in comparison with the UV-vis spectrum of the mixed system **15**. In case of highly effective energy transfer, the absorption spectrum of the mixed polymer and the fluorescence excitation spectrum of the acceptor fluorophore should be identical. The

opposite is observed in this case: the fluorescence excitation spectrum of the mixed system only matched the wavelength region with exclusive absorption of the perylene bisimide acceptor fluorophore (475–650 nm). In the lower wavelength region, the excitation spectrum shows even less intensity than the absorption spectrum of the pure perylene bisimide polymer (data not shown) which means that the supposed donor chromophore **8** acts more as a filter than as an energy donor. From this result, the absence of energy transfer within the mixed coordination polymer system **15** can be concluded.
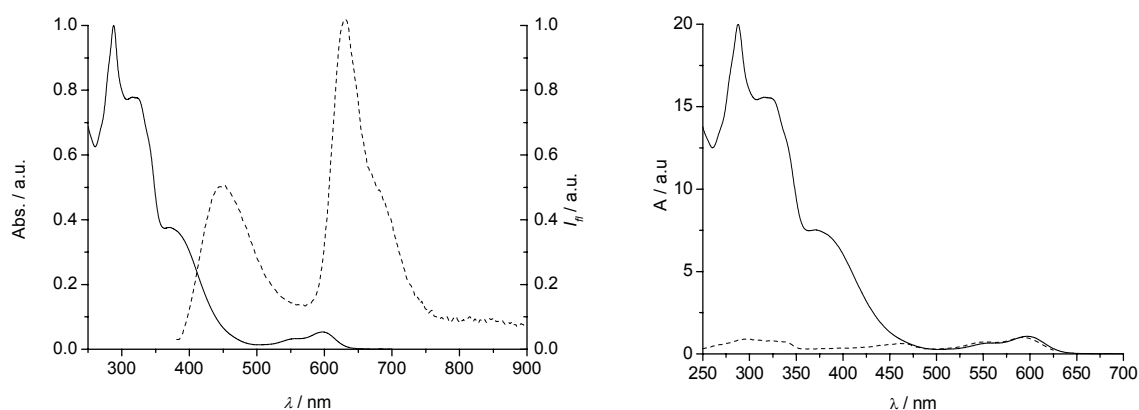

Figure 10. UV-Vis and fluorescence spectra of the mixed system **15** (1.25×10^{-5} M in CHCl$_3$/MeOH, 60:40). Left: UV-vis (solid line) and fluorescence emission spectrum ($\lambda_{ex} = 375$ nm, dashed line). Right: UV-vis (solid line) and fluorescence excitation spectrum ($\lambda_{em} = 630$ nm, dashed line) showing that no energy transfer is present in this system.

16
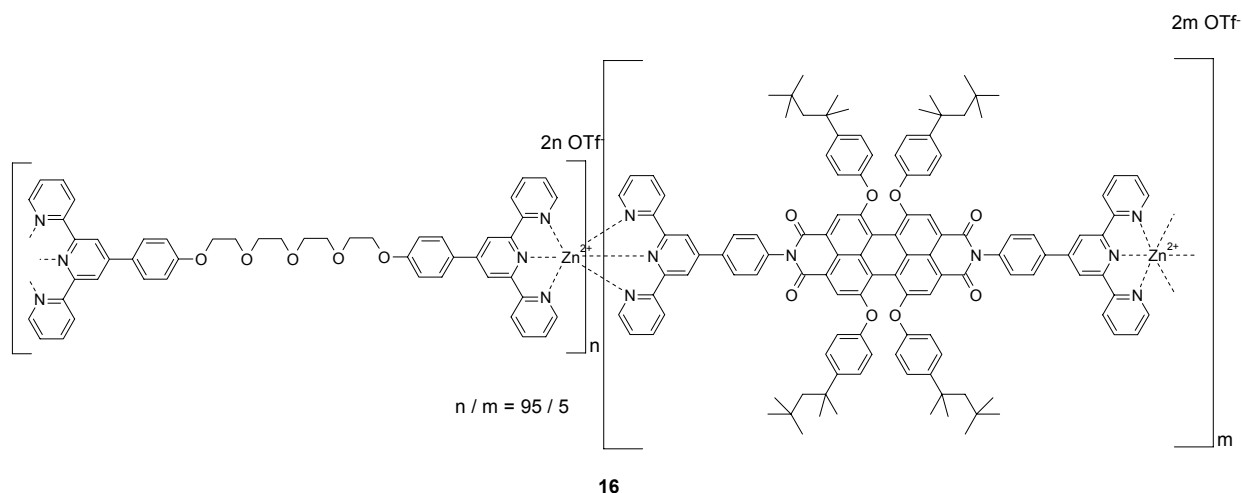
Chart 3

The same investigations with respect to energy transfer have also been conducted for the mixed system **16** consisting of the tetraethylene glycol spacered ligand **12** (95%) and the perylene bisimide unit **14** (5%). The results of the spectroscopic investigation are summarized in figure 11. Again, the left spectrum shows the UV-vis absorption and fluorescence emission spectra. The solid line represents the UV-vis absorption spectra of the mixed system **16**. The

dashed line is the fluorescence excitation spectrum detected in the fluorescence maximum of the ethylene glycol spacered ligand **8** at 490 nm. The green and red spectra represent the respective fluorescence bands when excited at 375 nm (dotted line) to obtain preferential excitation of the tpy-based fluorophore **8** and at 490 nm (dashed-dotted line) to provide exclusive excitation of the perylene bisimide moiety. Also here, the fluorescence of the energy donor is not quenched but even more intense than the acceptor fluorescence suggesting also for this system the absence of energy transfer.

The right chart shows the comparison of the UV-vis absorption spectrum (solid line) and the fluorescence excitation spectrum recorded at the perylene bisimide fluorescence at 630 nm (dotted line). In analogy to the previously discussed system **15**, also the present mixed system **16** does not show any sign of efficient energy transfer, as the fluorescence excitation spectrum does not resemble the absorption spectrum but, in contrast, shows significantly lower intensity in the wavelength range below 400 nm, which can again be interpreted as a filter effect of the tetraethylene glycol spacered ligand.
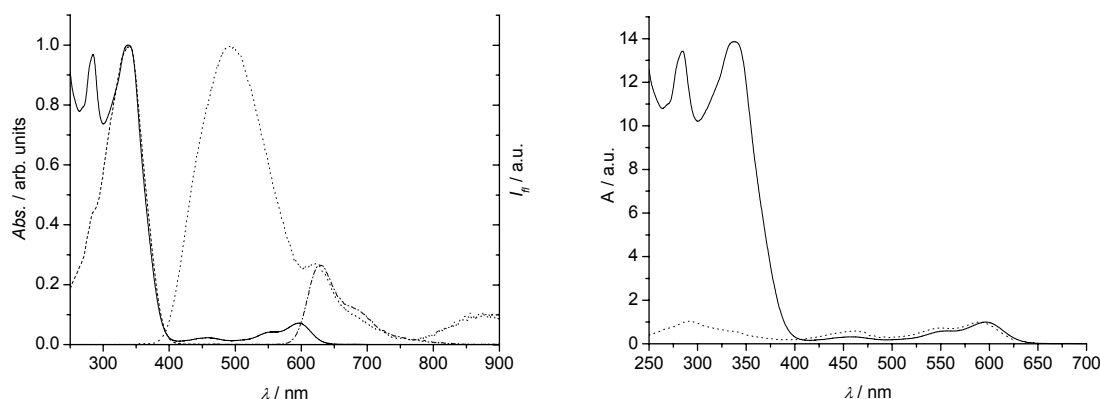
Figure 11. Spectroscopic study of the mixed system **16** (1.25×10^{-5} M in CHCl$_3$/MeOH, 60:40). Left: UV-vis (solid line) and fluorescence excitation (dashed line, λ_{em} = 450 nm) showing that only the highest wavelength band of ligand **12** at 340 nm contributes to the fluorescence of the emission. The fluorescence emission spectra are obtained by excitation at 375 nm (dotted line) and 550 nm (dash-dotted line), the latter exclusively exciting the perylene moiety. Right: UV-vis (solid line) and fluorescence excitation spectrum (dotted line, λ_{em} = 630 nm) showing the absence of energy transfer within the mixed system **16**.

The reason for the absence of energy transfer could be an unfavorable alignment of the absorption and fluorescence dipole moments of the two chromophores, since only the collinear or parallel orientation leads to effective enery transfer whereas orthogonal alignment does not allow effective energy transfer. A second reason could be that although the compounds are dissolved together and the Zn^{2+} is added to this homogeneous solution the complexation of similar units is favored which would also prevent energy transfer due to a too large distance between the chromophores.

Conclusion

The aim of this chapter was the application of 4'-substituted terpyridines as both structure determining and fluorescent units. A basic study with 4'-phenylterpyridine showed the general applicability of such units as fluorophores. Two ditopic ligands **8** and **12** have been synthesized and the optical properties and their change upon complexation have been studied. Due to its higher solubility, the complexation behavior of the oligoethylene glycol spacered ligand **12** with zinc triflate has been studied in more detail. Molecular modeling suggests that the flexible spacer unit also allows the formation of macrocyclic species. ^{1}H NMR titrations suggested that during a titration with zinc triflate indeed such macrocycles are present (approx. 20%) in addition to oligomeric/polymeric chains. Diffusion based experiments with DOSY NMR supported this interpretation by clearly showing two distinct species with different diffusion coefficient.

Although the absorption and fluorescence spectra suggest that Förster-type energy transfer from the two Zn^{2+}-complex species to the perylene bisimide chromophore should be possible, no energy transfer could be observed in mixed Zn^{2+}-coordination polymers constructed from the tpy-functionalized perylene bisimide unit and the ligands **8** or **12**, respectively. The reason – more likely - could by an unfavorable alignment of the fluorophore's transition dipole moments or an inhomogeneous distribution of the two ligands, i.e. the perylene bisimide and the tpy-ligand, within the polymer chain (block formation or existence of **12** as macrocycles). Nevertheless, the new oligoethylene glycol spacered ligand **12** is a promising highly soluble and flexible building block for the assembly of blue-fluorescent soluble terpyridine-based coordination compounds.

Experimental Section

General: Starting materials **6**, **7**, **10, 11** and 4'-phenyl-2,2':6',2"-terpyridine[12] have been synthesized according to the respective literature procedures. UV-vis spectra and titrations were performed on a Perkin Elmer Lambda40P spectrophotometer, fluorescence spectra were recorded on a PTI QM4-2003 fluorescence spectrometer. Emission and excitation fluorescence spectra are corrected against photomultiplier sensitivity and lamp intensity. Fluorescence quantum yields were determined against diphenylanthracene in cyclohexane (Φ_{Fl} = 1).[13] NMR spectra were recorded on a Bruker Avance 400, DOSY NMR experiments were performed with a Bruker DMX600 according to the details discussed in the experimental section of chapter 4.

Synthesis of the Terphenyl Spacered Ligand 8: To a solution of tetrakis(triphenyl-phosphane)palladium (41 mg, 36 µmol) in dimethoxyethane (3 ml) in a Schlenk tube under argon the boronic ester[6] **6** (250 mg, 0.6 mmol, solution in 4 ml dimethoxyethane) is added and the solution is stirred for 15 min. 1,4-Dibromo-2,5-bis(*n*-dodecyloxy)benzene[7] **7** (145 mg, 0.24 mmol, suspension in 18 ml dimethoxyethane) is added to the solution together with aqueous $NaCO_3$ solution (0.18 ml, 2 M) and the reaction mixture is heated to 90 °C for 24 h. An additional portion of the catalyst is added and the mixture is heated for another 24 h, after which it is cooled to room temperature to produce a precipitate which is isolated by filtration and washed with methanol. The filtrate is suspended in methanol (25 ml) in an ultrasonic bath at 35 °C for 15 min, subsequently reisolated by filtration and dried under vacuum to yield 214 mg (0.20 mmol, 84 %) of the greyish-yellow ditopic ligand **8**.

m.p. 198 °C (Lit. 198 °C), ^{1}H NMR spectrum corresponds to the literature.[5]

Synthesis of the Tetraethylene Glycol Spacered Ligand 12:

4'-p-Hydroxyphenyl-2,2':6',2"-terpyridine[8] **10** (400 mg, 1,2 mmol) is dissolved in *N,N*-dimethylformamide (25 ml) together with tetraethyleneglycol ditosylate **11** (300 mg, 0.6 mmol) and potassium carbonate (660 mg, 4.8 mmol) and heated to 80°C under a rgon for 48h. After filtration the solvent is evaporated and dichloromethane (50 ml) is added to precipitate toluenesulfonic acid, which is removed by filtration. The solvent is removed and acetonitrile (30 ml) is added to the residual oily residue. The suspension is treated in an ultrasonic bath for 15 min to afford the precipitation of the ditopic ligand **12** as a white solid, which is isolated (400 mg, 0.5 mmol, 83 %) by filtration and dried at room temperature.

m.p. 133 °C; ^{1}H NMR (400 MHz, CDCl$_3$, TMS): δ = 8.64 (ddd, J = 5.0, 1.5, 1.0 Hz, 4H; H6, H6"), 8.61 (s, 4H; H3', H5'), 8.57 (dt, J = 8.0, 1.0 Hz, 4H; H3, H3"), 7.79 (td, J = 7.5, 2.0 Hz, 4H; H4, H4"), 7.77 (d, J = 9.0 Hz, 4H; H$_{Ar}$), 7.26 (ddd, J = 7.5, 5.0, 1.0 Hz, 4H; H5, H5"), 6.94 (d, J = 9.0 Hz, 4H; H$_{Ar}$), 4.11 (t, J = 5.0 Hz, 4H; OCH$_2$), 3.82 (t, J = 5.0 Hz, 4H; OCH$_2$), 3.71-3.63 (m, 8H; OCH$_2$); ^{13}C NMR (100 MHz, CDCl$_3$): δ = 160.2 (C$_{Ar}$), 156.4 (C2', C6'), 155.8 (C2, C2"), 150.1 (C6, C6"), 149.2 (C4'), 137.6 (C4, C4"), 131.1 (C$_{Ar}$), 128.9 (C$_{Ar}$), 124.2 (C3, C3"), 121.9 (C5, C5"), 118.8 (C3', C5'), 115.4 (C$_{Ar}$), 71.3 (OCH$_2$), 71.1 (OCH$_2$), 70.1 (OCH$_2$), 67.9 (OCH$_2$) ppm; UV-vis (CHCl$_3$/MeOH 60/40): λ_{max} (ε) = 287 nm (76000 M^{-1} cm^{-1}); fluorescence (CHCl$_3$/MeOH 60/40): λ_{max} = 392 nm; fluorescence quantum yield Φ_{fl} = 0.30±0.1; MS (EI, 70 mV): m/z 808.4 [M]$^{+}$ calcd for C$_{50}$H$_{44}$N$_6$O$_5$: 808.3; elemental analysis calcd (%) for C$_{50}$H$_{44}$N$_6$O$_5$·0.5H$_2$O: C 73.42, H 5.55, N 10.27; found C 73.26, H 5.55, N 10.06.

UV-vis titration of ptpy with Zn(OTf)$_2$. A solution of ptpy (0.05 mM in acetonitrile, 1500 µl in a 1cm quartz UV-vis cuvette) is titrated with zinc triflate (0.5 mM in ptpy solution, 10 µl aliquots) in a constant-host titration. The UV-vis spectrum (200-400 nm) is recorded after each addition.

Fluorescence titration of ptpy with Zn(OTf)$_2$. A solution of ptpy (0.005 mM in acetonitrile, 1500 µl in a 1cm quartz fluorescence cuvette) is titrated with zinc triflate (0.05 mM in ptpy solution, 10 µl aliquots) in a constant-host titration. The fluorescence spectrum is recorded after each addition by excitation at the isosbestic point at λ_{ex} = 279 nm to avoid the necessity for absorption correction.

UV-vis titrations of ligands 8 and 12 with zinc triflate. The respective ligand **8** or **12** (0.05 mM in CHCl$_3$/MeOH 60:40, 1500 µl, 1cm quartz cuvette) is titrated with zinc triflate (0.5 mM in respective ligand solution, 10µl aliquots) and the UV-vis spectra are recorded after each addition.

Fluorescence titration of ligands 8 and 12 with zinc triflate. The respective ligands **8** or **12** (0.005 mM in CHCl$_3$/MeOH 60/40, 1500 µl, 1 cm fluorescence quartz cuvette) is titrated with zinc triflate (0.05 mM in respective ligand suolution, 10 µl aliquots) and the fluorescence spectrum is recorded after each addition by excitation at the isosbestic points to avoid the necessity for absorption correction (**8**: λ_{ex} = 310 nm; **12**: λ_{ex} = 312 nm).

^{1}H NMR titration of 12 with zinc triflate. To five identical samples of the ligand **12** (4 mg, 4.94 μmol, 4.94 mM in CDCl$_3$/d$_4$-MeOH, 60:40) are added 0, 0.5, 1, 1.5 and 3 equivalents of zinc triflate (0.5 eq.: 0.899 mg, 2.47 μmol; 1 eq.: 1.797 mg, 4.49 μmol; 1.5 eq.: 2.697 mg, 7.42 μmol; 3 eq.: 5.394 mg, 14.84 μmol) to yield clear homogeneous solutions, which were characterized by ^{1}H NMR. A DOSY NMR spectrum is recorded additionally for the pure ligand solution and the 1:1 mixture.

Preparation of mixed coordination polymer for energy transfer investigations. Stock solutions of the respective ligand **8**, **12**, **14** and zinc triflate were prepared (chloroform-methanol, 60:40 vv, 1.25×10^{-5} M) and the mixed polymers were prepared by combining 95 vol% of ligand solution **8** or **12** with 5 vol% of solution of **14** and subsequent addition of 100 vol% of zinc triflate solution to achieve complexation. The solutions were analyzed without prior isolation of the compounds.

References

(¹)   Goodall, W.; Gareth Williams, J. A. *Chem. Commun.* **2001**, 2514-2515.

(²)   Mutai, T.; Cheon, J.-D.; Arita, S.; Araki, K. *J. Chem. Soc., Perkin Trans. 2* **2001**, 1045-1050.

(³)   Schütte, M.; Kurth, D. G.; Linford, M. R.; Cölfen, H.; Möhwald, H. *Angew. Chem. Int. Ed.* **1998**, *37*, 2891-2893.

(⁴)   Kurth, D. G.; Schütte, M.; Wen, J. *Coll. Surf., A: Physicochem. Eng. Asp.* **2002**, *198-200,* 633-643.

(⁵)   Yu, S.-C.; Kwok, C.-C.; Chan, W. K.; Che, C.-M. *Adv. Mater.* **2003***, 15*, 1643-1647.

(⁶)   Aspley, C. J.; Gareth Williams, J. A. *New. J. Chem.* **2001**, *25*, 1136-1147.

(⁷)   Child, A. D.; Reynolds, J. R. *Macromolecules* **1994**, *27*, 1975-1977.

(⁸)   Hanabusa, K.; Hirata, T.; Inoue, D.; Kimura, M.; Shirai, H. *Coll. Surfaces, A: Physicochem. Eng. Asp.* **2000**, *169*, 307-316.

(⁹)   Marquis, D.; Desvergne, J.-P.; Bouas-Laurent, H. *J. Org. Chem.* **1995**, *60*, 7984-7996.

(¹⁰) Collin, J. P.; Guillerez, S.; Sauvage, J.-P.; Barigelletti, F.; De Cola, L.; Flamigni, L.; Balzani, V. *Inorg. Chem.* **1991**, *30,* 4230-4238.

(¹¹) Constable, E. C.; Ward, M. D. *Inorg. Chim. Acta* **1988**, 201-203.

(¹²) Constable, E.C.; Lewis, J.; Liptrot, M. C.; Raithby, P. R. *Inorg. Chim. Acta* **1990**, *178*, 47-54.

(¹³) Lakowicz, J. R. *Principles of Fluorescence Spectroscopy*, 2nd ed., Kluwer Academic/Plenum, New York, **1999**.

6

Electrostatic Self-Assembly
of Fluorescent Coordination Polymers

Abstract: In this chapter, the fluorescent coordination polymers **1** and **4**, which have been discussed in chapters 3 and 5, are applied to form fluorescent multilayer assemblies on quartz substrates by electrostatic self-assembly. Homogeneous films consisting of more than ten layers could be prepared by alternating immersion of the substrate in solutions of PSS and the coordination polymer respectively. UV-vis spectroscopy was applied to prove the build-up of the layers. By introduction of PSS/PAH layer as separators the substrates could also be covered with layers of both polymer types **1** and **4**. The fluorescence of the perylene bisimide unit is still observable when the units are assembled in multilayers, even though the fluorescence quantum yield is decreased.

Introduction

The construction of supramolecular systems of high complexity is scarcely possible by the application of one single type of noncovalent interaction, but affords the use of different interactions, whose binding strengths and orientations have to be well balanced. This approach is known as hierarchical self-assembly and is perfectly applied in natural systems. One example is given by the the light-harvesting system of green filamentous bacteria (chloroflexaceae) and green sulfur bacteria (chlorobiaceae), which consists of a large number of bacteriochlorophyll molecules that are organized in a tube-like structure. Each chromophore is fixed at its place by a network of hydrogen bonds, metal-ligand interactions and the mutual interaction of the chromophore's π-systems, the latter yielding excitonic coupling, which is the basis of the function of this aggregate, light energy absorption and transfer.[1] A number of examples have been published where the concept of hierarchical structure formation is adopted to the formation of complex synthetic structures.[2]

In the last years, great effort has been made to achieve noncovalent organization of molecules in the nanometer scale. Within this research area, the organization on surfaces is of special interest, since modified surfaces can be applied in a large number of applications as sensors or as electronic devices including organic transistors, organic solar cells or organic light emitting diodes. Supramolecular polyelectrolyte assemblies, which are prepared by alternating adsorption of polycations and polyanions, gained extensive interest[3] after the method was established by Decher and coworkers.[4] This method offers detailed control of surface layers comparable to the Langmuir-Blodgett-technique.[5] The important advantages of the so-called 'layer-by-layer' technique are its simplicity, since it can be applied without expensive machinery, and a wide range of materials that could be assembled. Examples for systems which have been assembled on surfaces include dendrimers, DNA and proteins, viruses, inorganic sheet structures or latex particles.[3] Furthermore, the method is not restricted to certain substrates but can be applied to all types and forms of substrates which bear surface charges. It needs to be mentioned that the layer assembly is not precise, but somewhat "fuzzy" and the adsorbed polyelectrolyte layers interpenetrate.

The layer-by-layer assembly was first applied to terpyridine coordination polymers by Kurth and coworkers.[6,7] In this chapter[8] the construction of multilayers from fluorescent metallosupramolecular coordination polyelectrolytes, which are formed by self-assembly of fluorescent tpy-functionalized units, is presented.

114

Results and Discussion

General Multilayer Formation. Figure 1 illustrates the principle of the layer-by-layer self-assembly. The substrate, in this case a transparent quartz slide, needs to be covered with a surface charge, which is dependent on the nature of the surface material and the previous cleaning and treatment. Dipping of the substrate into a solution of a polyelectrolyte of opposite charge results in the electrostatic adsorption of the polymer on the surface. The adsorption step has to be followed by a washing step. This is necessary to remove loosely adsorbed material, which would coprecipitate on the surface in the presence of oppositely charged material thereby causing irregularities or preventing the subsequent layer formation. After the washing step, the surface charge is reversed since more polyelectrolyte is adsorbed than would have been necessary just to compensate the charges. This charge overcompensation is the crucial point for the function of the layer-by-layer method. The most important parameters which can influence the adsorption behavior of the polymers on the surface are ionic strength, pH, the solvent and the concentration. The dipping time has to be long enough to ensure complete adsorption and lies in the range of 10-20 min for each adsorption step. The substrate is then dipped into the polyanion and polycation solution in a repetitive manner, always with an intermediate washing step, to form the individual layer pairs.
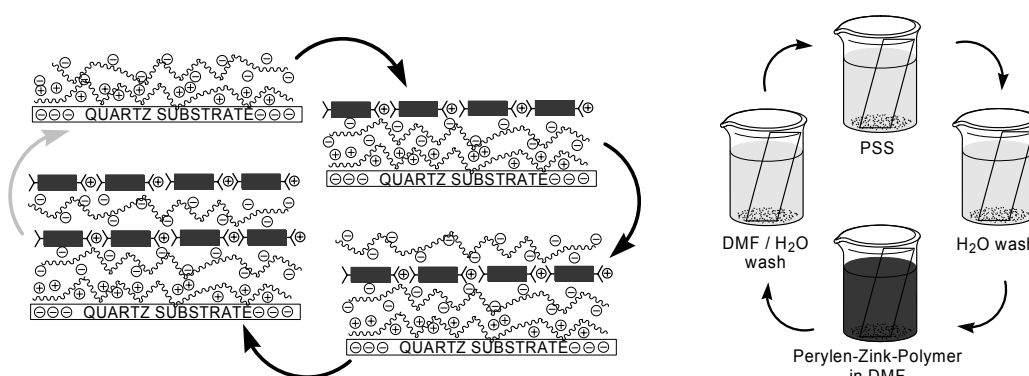

Figure 1. Schematic illustration of the principle of the layer-by-layer method, which is based on the surface charge reversal due to an overcompensation of the substrate's surface charge.
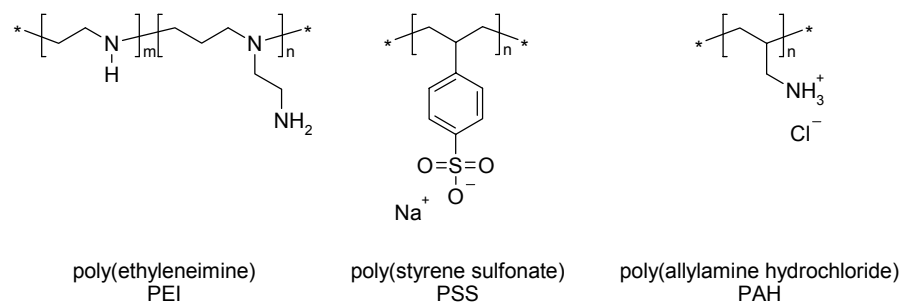

poly(ethyleneimine)
PEI

poly(styrene sulfonate)
PSS

poly(allylamine hydrochloride)
PAH

Chart 1.

115

There is a large number of polyelectrolytes which have been used for polyelectrolyte self-assembly. The polymers used in this work are depicted in chart 1. The highly branched poly(ethylene imine) (PEI) is only used for the first layer to ensure the contact between the quartz substrate and the subsequent layers. Poly(styrene sulfonate) (PSS) is an abundantly used polyanion which is applied as the counter-polyelectrolyte for all the polycations within this work.
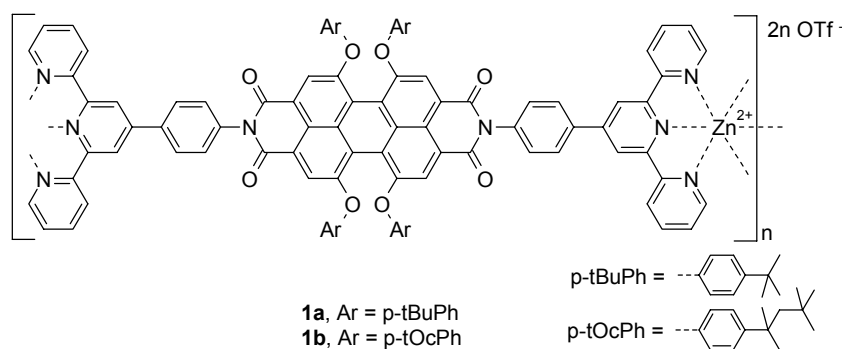

1a, Ar = p-tBuPh
1b, Ar = p-tOcPh

Chart 1.

Layers of Perylene Bisimide Containing Coordination Polymer 1: Since the perylene terpyridine coordination polymer **1a,b** is only soluble in chloroform–methanol mixtures and DMF (refer to chapters 3 and 4 for detailed discussion), the procedure was adapted and DMF was chosen for the deposition of the polycationic perylene bisimide coordination polymers **1a,b**. After covering of the surface with one layer of PEI to form a cationic surface, and the first adsorption of PSS from aqueous solution, the substrate was dipped into the coordination polymer solution in DMF. After every adsorption of the perylene polymer from DMF, the substrate was washed subsequently with pure DMF, a 1:1 mixture of DMF–water, and pure water. This successive change of the solvent ensures that there is no uncontrolled precipitation of the perylene coordination polymer on the surface due to solvent changes, since it is insoluble in water. The growth of the layers can be easily monitored by UV/Vis spectroscopy, which is shown in figure 2 for up to ten layers of coordination polyelectrolyte **1a** on a quartz substrate and for 6 layers of **1b** in figure 3. For **1b**, after five layers, the amount of adsorbed polymer **1b** decreases and after the seventh layer no further layer buildup could be monitored, but in contrast, partial detachment of the film occurred.
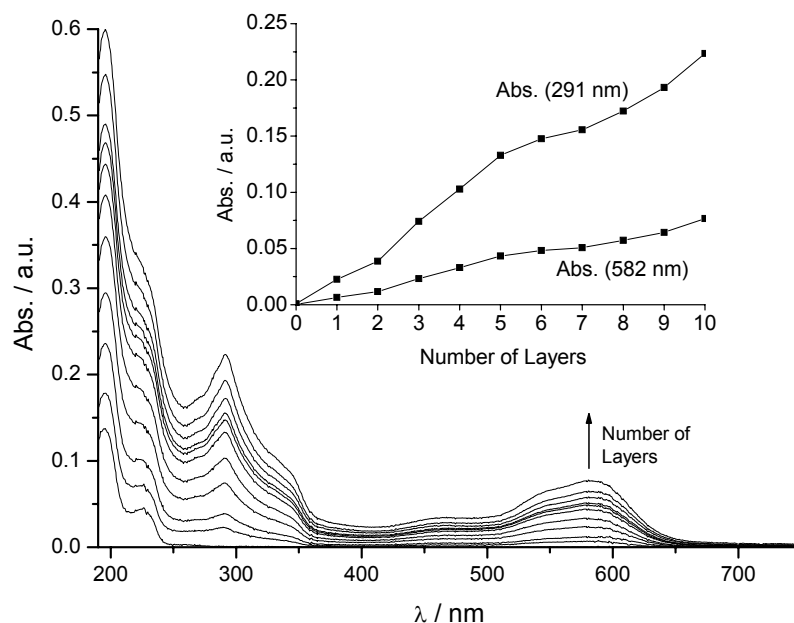
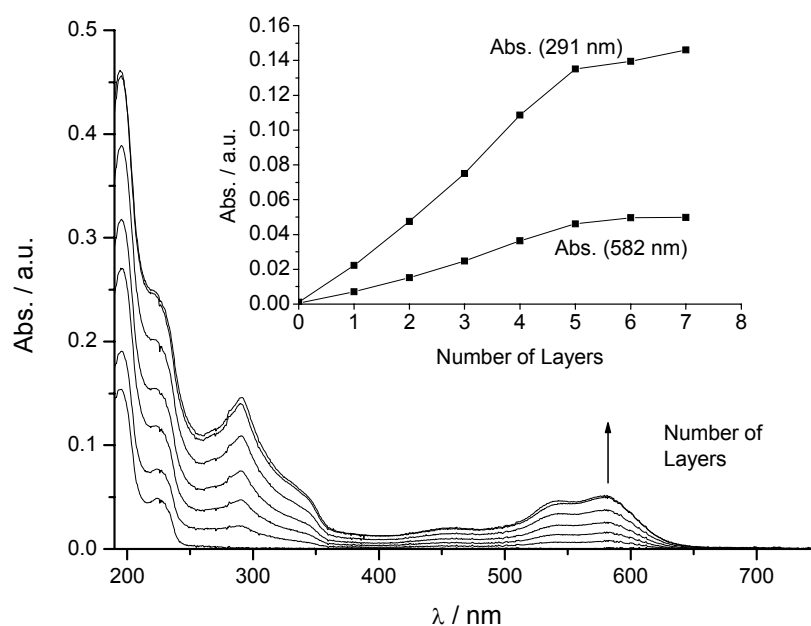**Figure 2.** UV/Vis Spectra of Self-Assembled Multilayers [Quartz/PEI/(PSS/**1a**)$_n$/PSS] (n=1-10).

Figure 3. UV/Vis Spectra of Self-Assembled Multilayers [Quartz/PEI/(PSS/**1b**)$_n$/PSS] (n=1-7).

As depicted in the insets of figures 2 and 3, the growth of the multilayers is not perfectly linear, i.e. the amount of adsorbed polymer varies in different adsorption steps. Nevertheless, the amount of polymer adsorbed to the surface is enough in every step to change the surface charge and thereby facilitate successive adsorption of the next layer with opposite charge. Investigation of the substrates under an optical microscope shows a homogeneous film.

From the UV/Vis absorbance data the surface coverage of the layers can be estimated using Beer's Law, if some approximations are made. The calculated value for the surface coverage is 0.4 monomer units/nm^2 which corresponds to a space demand of 2.4

nm^2/monomer unit. From molecular modeling studies[9] the space demand of one perylene building block can be estimated to be 6 – 8 nm^2 depending on the conformation of the phenoxy substituents, provided that the units are aligned parallel to the surface. From the basis of this estimation, one layer of the perylene polymer consists of approximately three polymer strands. These results imply that aggregation of the polymer strands takes place on the substrate surface. The observation of aggregation is also consistent with the shape of the UV/Vis bands, which are broadened significantly compared to those of the solution, as can be seen from the comparison in Figure .

Fluorescence Properties. The fluorescence properties of the coordination polymers are still retained in the polyelectrolyte films, but quantum yield and lifetime of the fluorescence are significantly decreased. The quantum yield of **1a,b**, which is $\Phi_{Fl} = 0.6$ in DMF solution, is lowered to 0.04±0.05 for **1a** and 0.06±0.05 for **1b**. For the lifetimes (figure 6) a decrease from 5±0.4 ns in DMF solution to 0.5±0.4 ns in the polyelectrolyte layers is observed. The reasons for this low fluorescence within the layers could be the highly polar and ionic environment, as well as aggregation of the perylene bisimide unit, which both promote fluorescence quenching. The fluorescence spectrum (figure 4 and 5) shows significantly broadened bands compared to the spectrum in solution while the fluorescence maximum is shifted bathochromically and the Stokes shift is increased from 36 nm in DMF solution to 74 nm in the multilayer film.
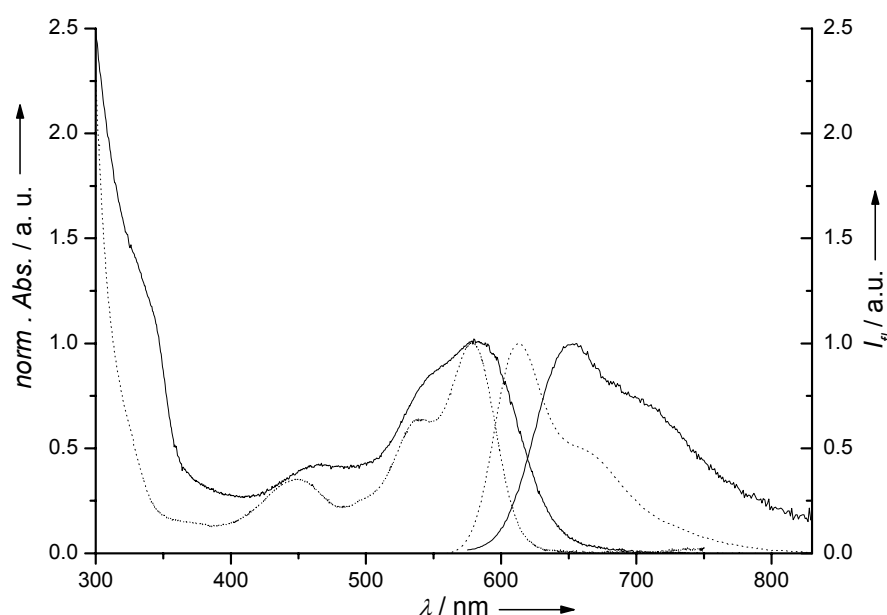

Figure 4. Comparison of UV-vis and fluorescence spectra of coordination polymer **1a** in DMF solution (dotted line) and in the polyelectrolyte multilayer assembly. Note the significant red-shift of luminescence and the broadening of both absorption and fluorescence spectra in the case of the multilayer system.
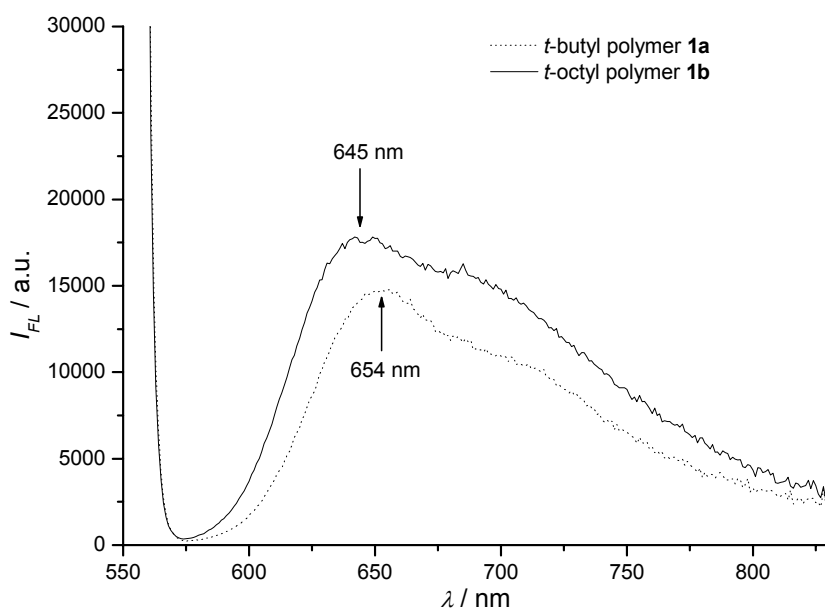
Figure 5. Comparison of the fluorescence spectra of the *t*-butyl- and the *t*-octyl-substituted perylene coordination polymers **1a** (dotted line) and **1b** (solid line).
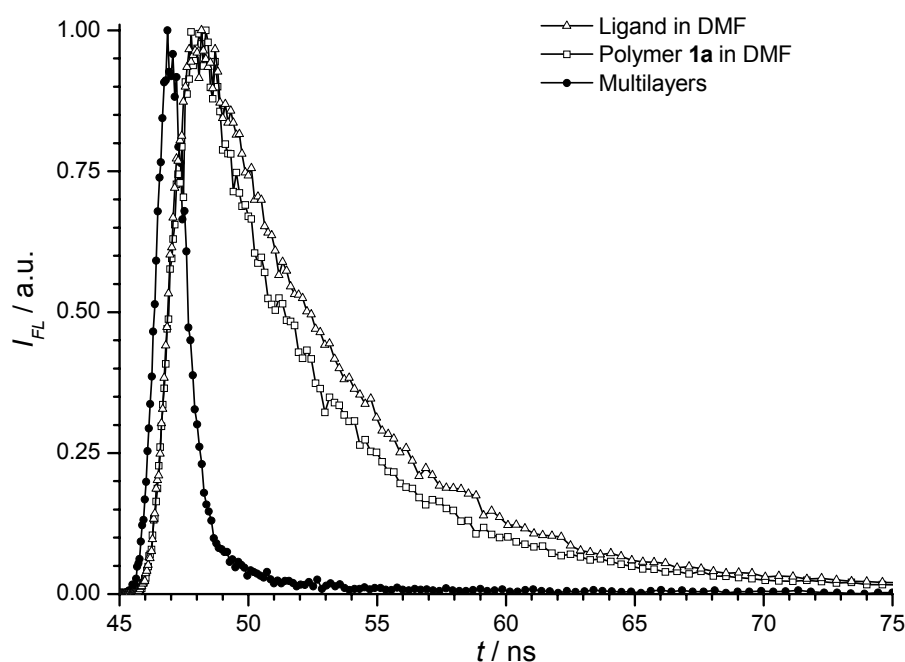

Figure 6. Fluorescence lifetime of ligand **1a** and polymer **2a** in DMF and multilayer [quartz/PEI/(PSS/**1a**)$_{10}$/PSS]; Inset: fluorescence spectrum of polymer **2a** in DMF (dotted line) and multilayer.

Alternative Substrate Preparation for Enhanced Layer Stability: Although the layer formation could be achieved directly on PEI-coated quartz substrates, the stability of the layers decreased significantly when more than 5 layers are adsorbed. During the washing procedure, some parts of the film lost contact with the substrate and were washed off, with the phenomenon getting more critical with increasing number of layers. This observation indicates that the films themselves are stable, but suffer from bad adhesion to the quartz

substrate. To improve the film adhesion, the perylene bisimide coordination polymers were adsorbed on a pretreated substrate, which was first covered with two double-layers of PSS/PAH on the initial PEI-treated substrate. This method significantly increased the stability of the films and no film detachment or rupture was observed also when more than ten layer pairs were adsorbed.

Film Formation with Oligoethylene Glycol Spacered Tpy-Coordination-Polymer 4: Layer formation was also investigated with the oligoethylene glycol spacered coordination polymer **4**, which was introduced in chapter 5. The adsorption procedure was exactly identical to the one applied for the perylene bisimide coordination polymer and also DMF was applied as solvent. The UV-vis spectra in figure 7 were recorded after each double-layer adsorption step. Also for this coordination polymer, the amount of adsorbed material is not exactly the same for each step. Remarkably, the fluorescence of the coordination polymer is retained upon assembly within the polyelectrolyte layers and the layers show a bright blue-green fluorescence when watched under UV-light.
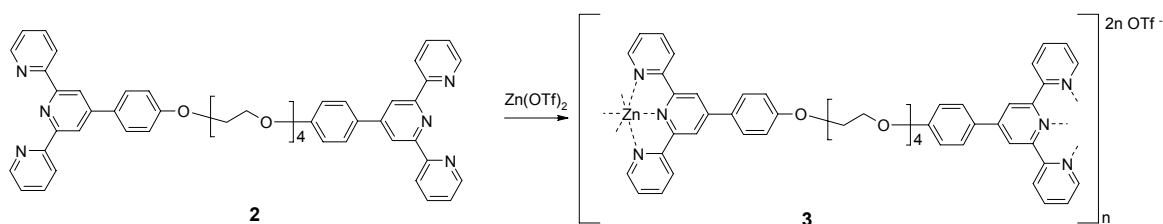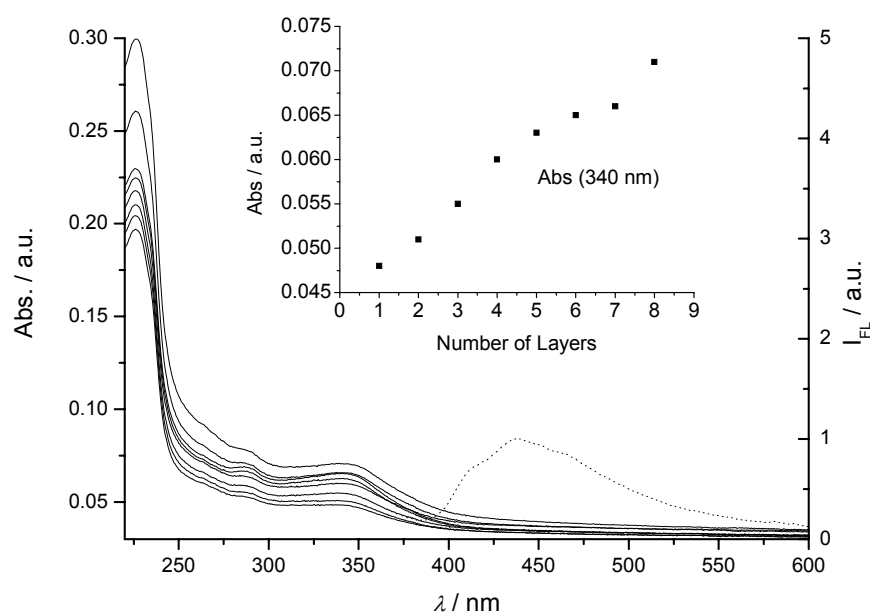

Scheme 1

Figure 7. Layer assembly of the oligoethylene glycol spacered coordination polymer **3** monitored by UV-vis spectroscopy. Also the fluorescence spectrum (dotted line, $\lambda_{ex} = 350$ nm) of the compound when assembled within the layers is shown (right axis). Inset: Increase in absorption (340 nm) against the number of adsorbed layers.

Construction of Mixed Layers: Since both layers of the perylene bisimide containing coordination polymer **1** and the oligoethylene glycol spacered coordination polymer **3** exhibit fluorescence, the formation of mixed layers was studied with the goal of realizing a white light-emitting system[10] by a mixture of fluorophores emitting at different wavelengths. The construction of substrates bearing layers of both polymer types is shown in figure 8 and figure 9. In figure 8, the perylene bisimide containing polymer (in this case the octyl-substituted type **1b**) is adsorbed first in six layers followed by one double layer of PAH/PSS. Subsequently, seven layers of the tetraethylene glycol spacered polymer **3** are adsorbed.
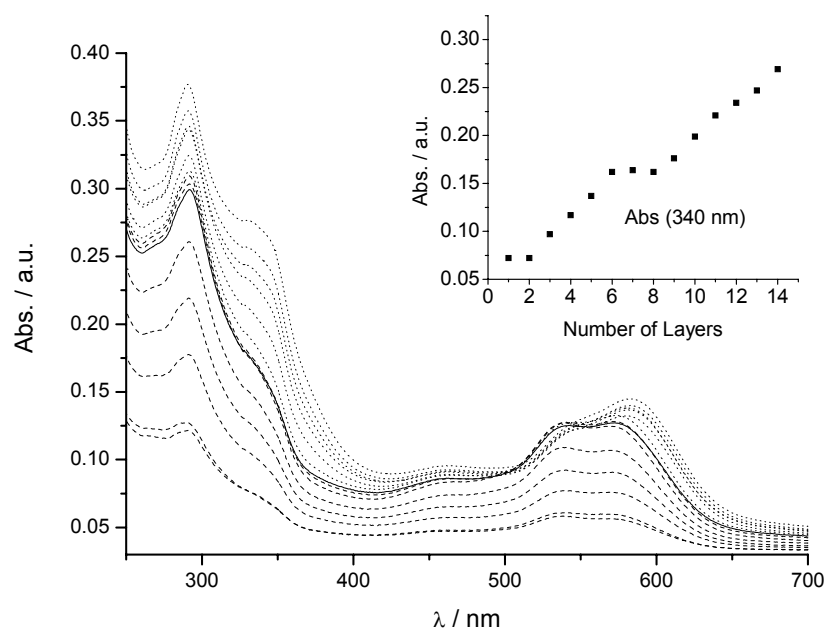

Figure 8. Layer assembly consisting of 6 layers of the perylene bisimide polymer **1b** (dashed lines), a PAH/PSS double layer (solid line) and 7 layers of the tetraethylene glycol polymer **3** (dotted lines): [quartz/PEI/(PSS/PAH)$_2$/(PSS/**1b**)$_6$/(PSS/PAH)$_2$/(PSS/**3**)$_7$]. The inset shows the absorption spectra at 340 nm.

In figure 9, the situation is inverse and the perylene bisimide coordination polymer is adsorbed on top of the ethylene glycol spacered polymer **3** and the intermediate PAH/PSS layer. Although the additional intermediate PAH/PSS layer increases the distance between the two types of dye-containing polymers it was found to be necessary to allow the effective adsorption of a second type of polymer. When polymer **3** was directly adsorbed onto the perylene bisimide layers, the UV-vis spectra showed a drastic decrease of perylene bisimide absorbance pointing towards the destruction of the perylene bisimide layers by polyelectrolyte **3**.
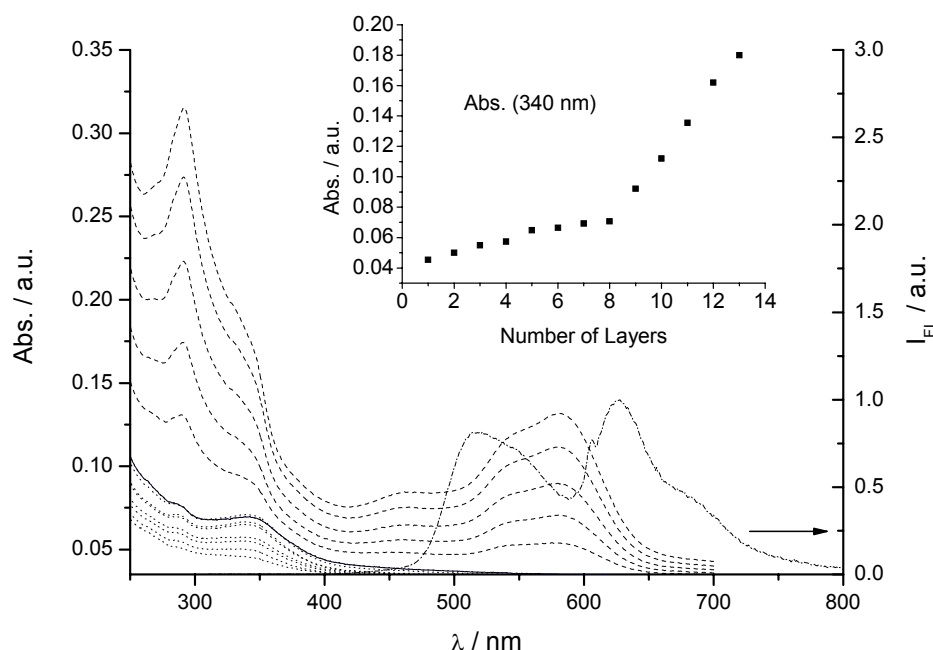
Figure 9. Layer assembly consisting of 6 layers of the tetraethylene glycol polymer **3** (dotted lines), a PAH/PSS double layer (solid line) and 5 layers of the perylene bisimide polymer **1b** (dashed lines):[quartz/PEI/(PSS/PAH)$_2$/(PSS/**3**)$_6$/(PSS/PAH)$_2$/(PSS/**1b**)$_5$]. The inset shows the absorption spectra at 340 nm. Dashed-dotted line: the fluorescence spectrum of the layer upon excitation at 300 nm.

The fluorescence spectrum of this multilayer assembly (figure 9, dotted line) shows the emission of both coordination polymers. The emission of polymer **3** is shifted by more than 50 nm to the red and shows a fluorescence maximum at 505 nm. Since both types of fluorophores are separated by the two PAH/PSS layer pairs, energy transfer is not likely due to the relatively large distance of the two systems.

Conclusion

In the present chapter, the formation of polyelectrolyte multilayers by electrostatic self-assembly was accomplished with two of the Zn^{2+} mediated coordination polymers which were introduced in the preceding chapters of this thesis. The multilayers are fabricated by simple immersion of a quartz substrate alternatingly into a solution of a polystyrene sulfonate polyanion and the respective zinc-terpyridine based coordination polymers, which are polycations. Layer formation can be easily monitored by UV-vis spectroscopy and showed continuous adsorption of the polyelectrolytes.

The fluorescence of the perylene bisimide units can still be investigated when adsorbed within such multilayer assemblies, but a decrease of the fluorescence quantum yield was noted. In contrast, the blue-fluorescent coordination polymer constructed from the oligoethylene glycol spaced 4'-phenylterpyridine ligand retains its fluorescence intensity also within the deposited assemblies.

Quartz substrates could also be covered with layers of both types showing both the blue fluorescence of the phenylterpyridine based polymer and the red fluorescence of the perylene bisimide based polymer. Energy transfer was not observed due to the significant distance of the two different fluorophores within these layers.

The layer-by-layer method enables easy three dimensional assembly of these fluorescent supramolecular coordination polymers. Surfaces covered with fluorescent coordination polymers could be useful for applications like light-harvesting in dye-sensitized solar cells, or as fluorescent units in organic light emitting diodes.

Experimental Section

Materials. Quartz substrates were supplied by Hellma GmbH, Müllheim, Germany, and cleaned by immersing into conc. H_2SO_4/H_2O_2 (ca. 1:1) for 10 min followed by intensive rinsing with water. Polyethyleneimine (PEI, branched, MW ca. 750.000) and polystyrene sulfonate (PSS, MW ca. 70.000) were obtained from Sigma-Aldrich Chemie GmbH, and applied as 0.01 M solutions in 0.5 M aqueous NaCl solution. Zinc trifluoromethanesulfonate (triflate) was purchased from ABCR GmbH, Karlsruhe, Germany. Solvents were purchased from Merck KG and used without further purification. UV/Vis spectra were recorded with a Varian Cary-50 spectrophotometer and fluorescence spectra on a Spex Fluorolog 212. Fluorescence lifetimes are determined with a fluorescence lifetime system using a PTI GL330 nitrogen laser (337 nm) and a PTI GL302 dye laser. Fluorescence decay curves were evaluated using the software supplied with the instrument. Fluorescence quantum yields are relative to *N,N'*-di(2,6-diisopropylphenyl)-1,6,7,12-tetraphenoxyperylene-3,4:9,10-tetra-carboxylic acid bisimide ($\Phi_{Fl} = 0.96$ in $CHCl_3$).[11]

Perylene coordination polymer. An exact 1:1 mixture was prepared by using stock solutions of ligand **1** (1.97 μM, 16.0 ml) and zinc triflate (22.3 μM, 1.41 ml) in chloroform–methanol (60:40), the mixture was stirred over night at room temperature. An aliquot of the solution was evaporated and the residue was redissolved in $CDCl_3$–CD_3OD (60:40) for ^{1}H-NMR measurements to ensure the 1:1 ratio. The reaction mixture was condensed, the product precipitated by addition of more methanol and isolated by centrifugation.

Multilayer formation. A freshly cleaned quartz substrate was immersed into a solution of PEI for 20 min, washed with water and dried under a gentle stream of nitrogen gas. Multilayers are formed by subsequent dipping of the substrate in solutions of PSS and te respective coordination polymer (1 mM in DMF). After each adsorption step in DMF the substrate is subsequently immersed in DMF, DMF–water (1:1) and water to avoid undesired

precipitation of polymer **2** in the next adsorption step. The formation of the layers was controlled by UV/Vis spectroscopy after each adsorption step.

Calculation of surface coverage. The surface coverage Γ of the perylene chromophores was calculated according to the equation $\Gamma = A \cdot l^{-1} \cdot \varepsilon^{-1}$, where A is the absorbance of the film, l is the number of layers, and ε is the molecular extinction coefficient of the polymer. As only the molar extinction coefficient of the isotropic solution in CH_2Cl_2 is known, it is important to note that the calculated surface coverage is only an approximation.

References

(1)   Olson, J. M. *Photochem. Photobiol.* **1998**, *67*, 61-75.

(2)   For a recent review on the concept of hierarchical self-assembly refer to: Elemans, J. A. A. W.; Rowan, A. E., Nolte, R. J. M. *J. Mater. Chem.* **2003**, *13*, 2661-2670.

(3)   For current reviews on electrostatic self-assembly refer to: Arys, X.; Jonas, A. M., Laschewsky, A.; Legras, R. *Supramolecular Polyelectrolyte Assemblies* in: A. Ciferri (Ed.) *Supramolecular Polymers*, 505-564, Marcel Dekker, New York, Basel: **2000**; Decher, G.; Schlenloff, J. B. *Multilayer Thin Films. Sequential Assembly of Nanocomposite Materials*, 177-205, Wiley-VCH, Weinheim: **2003**.

(4)   Decher, G. *Science* **1997**, *277*, 1232-1237.

(5)   Petty, M. C. *Langmuir Blodgett films: an introduction* Cambridge Univ. Press, Cambridge: **1996**.

(6)   Schütte, M.; Kurth, D. G.; Linford, M. R.; Cölfen, H.; Möhwald, H. *Angew. Chem. Int. Ed.* **1998**, *37*, 2891-2893.

(7)   Kurth, D. G.; Schütte, M.; Wen, J. *Coll. Surf., A: Physicochem. Eng. Asp.* **2002**, *198-200,* 633-643.

(8)   A part of this chapter is published as: Dobrawa, R.; Kurth, D. G., Würthner, F. *Polymer Prepr.* **2004**, *45*, 378-379.

(9)   Fujitsu Quantum CAChe 5, MM3 force field.

(10)   Gong, X.; Ma, W.; Ostrowski, J. C.; Bazan, G. C.; Moses, D.; Heeger, A. J. *Adv. Mater.* **2004**, *16*, 615-619.

(11)   Gvishi, R.; Reisfeld, R.; Burshtein, Z. *Chem. Phys. Lett.* **1993**, *213*, 338-344.

7

Summary

Thin films of organic dyes are currently investigated for application in organic solar cells and organic light emitting diodes. By incorporation of dyes into supramolecular polymers, interesting possibilities could arise for the preparation of such layers. By application of noncovalent, reversible interactions, structure formation occurs in a dynamic way, giving rise to self-assembly processes.

The topic of the present word is the synthesis and characterization of fluorescent supramolecular coordination polymers based on terpyridine metal complexes. Several building blocks have been used, based on the blue-fluorescent 4'-phenylterpyridine unit as well as a red fluorescent perlyene bisimide unit equipped with two terpyridine receptors. In both cases, chain growth reaction occurs upon addition of metal ions. To characterize this in detail, the thermodynamics of the terpyridine-metal ion interaction as well as the resulting polymeric structures and their fluorescence properties have been investigated.

The first chapter deals with the basic correlation between complex binding constant, concentration and the resulting polymer chain length. Furthermore, an overview of known

coordination polymer systems, which are based on various metal-ligand interactions, and their properties is given.

Investigation of the coordination interaction between the terpyridine ligand and a series of transition metal ions is the topic of the second chapter. By UV-vis and titration experiments and isothermal titration calorimetry (ITC), insight into the thermodynamics of complex formation and its reversibility could be gained. Enthalpies of reaction could be determined for the complexation of iron(II), cobalt(II), nickel(II), copper(II) and zinc(II) with terpyridine by ITC measurements. For the copper complex, the formation of a pentadentate complex could be proven, with one of the two tpy units in $Cu(tpy)_2^{2+}$ only acting as a bidentate ligand. Especially promising with regard to the aim of the present work is the zinc(II)-terpyridine complex, since despite its high binding constant ($K > 10^{10} \, M^{-1}$) complexation is reversible and due to its closed-shell d^{10} electron configuration no low-lying state can be populated, which quench the fluorescence.
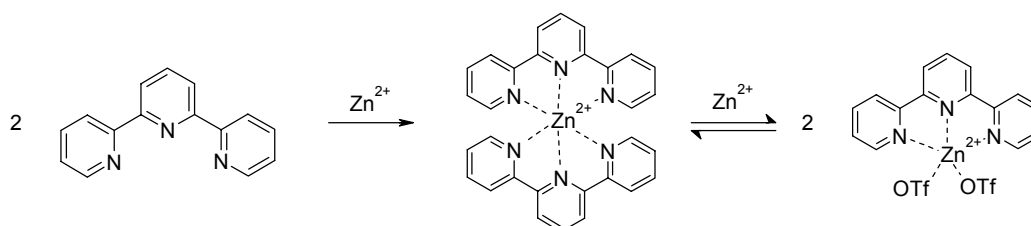
Scheme 1. Reversible complexation of the zinc-terpyridine system.

The synthesis of zinc(II)-terpyridine coordination polymer containing fluorescent perylene bisimide units is presented in chapter. The ligand is synthesized by reaction with 4'-aminophenylterpyridine with the fourfold phenoxy-substituted perylene bisanhydride thus forming the respective perylene bisimide. By application of a model compound bearing only one terpyridine receptor, the formation of the dimer complex is investigated first by NMR titration experiments. Reaction of the respective ditopic ligand with exactly one equivalent of zinc(II) causes the formation of the coordination polymer, which was also characterized by NMR titration studies. The advantageous properties of the perylene bisimide unit are scarcely influenced, thus producing a fluorescent coordination polymer. Addition of an excess amount of zinc(II) results in the fragmentation of the extended polymer into smaller monomeric and oligomeric fragments by transformation of the $Zn(tpy)_2^{2+}$ unit into the respective monocomplexed $Zn(tpy)^{2+}$ species.
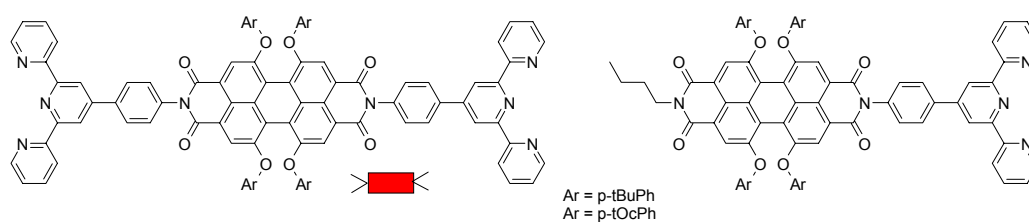
Chart 1. Ditopic and monotopic perylene bisimide-terpyridine ligands

The reversibility of the zinc(II)-mediated polymerization is discussed in the fourth chapter. By means of diffusion-based NMR methods (DOSY NMR) a significant decrease of the diffusion coefficient could be proven upon addition of one equivalent of zinc(II), suggesting a distinct increase of the molecular mass. Fragmentation of the polymer upon addition of an excess amount of zinc(II) can be observed by an increase in diffusion coefficient. A similar result was obtained by fluorescence anisotropy titration experiments. Here, the coordination polymer produced a clearly higher anisotropy value compared to the uncomplexed monomer or the fragmented species.
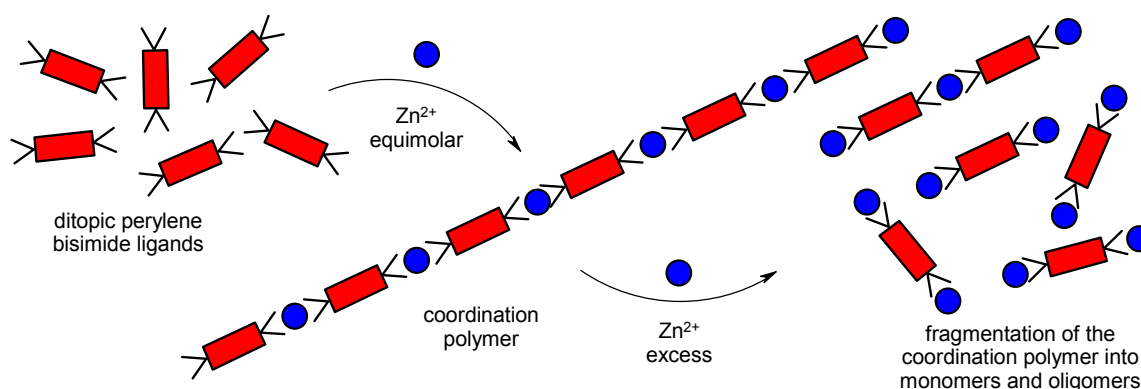

Figure 1. Reversible formation of the zinc coordination polymer.

Visualization of the polymer chains could be obtained by atomic force microscopy (AFM). Evaluation of the micrographs give an average chain length of approx. 15 repeat units, corresponding to a molecular mass of approx. 25000 g/mol. Sample preparation form concentrated solution resulted in the formation of a dense monolayer on the substrate by lateral aggregation of the individual polymer strands.

By application of the 4'-phenylterpyridine, which acts both as a structure determining unit and as a fluorophore, blue fluorescent terpyridine-based coordination polymers could be obtained (Chapter 5). By connection of two units by a tetraethylene glycol chain a ditopic ligand was obtained and its complexation behavior was investigated by NMR titration experiments. The titration experiments and additional DOSY NMR spectra revealed the

formation of a macrocyclic product, which is formed in the millimolar concentration range in 20 % in competition to the coordination polymer. By coordination of zinc(II) the fluorescence properties are increased, making this system an attractive building block for the formation of fluorescent supramolecular architectures. The possibilities regarding the construction of switchable structures as well as the preparation of catenanes and rotaxanes could be of special interest.
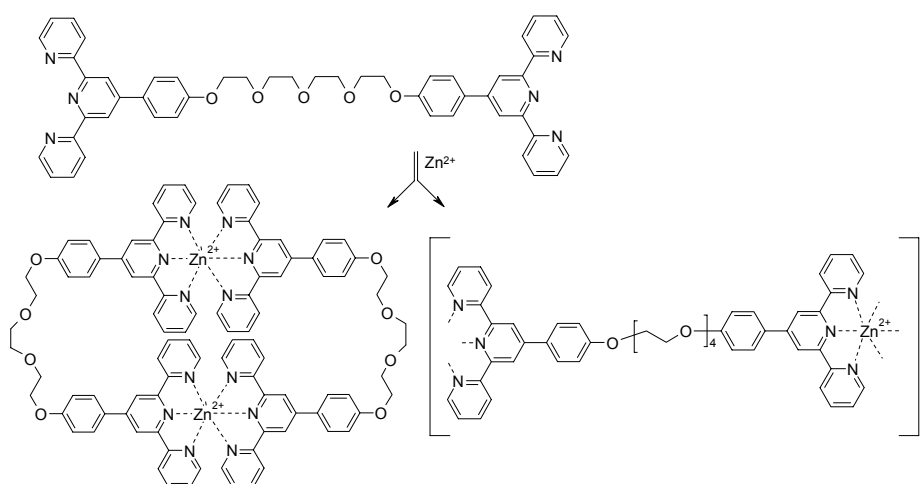
Scheme 2. Formation of macrocyclic and linear fluorescent coordination compounds.

An additional supramolecular structure formation process is described in chapter six, discussing the construction of defined polyelectrolyte layers from the fluorescent coordination polymers. The polycationic character of the coordination polymers is applied to obtain alternating adsorption of fluorescent terpyridine-polycations and polystyrene sulfonate polyanions by the so-called layer-by-layer method. Layer formation can be monitored by UV-vis spectroscopy. The characteristic fluorescence properties of the both terpyridine-based coordination polymers are retained; however, the fluorescence quantum yield is decreased.
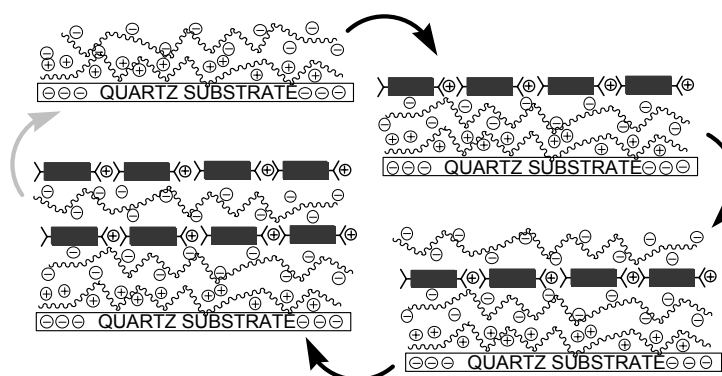

Figure 2. Construction of polyelectrolyte multilayers from the fluorescent coordination by the "layer-by-layer" method.

In conclusion, the present work presents a concept for the preparation of fluorescent supramolecular materials over a number of steps (hierarchical self-assembly) beginning with an investigation of the receptor system, the synthesis of ditopic ligands, the formation of 1D polymer chains by metal ion induced polymerization, the adsorption of the latter in 2D monolayers on negatively charged mica substrate up to the formation of controlled 3D layer formation.

8

Zusammenfassung

Dünne Schichten organischer Farbstoffe werden derzeit intensiv für Anwendungen in organischen Solarzellen und organischen Leuchtdioden (OLEDs) untersucht. Durch den Einbau von Farbstoffen in supramolekulare Polymere könnten sich interessante Möglichkeiten für die Herstellung solcher Schichten ergeben. Unter Verwendung von nichtkovalenten, reversiblen Wechselwirkungen resultiert die Strukturbildung in dynamischer Weise, so dass Selbstorganisationsprozesse möglich werden.

Die vorliegende Arbeit beschäftigt sich mit der Synthese und der Charakterisierung von fluoreszierenden supramolekularen Koordinationspolymeren auf der Basis von Terpyridin-Metallkomplexen. Dabei wurden mehrere Bausteine verwendet, zum einen die blau-fluoreszierende 4'-Phenylterpyridin-Einheit, zum anderen intensiv rot fluoreszierende Perylenbisimid-Fluorophore, die mit Terpyridin-Rezeptoren ausgestattet wurden. In beiden Fällen findet bei Zugabe von Übergangsmetallionen eine Kettenwachstumsreaktion statt. Um diese zu charakterisieren, wurden die Thermodynamik der Terpyridin-Metallionen-Wechselwirkung sowie die gebildeten Strukturen und deren Fluoreszenzeigenschaften eingehend untersucht.

Das erste Kapitel der Arbeit behandelt grundlegende Zusammenhänge zwischen Komplexbindungskonstante, Konzentration und der daraus resultierenden Polymerkettenlänge. Weiterhin wird ein Überblick über bereits bekannte Koordinationspolymere, welche auf unterschiedlichen Metall-Ligand-Systemen beruhen, und deren Eigenschaften gegeben.

Die Untersuchung der Koordinationswechselwirkung zwischen einem Terpyridin-Liganden und einer Reihe von Übergangsmetallionen ist Thema des zweiten Kapitels. Durch UV/Vis- und NMR-Titrationsexperimente sowie durch Isotherme Titrationskalorimetrie (ITC) konnte Einblick in die Thermodynamik der Komplexbildung und deren Reversibilität erhalten werden. Für die Metallionen Eisen(II), Cobalt(II), Nickel(II), Kupfer(II) und Zink(II) konnten die Reaktionsenthalpien der Komplexbildung durch ITC bestimmt werden. Für den Kupferkomplex wurde die Bildung eines fünffach koordinierten Komplexes festgestellt, in dem eine der Terpyridin-Einheiten nur als zweizähniger Komplex wirkt. Besonders vielversprechend im Hinblick auf die Zielsetzung der vorliegenden Arbeit erwies sich der Zink(II)-Terpyridin Komplex, da seine Bildung trotz hoher Bindungskonstante ($K > 10^8$ M^{-1}) rasch und reversibel verläuft und für das d^{10}-Metallion Zink(II) keine tiefliegenden Anregungszustände vorliegen, die zur Fluoreszenzlöschung führen.
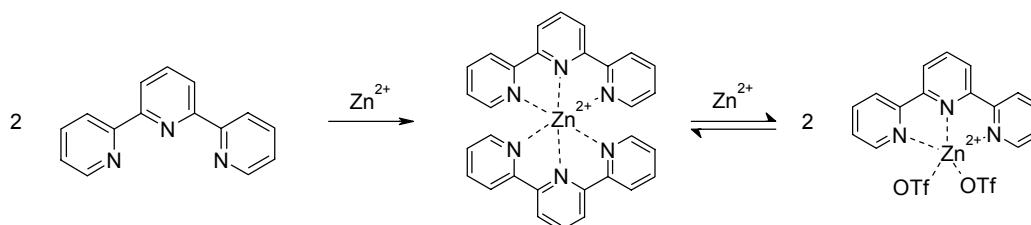
Schema 1. Reversible Komplexierung im Zink-Terpyridin System

Die Synthese von Zink-Terpyridin-Koordinationspolymeren mit eingebauten fluoreszierenden Perylenbisimid-Einheiten wird in Kapitel 3 vorgestellt. Die Darstellung der Liganden erfolgt durch Umsetzung von 4'-Aminoterpyridin mit dem vierfach Phenoxy-substituierten Perylenbisanhydrid unter Bildung des entsprechenden Perylenbisimids. Anhand einer Modellverbindung, die nur einen Terpyridin-Rezeptor trägt, wurde zunächst die Komplexierung zum dimeren Komplex durch NMR-Titrationsexperimente untersucht. Die Umsetzung des entsprechenden ditopen Perylenbisimid-Liganden mit exakt einem Äquivalent Zink(II) bewirkt die Bildung des Koordinationspolymers, welche ebenfalls durch NMR-Titration charakterisiert werden konnte. Bei der Koordination des Zink-Metallions werden die vorteilhaften Fluoreszenzeigenschaften der Perylenbisimid-Einheit nur geringfügig

beeinflusst, so dass sich ein fluoreszierendes Koordinationspolymer ergibt. Die Zugabe eines Zink-Überschusses bewirkt die Fragmentierung des ausgedehnten Polymers in kleine monomere und oligomere Bruchstücke durch die Umwandlung der $Zn(tpy)_2^{2+}$-Einheit in die entsprechende einfach-komplexierte $Zn(tpy)^{2+}$-Spezies.
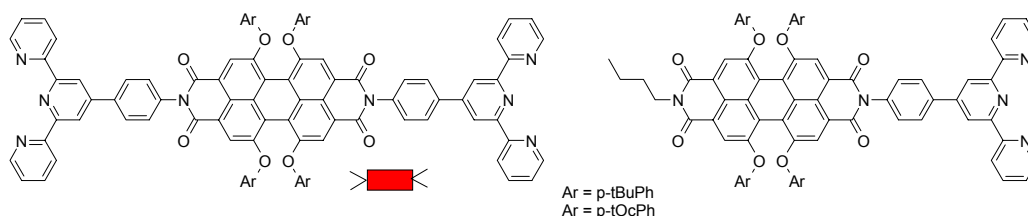

Chart 1. Ditope und monotope Perylenbisimid-Terpyridin Liganden

Die genaue Charakterisierung der Reversibilität der Zink-Ionen kontrollierten Polymerisation ist Inhalt des 4. Kapitels. Mittels diffusionsabhängiger NMR-Methoden (DOSY NMR) konnte eine signifikante Abnahme des Diffusionskoeffizienten nach Umsetzung mit einem Äquivalent Zink(II) nachgewiesen werden, was auf eine deutliche Zunahme der Molekülmasse schließen lässt. Die Fragmentierung nach Zugabe eines Zink(II)-Überschusses zeigt sich durch eine Erhöhung des Diffusionskoeffizienten. Ein entsprechendes Ergebnis konnte auch durch Fluoreszenzanisotropie-Titrationsexperimente erhalten werden. Hier ergibt sich für das Koordinationspolymer ein deutlich erhöhter Anisotropie-Wert im Vergleich zum unkomplexierten Monomer und der fragmentierten Spezies.
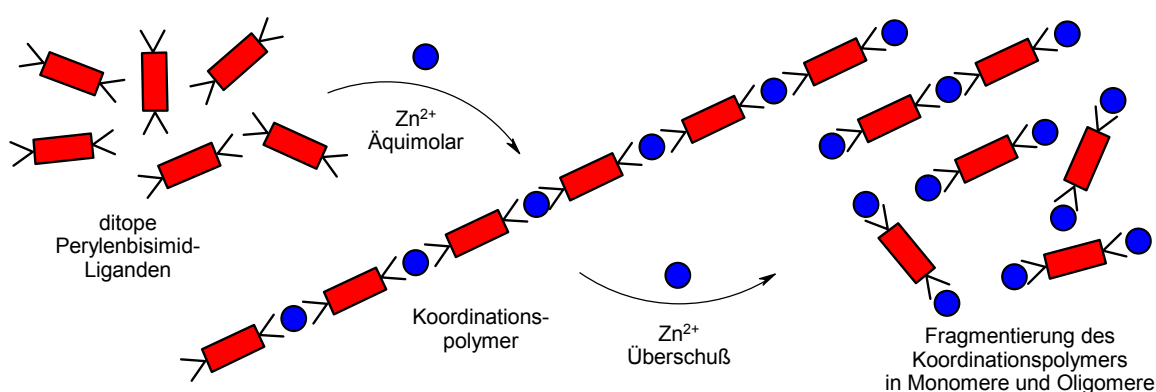

Abbildung 1. Reversible Bildung des Zink-Koordinationspolymers

Durch Rasterkraftmikroskopie-Messungen (AFM) konnten die Polymerstränge abgebildet werden. Die Auswertung der Bilder ergibt eine Kettenlänge von ca. 15 Wiederholungseinheiten, was einer Molekülmasse von ca. 25000 g/mol entspricht.

Messungen bei hoher Konzentration führten zur Ausbildung einer dichten Monolage auf dem Substrat, indem sich benachbarte Polymerketten aneinanderlagern.

Blau-fluoreszierende Terpyridin-basierte Koordinationspolymere wurden durch die Nutzung der 4'-Phenylterpyridin-Einheit erhalten, die sowohl als strukturgebende Einheit als auch als Fluorophor fungiert (Kapitel 5). Durch die Verbindung zweier Einheiten über eine Tetraethylenglykol-Brücke konnte ein ditoper Ligand erhalten werden, dessen Komplexbildung wiederum über NMR-Titrationen untersucht wurde. Dabei konnte durch NMR-Titrationsexperimente sowie DOSY NMR die Bildung einer makrocyclischen Spezies beobachtet werden, die sich als Konkurrenzprodukt zum Koordinationspolymer zu 20 % im millimolaren Konzentrationsbereich bildet. Durch die Koordination mit Zink(II) werden die Fluoreszenzeigenschaften dieses Liganden noch verbessert, so dass ein attraktiver Baustein zur Bildung von fluoreszierenden supramolekularen Architekturen erhalten werden konnte. Hier erscheinen insbesondere interessante Möglichkeiten im Hinblick auf schaltbare Strukturen sowie die Herstellung von Catenanen und Rotaxanen gegeben.
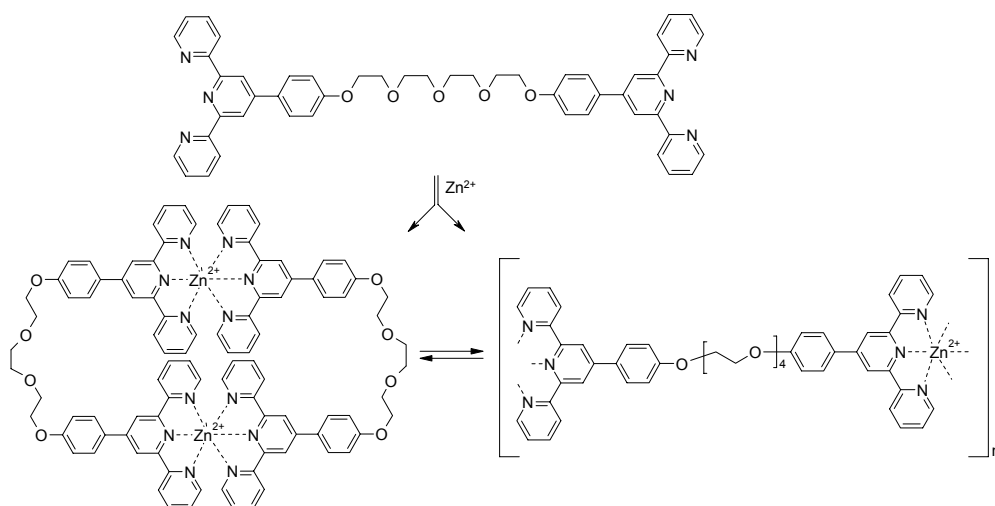
Schema 2. Bildung von makrocyclischen und linearen fluoreszierenden Koordinationsverbindungen

Ein weitergehender supramolekularer Strukturbildungsprozess wird in Kapitel 6 beschrieben, wo definierte Polyelektrolytschichten aus den fluoreszierenden Koordinationspolymeren hergestellt werden. Der polykationische Charakter der Koordinationspolymere wird hier zur alternierenden Adsorption von fluoreszierenden Terpyridin-Polykationen mit Polystyrolsulfonat-Polyanionen nach der sog. Layer-by-Layer Methode genutzt. Der Aufbau der Schichten aus den beiden bisher vorgestellten Polymeren lässt sich über UV/Vis-Spektroskopie verfolgen. Dabei bleiben bei beiden Polymertypen die charakteristischen Fluoreszenzeigenschaften – zum Teil allerdings mit verringerter Quantenausbeute – erhalten.
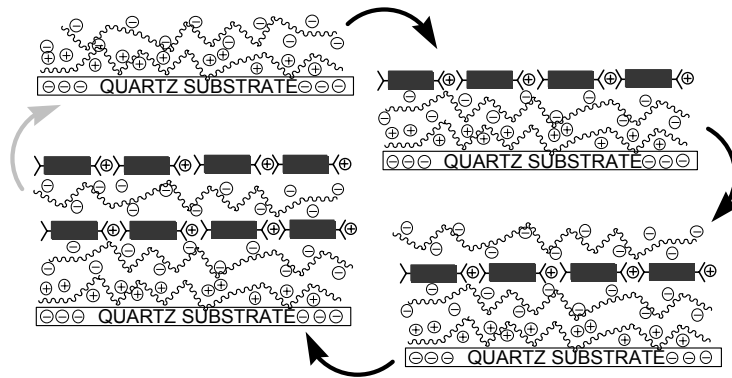
Abbildung 2. Aufbau von Polyelektrolyt-Multischichten aus den fluoreszierenden Koordinationspolymeren durch die "Layer-byLayer"-Methode.

Zusammenfassend wurde in dieser Arbeit ein Konzept für die Herstellung fluoreszierender supramolekularer Materialien über mehrere Stufen ("hierarchical self-assembly") beschrieben, beginnend mit Studien zum Bindungssystem, der Darstellung ditoper Liganden, dem Aufbau eindimensionaler Polymerstränge durch Metallionen-induzierte Polymerisation, deren Abscheidung in zweidimensionalen Monolagen auf negativ geladenem Glimmer-Substrat bis hin zum dreidimensionalen, kontrollierten Schichtaufbau.

DOBRAWA, RAINER ANTON

Date of Birth: June 13th, 1975
in Kaufbeuren, Germany

single; no children
nationality: german

DISSERTATION

since Oct. 2002	Continuing the dissertation at the Institut für Organische Chemie, Universität Würzburg, group of Prof. Dr. Frank Würthner
Oct. 2000 – Oct. 2002	Abteilung für Organische Chemie II, Universität Ulm Supervisor: Prof. Dr. Frank Würthner *"Synthesis and Characterization of Terpyridine-based Fluorescent Coordination Polymers""*

UNIVERSITY EDUCATION

March – Sept. 2000	Diploma Thesis, Abteilung für Organische Chemie II, Universität Ulm, Supervisor: Prof. Dr. Bäuerle *"Synthesis of 2,2':6',2"-Terpyridine-functionalized Perylene Bisimides"*
22.09.2000	Diplom (diploma, corresponds to master's degree)
22.10.1997	Vordiplom (corresponds to bachelor's degree)
Oct. 1995 – Sept. 2000	started studies in chemistry at the University of Ulm, Germany

COMMUNITY SERVICE

Aug. 1994 – Oct. 1995	Fachklinik Enzensberg (rehabilitation clinic)

SCHOLASTIC EDUCATION

1985–1994	mathemat.-naturwiss. Gymnasium Marktoberdorf (high school) Abitur (corresponds to A-levels)
1981-1985	Volksschule Thalhofen a.d.W. (primary school)

List of Publications

"Electrostatic Self-Assembly of Fluorescent Perylene Bisimide Coordination Polymers"
R. Dobrawa, D. G. Kurth, F. Würthner
Polymer Preprints **2004**, *45*, 378-379.

"Photoinduced Electron and Energy Transfer Processes in a Bichromophoric Pyrene-Perylene Bisimide System"
B. K. Kaletas, R. Dobrawa, A. Sautter, F. Würthner, M. Zimine, L. De Cola, R. M. Williams
J. Phys. Chem. **2004**, *108*, 1900-1909.

"Fabrication and Fluorescence Properties of Perylene Bisimide Dye Aggregates bound to Gold Surfaces and Nanopatterns"
U. Haas, C. Thalacker, J. Adams, J. Fuhrmann, S. Riethmüller, U. Beginn, U. Ziener, M. Möller, R. Dobrawa, F. Würthner
J. Mater. Chem. **2003**, *13*, 767-772.

"Photoluminescent Supramolecular Polymers: Metal-Ion Directed Polymerization of Terpyridine-Functionalized Perylene Bisimide Dyes"
R. Dobrawa, F. Würthner
Chem. Commun. **2002**, 1878-1879.